



January 2016

Synthesis And Applications Of Symmetric Building Blocks In Supramolecular, Single-Stranded, And Double-Stranded Polymers

Zijun Dave Wang

Follow this and additional works at: <https://commons.und.edu/theses>

Recommended Citation

Wang, Zijun Dave, "Synthesis And Applications Of Symmetric Building Blocks In Supramolecular, Single-Stranded, And Double-Stranded Polymers" (2016). *Theses and Dissertations*. 2085.
<https://commons.und.edu/theses/2085>

This Thesis is brought to you for free and open access by the Theses, Dissertations, and Senior Projects at UND Scholarly Commons. It has been accepted for inclusion in Theses and Dissertations by an authorized administrator of UND Scholarly Commons. For more information, please contact zeinebyousif@library.und.edu.

SYNTHESIS AND APPLICATIONS OF SYMMETRIC BUILDING BLOCKS IN
SUPRAMOLECULAR, SINGLE-STRANDED, AND DOUBLE-STRANDED
POLYMERS

by

Zijun (Dave) Wang

Bachelor of Chemical Engineering, Harbin University of Science and Technology,
Harbin, China 2011

A Thesis

Submitted to Graduate Faculty

of the

University of North Dakota

In partial fulfillment of the requirements

for the degree of

Master of Science

Grand Forks, North Dakota

December

2016

This thesis, submitted by Zijun D. Wang in partial fulfillment of the requirements for the Degree of Master of Science from the University of North Dakota, has been read by the faculty Advisory Committee under whom the work has been done and is hereby approved.



Chairperson





This thesis meets the standard for appearance, conforms to the style and format requirements of the Graduate School of the University of North Dakota, and is hereby approved.


Dean of the Graduate School


Date

PERMISSION

Title Synthesis and Applications of Symmetric Building Blocks in
 Supramolecular, Single-stranded, and Double-stranded Polymers

Department Chemistry

Degree Master of Science

In presenting this thesis in partial fulfillment of the requirements for a graduate degree from the University of North Dakota, I agree that the library of this University shall make it freely available for inspection. I further agree that permission for extensive copying for scholarly purposes may be granted by the professor who supervised my thesis work or, in his absence, by the Chairperson of the department or the dean of the Graduate School. It is understood that any copying or publication or other use of this thesis or part thereof for financial gain shall not be allowed without my written permission. It is also understood that due recognition shall be given to me and to the University of North Dakota in any scholarly use which may be made of any material in my thesis.

Zijun (Dave) Wang

12/12/2016

TABLE OF CONTENTS

LIST OF ABBREVIATIONS.....	viii
LIST OF FIGURES.....	ix
LIST OF SCHEMES.....	xiv
LIST OF TABLES.....	xv
LIST OF CHARTS.....	xvi
ACKNOWLEDGEMENTS.....	xvii
ABSTRACT.....	xix

CHAPTER

1. INTRODUCTION AND BACKGROUND.....	1
1.1 Supramolecular Polymers.....	2
1.2 Bio-based Single-stranded Polymers.....	3
1.3 Double-stranded Polymers.....	4
2. STUDY OF THREE-FOLD SYMMETRIC CARBAMATES AS BUILDING BLOCKS FOR SUPRAMOLECULAR POLYMERS.....	6
2.1 Goals of the Study.....	6
2.2 Synthesis of Three-fold Symmetric Carbamates	7
2.3 Self-assembly of Three-fold Symmetric Carbamates to Supramolecular Polymers.....	8
2.4 Hydrogen-bonded Network of Supramolecular Polymers from Carbamates	9
2.5 Odd-even Effect of the Carbamates with a Similar H-bonded Network.....	14

2.6	Organogelators Derived from Carbamates 7-11	16
2.7	Conclusions.....	18
3.	A POTENTIAL BUILDING BLOCK FOR FURFURAL-BASED POLYMER.....	19
3.1	Goals of the Study.....	19
3.2	Synthesis and Characterization of the Furfural-derived Monomer.....	20
3.2.1	Synthesis of Monomer 12 and its Precursor 12'	20
3.2.2	Crystalline Structure of 12	22
3.2.3	Photo, Thermal, and Chemical Stability of 12	23
3.3	Polymerization and Detection of 12	25
3.4	Conclusions.....	25
4.	BUILDING BLOCKS FOR DOUBLE-STRANDED POLYMERS.....	27
4.1	Goals of the Study.....	27
4.2	Synthesis of the Monomers.....	28
4.3	Self-assembly of the Monomers.....	32
4.4	Cis-trans isomerization of the Monomers.....	36
4.5	Synthesis of the Polymers.....	39
4.6	Conclusions.....	41
5.	EXPERIMENTAL SECTION.....	43
5.1	General Procedure and Instrumentation.....	43
5.2	Synthetic Procedures.....	44

5.2.1	Synthesis of benzene-1,3,5-triyl tris(propylcarbamate) 1	44
5.2.2	Synthesis of benzene-1,3,5-triyl tris(butylcarbamate) 2	44
5.2.3	Synthesis of benzene-1,3,5-triyl tris(pentylcarbamate) 3	45
5.2.4	Synthesis of benzene-1,3,5-triyl tris(hexylcarbamate) 4	46
5.2.5	Synthesis of benzene-1,3,5-triyl tris(heptylcarbamate) 5	46
5.2.6	Synthesis of 1,3,5-Triisocyanatobenzene 6	47
5.2.7	Synthesis of tripropanyl <i>N',N'',N'''</i> -benzene-1,3,5- tricarbamate 7	48
5.2.8	Synthesis of tributyl <i>N',N'',N'''</i> -benzene-1,3,5- tricarbamate 8	48
5.2.9	Synthesis of tripentyl <i>N',N'',N'''</i> -benzene-1,3,5- tricarbamate 9	49
5.2.10	Synthesis of trihexyl <i>N',N'',N'''</i> -benzene-1,3,5- tricarbamate 10	50
5.2.11	Synthesis of triheptyl <i>N',N'',N'''</i> -benzene-1,3,5- tricarbamate 11	50
5.2.12	Synthesis of 3,4-di(furan-2-yl)cyclobutane-1,2- dicarboxylic acid 12	51
5.2.13	Preparation of Polymer from 12 and 1,5-Pentanediol.....	52
5.2.14	Synthesis of (2 <i>Z</i> ,2' <i>Z</i>)-4,4'-[propane-1,3-diylbis(oxy)] bis(4-oxobut-2-enoic acid) 13	52
5.2.15	Synthesis of (2 <i>Z</i> ,2' <i>Z</i>)-4,4'-[butane-1,4-diylbis(oxy)] bis(4-oxobut-2-enoic acid) 14	53
5.2.16	Synthesis of (2 <i>Z</i> ,2' <i>Z</i>)-4,4'-[pentane-1,5-diylbis(oxy)] bis(4-oxobut-2-enoic acid) 15	53
5.2.17	Synthesis of (2 <i>E</i> ,2' <i>E</i>)-4,4'-[butane-1,4-diylbis(oxy)] bis(4-oxobut-2-enoic acid) 16	54
5.2.18	Synthesis of (3 <i>Z</i> ,14 <i>Z</i>)-1,6,12,17-tetraoxacyclodocosa- 3,14-diene-2,5,13,16-tetraone 17	55

5.2.19 Synthesis of (3 <i>E</i> ,14 <i>E</i>)-1,6,12,17-tetraoxacyclodocosa-3,14-diene-2,5,13,16-tetraone 18	56
5.2.20 Synthesis of a Double-stranded Polymer from 17	56
APPENDIX.....	57
REFERENCES.....	103

LIST of ABBREVIATIONS

Abbreviations	Definitions
1D	one-dimensional
2D	two-dimensional
DMF	<i>N,N</i> -dimethyl formamide
DMSO	dimethyl sulfoxide
EA	ethyl acetate
FT-IR	Fourier transform infrared
NMR	nuclear magnetic resonance
THF	tetrahydrofuran
TEA	triethylamine
TLC	thin-layer chromatography
TGA	thermal gravimetric analysis
UV	ultraviolet
SCXRD	single crystal X-ray diffraction

LIST OF FIGURES

Figure	Page
Figure 1. ¹ H NMR spectra of carbamate 4 in CDCl ₃ at different concentrations at room temperature.....	8
Figure 2. IR spectra of carbamates 1-5	9
Figure 3. Comparison of the crystal structures of 1 and 2	11
Figure 4. Comparison of hydrogen-bond networks in 1 and 5	11
Figure 5. Crystal packing for two supramolecular polymer layers of carbamates 1-5	13
Figure 6. Side chain conformations in carbamates 3 and 5	15
Figure 7. Dihedral angles between the aromatic core and the arm with three hydrogen bonds in carbamates 2-5	15
Figure 8. Melting points of carbamates 2-5	16
Figure 9. Carbamates 7-11 at 20 g/L (2.6 × 10 ⁻² M) in <i>n</i> -dodecane.....	17
Figure 10. Crystal structure of 3-(2-furyl)acrylic acid 12'	21
Figure 11. The UV-Vis spectra of 12 in the solid state and in MeOH solution.....	21
Figure 12. Image of 12 from single crystal X-ray diffraction.....	23
Figure 13. TGA curve of 12	24
Figure 14. Single crystal structure of 17	33
Figure 15. Powder XRD of 17	34
Figure 16. Single crystal structure of 18	35
Figure 17. Powder XRD of 18	36
Figure 18. ¹ H NMR (CDCl ₃) spectra of 14 and 16	37
Figure 19. ¹ H NMR (CDCl ₃) spectrum of 16 after UV irradiation.....	37

Figure 20. ¹ H NMR spectra of the compounds 17 and 18 in cis to trans and trans to cis isomerization.....	38
Figure 21. UV spectra of the cis isomer 17 and trans isomer 18 in hexane.....	39
Figure 22. The image of product obtained from polymerization trial.....	40
Figure 23. IR spectra of monomer 17 and its polymer 17'	40
Figure 24. Solid state ¹³ C{ ¹ H} NMR spectra of monomer 17 and polymer 17'	41
Figure 25. ¹ H NMR spectrum of benzene-1,3,5-triyl tris(propylcarbamate) 1 in CDCl ₃	58
Figure 26. ¹³ C{ ¹ H} NMR spectrum of benzene-1,3,5-triyl tris(propylcarbamate) 1 in CDCl ₃	59
Figure 27. IR spectrum of benzene-1,3,5-triyl tris(propylcarbamate) 1	60
Figure 28. IR spectrum of benzene-1,3,5-triyl tris(butylcarbamate) 2	61
Figure 29. ¹ H NMR spectrum of benzene-1,3,5-triyl tris(pentylcarbamate) 3 in CDCl ₃	62
Figure 30. ¹³ C{ ¹ H} NMR spectrum of benzene-1,3,5-triyl tris(pentylcarbamate) 3 in CDCl ₃	63
Figure 31. IR spectrum of benzene-1,3,5-triyl tris(pentylcarbamate) 3	64
Figure 32. ¹ H NMR spectrum of benzene-1,3,5-triyl tris(heptylcarbamate) 5 in CDCl ₃	65
Figure 33. ¹³ C{ ¹ H} NMR spectrum of benzene-1,3,5-triyl tris(heptylcarbamate) 5 in CDCl ₃	66
Figure 34. IR spectrum of benzene-1,3,5-triyl tris(heptylcarbamate) 5	67
Figure 35. ¹ H NMR spectrum of 3,4-di(furan-2-yl)cyclobutane-1,2-dicarboxylic acid 12 in DMSO- <i>d</i> ₆	68
Figure 36. ¹³ C{ ¹ H} NMR spectrum of 3,4-di(furan-2-yl)cyclobutane-1,2-dicarboxylic acid 12 in DMSO- <i>d</i> ₆	69
Figure 37. IR spectrum of 3,4-di(furan-2-yl)cyclobutane-1,2-dicarboxylic acid 12	70
Figure 38. IR spectrum of 3-(2-furyl)acrylic acid 12'	71

Figure 39. ¹ H NMR (DMSO- <i>d</i> ₆) spectrum of 3,4-di(furan-2-yl)cyclobutane-1,2-dicarboxylic acid 12 after 6 M HCl (aq.) treatment overnight.....	72
Figure 40. ¹ H NMR (DMSO- <i>d</i> ₆) spectrum of 3,4-di(furan-2-yl)cyclobutane-1,2-dicarboxylic acid 12 after 1 month heat treatment at 100 °C.....	73
Figure 41. ¹ H NMR (DMSO- <i>d</i> ₆) spectrum of the polymer product obtained from 3,4-di(furan-2-yl)cyclobutane-1,2-dicarboxylic acid 12 and 1,5-pentanediol.....	74
Figure 42. ¹³ C{ ¹ H} NMR (DMSO- <i>d</i> ₆) spectrum of the polymer product from 3,4-di(furan-2-yl)cyclobutane-1,2-dicarboxylic acid 12 and 1,5-pentanediol.....	75
Figure 43. ¹ H NMR (CDCl ₃) spectrum of the polymer product prepared from 3,4-di(furan-2-yl)cyclobutane-1,2-dicarboxylic acid 12 and glycerol.....	76
Figure 44. IR spectrum of the polymer product from 3,4-di(furan-2-yl)cyclobutane-1,2-dicarboxylic acid 12 and glycerol.....	77
Figure 45. ¹ H NMR spectrum of (2 <i>Z</i> ,2' <i>Z</i>)-4,4'-[propane-1,3-diylbis(oxy)]bis(4-oxobut-2-enoic acid) 13 in DMSO- <i>d</i> ₆	78
Figure 46. IR spectrum of (2 <i>Z</i> ,2' <i>Z</i>)-4,4'-[propane-1,3-diylbis(oxy)]bis(4-oxobut-2-enoic acid) 13	79
Figure 47. ¹ H NMR spectrum of (2 <i>Z</i> ,2' <i>Z</i>)-4,4'-[butane-1,4-diylbis(oxy)]bis(4-oxobut-2-enoic acid) 14 in DMSO- <i>d</i> ₆	80
Figure 48. ¹³ C{ ¹ H} NMR spectrum of (2 <i>Z</i> ,2' <i>Z</i>)-4,4'-[butane-1,4-diylbis(oxy)]bis(4-oxobut-2-enoic acid) 14 in DMSO- <i>d</i> ₆	81
Figure 49. IR spectrum of (2 <i>Z</i> ,2' <i>Z</i>)-4,4'-[butane-1,4-diylbis(oxy)]bis(4-oxobut-2-enoic acid) 14	82
Figure 50. ¹ H NMR spectrum of (2 <i>Z</i> ,2' <i>Z</i>)-4,4'-[pentane-1,5-diylbis(oxy)]bis(4-oxobut-2-enoic acid) 15 in DMSO- <i>d</i> ₆	83
Figure 51. ¹³ C{ ¹ H} NMR spectrum of (2 <i>Z</i> ,2' <i>Z</i>)-4,4'-[pentane-1,5-diylbis(oxy)]bis(4-oxobut-2-enoic acid) 15 in DMSO- <i>d</i> ₆	84
Figure 52. IR spectrum of (2 <i>Z</i> ,2' <i>Z</i>)-4,4'-[pentane-1,5-diylbis(oxy)]bis(4-oxobut-2-enoic acid) 15	85
Figure 53. ¹ H NMR spectrum of (2 <i>E</i> ,2' <i>E</i>)-4,4'-[butane-1,4-diylbis(oxy)]bis(4-oxobut-2-enoic acid) 16 in DMSO- <i>d</i> ₆	86

Figure 54. $^{13}\text{C}\{^1\text{H}\}$ NMR spectrum of (2 <i>E</i> ,2' <i>E</i>)-4,4'-[butane-1,4-diylbis(oxy)]bis(4-oxobut-2-enoic acid) 16 in DMSO- <i>d</i> ₆	87
Figure 55. IR spectrum of (2 <i>E</i> ,2' <i>E</i>)-4,4'-[butane-1,4-diylbis(oxy)]bis(4-oxobut-2-enoic acid) 16	88
Figure 56. ^1H NMR spectrum of (3 <i>Z</i> ,14 <i>Z</i>)-1,6,12,17-tetraoxacyclodocosa-3,14-diene-2,5,13,16-tetraone 17 in DMSO- <i>d</i> ₆	89
Figure 57. ^1H NMR spectrum of (3 <i>Z</i> ,14 <i>Z</i>)-1,6,12,17-tetraoxacyclodocosa-3,14-diene-2,5,13,16-tetraone 17 in CDCl ₃	90
Figure 58. $^{13}\text{C}\{^1\text{H}\}$ NMR spectrum of (3 <i>Z</i> ,14 <i>Z</i>)-1,6,12,17-tetraoxacyclodocosa-3,14-diene-2,5,13,16-tetraone 17 in CDCl ₃	91
Figure 59. IR spectrum of (3 <i>Z</i> ,14 <i>Z</i>)-1,6,12,17-tetraoxacyclodocosa-3,14-diene-2,5,13,16-tetraone 17	92
Figure 60. ^1H NMR spectrum of (3 <i>E</i> ,14 <i>E</i>)-1,6,12,17-tetraoxacyclodocosa-3,14-diene-2,5,13,16-tetraone 18 in CDCl ₃	93
Figure 61. $^{13}\text{C}\{^1\text{H}\}$ NMR spectrum of (3 <i>E</i> ,14 <i>E</i>)-1,6,12,17-tetraoxacyclodocosa-3,14-diene-2,5,13,16-tetraone 18 in CDCl ₃	94
Figure 62. IR spectrum of (3 <i>E</i> ,14 <i>E</i>)-1,6,12,17-tetraoxacyclodocosa-3,14-diene-2,5,13,16-tetraone 18	95
Figure 63. IR spectrum of (2 <i>Z</i> ,2' <i>Z</i>)-4,4'-[propane-1,3-diylbis(oxy)]bis(4-oxobut-2-enoic acid) 14 after 27 h mercury lamp UV irradiation.....	96
Figure 64. IR spectrum of (2 <i>Z</i> ,2' <i>Z</i>)-4,4'-[butane-1,3-diylbis(oxy)]bis(4-oxobut-2-enoic acid) 14 after 27 h mercury lamp UV irradiation.....	97
Figure 65. IR spectrum of (2 <i>Z</i> ,2' <i>Z</i>)-4,4'-[pentane-1,3-diylbis(oxy)]bis(4-oxobut-2-enoic acid) 15 after 27 h mercury lamp UV irradiation.....	98
Figure 66. ^1H NMR (DMSO- <i>d</i> ₆) spectrum of (2 <i>E</i> ,2' <i>E</i>)-4,4'-[butane-1,3-diylbis(oxy)]bis(4-oxobut-2-enoic acid) 16 after 72 h mercury lamp UV irradiation.....	99
Figure 67. IR spectrum of (3 <i>Z</i> ,14 <i>Z</i>)-1,6,12,17-tetraoxacyclodocosa-3,14-diene-2,5,13,16-tetraone 17 after 2-day mercury lamp UV irradiation.....	100
Figure 68. ^1H NMR (CDCl ₃) spectrum of (3 <i>E</i> ,14 <i>E</i>)-1,6,12,17-tetraoxacyclodocosa-3,14-diene-2,5,13,16-tetraone 18 after 12 h mercury lamp UV irradiation.....	101

Figure 69. IR spectrum of the product obtained from the solution of (3Z,14Z)-1,6,12,17-tetraoxacyclodocosa-3,14-diene-2,5,13,16-tetraone **17** in hexane after 12 h mercury lamp UV irradiation.....102

LIST OF SCHEMES

Scheme	Page
1. Synthesis of carbamate 1 to 5	7
2. Synthesis of carbamate 7 to 11	8
3. General synthetic route to the furfural-based polymer in this study.....	20
4. Synthesis of the furfural-based carboxylic acid 12'	21
5. Synthesis of furfural-based monomer 12	22
6. Synthesis of the polymer from 12 and 1,5-pentanediol.....	25
7. Synthetic route 1 of double-stranded polymers from cyclic monomers.....	30
8. Synthetic route 2 of double-stranded polymers from cyclic monomers.....	31
9. Synthetic route 3 of double-stranded polymers from cyclic monomers	32
10. Cis-trans isomerization of 14	36
11. Cis-trans isomerization of 17	38

LIST OF TABLES

Table	Page
1. Crystal data of carbamates 1-5	10
2. Gelation capability of carbamates 7-11 in <i>n</i> -dodecane (20 g/L)	16

LIST OF CHARTS

Chart	Page
1. General structure of non-covalently bonded double-stranded polymers.....	5
2. General structure of our proposed covalently bonded double-stranded polymers.....	5
3. Column-like and sheet-like supramolecular polymers	6
4. The general structure of the carbamates synthesized and studied in this work.....	7
5. The structure of 3,4-di(furan-2-yl)cyclobutane-1,2-dicarboxylic acid 12 , phthalic acid, and glyptal.....	20
6. The proposed three-step preparation for double-stranded polymers.....	27
7. General designs of the monomers for double-stranded polymers.....	28
8. The starting materials chosen for monomers.....	29
9. The crystal packing expected to form a polymer.....	33

ACKNOWLEDGEMENTS

Firstly, I would like to express my sincere gratitude to my advisor Prof. Qianli Rick Chu for the continuous support of my graduate study and related research, for his patience, motivation, and immense knowledge. His guidance helped me in all the time of research and writing of this thesis. I could not have imagined having a better advisor and mentor for my graduate study.

I want to thank the members of my committee: Dr. Kathryn A. Thomasson and Dr. Irina P. Smoliakova for helping me during annual meetings of the committee as well as private consultations. I am also grateful to Dr. Guodong Du and Dr. Alexei Novikov for being so encouraging and helpful to me whenever I need their advice. I am also thankful to Dr. Julia Xiaojun Zhao for teaching me about the SEM technique, thankful to Dr. Lothar Stahl for help with XRD equipment. I wish to thank Dr. Alena Kubatova and her students for helping me with high resolution mass spectroscopic analysis of some of my compounds.

I thank my fellow labmates Dr. Xiaodong Hou, Zhihan Wang, Brent Kastern, Katelyn Randazzo, Jonathan Butz, Jenna Puttkammer, Rahul Shahni, Benjamin Miller, Joseph Lee, Tiffany Shui, Micah Mabinn, Quintin Elliot, and Fang Ben for the sleepless nights we were working together, and for all the fun we have had in the last three years. Also I thank my friend Wang Wan in Clemson University.

I am sincerely thankful to the Chemistry Department for providing me the financial support during my graduate study. I would like to thank ND EPSCoR, the Center for Sustainable Materials Science, and the Chemistry Graduate Students Association. I would also like to thank faculty of the Chemistry Department for providing me good education and being always supportive to me. I am also thankful to the staff members of the Chemistry Department for their support to me during my study at the University of North Dakota.

Last but not least, I would like to thank my father Kairu and mother Ling for always being supportive in my every endeavor.

ABSTRACT

In this study, supramolecular polymers from carbamates are studied. A number of three-fold symmetric carbamates have been synthesized, characterized and their self-assembly structure are studied. The lamellar structures are detected and compared by using their melting points, NMR and FT-IR spectroscopy, and single crystal X-ray diffraction. The hydrogen-bond networks of each compound in crystalline state are examined. A new hydrogen bonded network self-assembles under mild conditions from benzene-1,3,5-triyl tris(butyl carbamate) (**2**), benzene-1,3,5-triyl tris(pentyl carbamate) (**3**), benzene-1,3,5-triyl tris(hexyl carbamate) (**4**), and benzene-1,3,5-triyl tris(heptyl carbamate) (**5**). One of the carbonyl groups in the molecules **2-4** does not form a C=O...H-N hydrogen bond in the sheet-like structure. Three different types of hydrogen bonding sites are observed. Although the building blocks only differ in the number of carbons in their side chains, this 2D unsaturated hydrogen bonded network is different from the saturated one which is self-assembled from benzene-1,3,5-triyl tris(propyl carbamate) **1**. For compounds **2-5**, the odd-even effect is also observed in terms of melting point, as well as the dihedral angle between the aromatic core and the arm with an oversaturated hydrogen bond. The inverted carbamates **7-11** are also synthesized and studied. An organic gel is found in triheptyl *N',N'',N'''*-benzene-1,3,5-tricarbamate **11** with a concentration of 20 g/L (2.6×10^{-2} M) in *n*-dodecane.

A mirror-symmetric building block for linear polymer is designed. 3,4-Di(furan-2-yl)cyclobutane-1,2-dicarboxylic acid (**12**) is synthesized from 3-(2-furyl)acrylic acid (**12'**) through a solid-state [2+2] photocycloaddition by UV-A irradiation in quantitative yield. This building block molecule is derived from furfural and malonic acid. Thus, a novel 100% bio-based monomer has been successfully synthesized. For the first time, the single crystal is obtained in MeOH/DCM at room temperature. The thermal stability and acidic resistance of the cyclobutane ring of this building block is tested by thermal gravimetric analysis (GTA) and acid treatment. As a proof-of-concept, the condensation of **12** and 1,5-pentanediol is evaluated in this study. MS and NMR spectra of the product prove the formation of the target polymer.

A series of cyclic C₂-symmetric building blocks for double-stranded polymers are designed. Our goal is to synthesize a linear polymer with double-stranded chains. The two strands are anchored by a C-C single bond so that the width is only extended by one covalent bond while the strength of the chain is enhanced. To achieve this polymer, a three-step strategy has been designed. The first step is to synthesize a cyclic monomer with a C=C bond at each end of the molecule. The second step is to apply intermolecular interactions for self-assembling the monomer. When desirable crystalline packing is obtained, the third step is to generate cyclobutane rings between each neighboring C=C bond by solid-state [2+2] photocycloaddition to form the double-stranded polymer. A series of lactone monomers have been successfully synthesized and their structures are confirmed by NMR spectroscopy. (3*Z*,14*Z*)-1,6,12,17-tetraoxacyclodocosa-3,14-diene-2,5,13,16-tetraone (**17**) is synthesized from maleic anhydride and 1,5-pentanediol. Then isomerization of compound **17** afford (3*E*,14*E*)-1,6,12,17-tetraoxacyclodocosa-3,14-

diene-2,5,13,16-tetraone (**18**). Crystalline structures of these two compounds are analyzed by SCXRD and their photoreactivity is examined. The photopolymerization of **17** is supported by IR and solid state ^{13}C NMR spectra.

CHAPTER 1

INTRODUCTION AND BACKGROUND

Polymers are defined as large molecules or macromolecules, which are composed of many repeated subunits.¹ They play an essential part in our life. Vegetables and meat all contain natural polymers such as lignin, polysaccharides, nucleic acids, and protein. Almost all our clothes, CDs, paint oil, and plastic products contains man-made polymers such as polyethylene, polyester, and nylons.² Among those factors that affect the property and applications of polymers, the monomers always play an important role.

Researchers are pursuing monomers that are functionalized and easy to synthesize. For the most part, one needs to find a balance between these two aspects. In terms of the monomer candidates, the more complicated the synthesis is, the more time and resources are needed to explore the processing. If cost-efficient procedures are not developed, the commercial acceptability of this polymer may be limited.³ Due to ease of synthesis, symmetric molecules are one of the most popular candidates for monomers.

There is an old saying that necessity is the mother of invention. Charles E. Carraher said “it has led to the sequence of chemical reactions where little is wasted and byproducts from one reaction are employed in another reaction as an integral starting material.”⁴ This can be used as an explanation for the rise of today’s sustainable

chemistry. It would be ideal if I make full use of the ‘waste’ produced by nature, and extract our starting materials from it.⁵

In summary, developing monomers from readily available inexpensive feedstocks is our basic goal. Furthermore, exploring the synthesis of high performance polymers, which is built on renewable resources, is both an art and a science. Monomer and polymer synthesis continues to undergo change and improvement.

1.1 Supramolecular Polymers

Supramolecular polymers are polymeric arrays of monomeric units which are connected to each other by noncovalent bonds such as hydrogen bonds. These reversible and highly directional interactions give this class of polymers low viscosity that are easy to handle.⁶ Some of them can even self-heal their fractures in certain environments.⁷ Organic sheets can be found in many natural applications such as the β -pleated sheet of polypeptides and the lipid bilayer in the cell membrane.⁸⁻¹⁰ Recently, our research group has discovered and studied a series of hydrogen bonded sheets that self-assembled from three-fold symmetric triamides or tricarbamates.¹¹⁻¹³ These organic sheets have displayed chirality generated from achiral molecules with stereogenic axes (supramolecular atropisomers).^{11,12} By introducing cyclohexyl side chains onto the surface of the carbamate sheet, the derived two-dimensional (2D) hydrogen bonded framework has demonstrated applications in host–guest chemistry.¹³ Another significant characteristic of the hydrogen bonded sheets is structural adaptability and generality. To adapt the structural variations of the supramolecular building blocks, the hydrogen bonded networks were changed correspondingly while the lamellar structures remained unaltered.

Herein, I report two new unsaturated hydrogen bonded sheets obtained from three-fold symmetric carbamates.

1.2 Bio-based Single-stranded Polymers

Growing ecological and economic concerns have resulted in a global pursuit for renewable and bio-based materials.¹⁴⁻¹⁷ To achieve this goal, a vast amount of research has been conducted¹³⁻¹⁹ and also backed by both local and foreign governments.^{25,26} One promising bio-based building block is furfural.^{27,28} It can be derived from pentoses found within the hemicellulose of a variety of biomass sources,³⁰ such as corncobs, rice hulls, and sugarcane bagasse.²⁵⁻²⁹ In addition to being used as a lubricating oil, fungicide and organic solvent, furfural can also be used to synthesize other furan-based chemicals.^{27,31-34} Recently, furan-based monomers have been getting increasing attention.³⁵

3-(2-Furyl)acrylic acid (**12'**) is a furan-based chemical and the starting material for a novel monomer studied in this paper. Compound **12'** can be readily obtained from furfural and malonic acid via Knoevenagel condensation.³⁶ Malonic acid can be obtained directly from renewable sources as well, such as glucose or 3-hydroxypropionic acid.^{37,38} Acid **12'** contains only one carboxyl group, which makes it unsuitable for classic polymerization. However, instead of synthesizing another carboxyl group on the furan ring, solid-state photoreaction provides an alternative to double the number of this functional group.³⁹ G. Schmidt found that upon exposure to ultraviolet light, crystals of **12'** underwent dimerization through [2+2] photocycloaddition. UV light excites the C=C bond in **12'** and forms a cyclobutane ring between the two neighboring molecules.³⁹⁻⁴¹

Thus, 3,4-di(furan-2-yl)cyclobutane-1,2-dicarboxylic acid (**12**) was obtained with the doubling of carboxyl groups in one simple step in a 51% yield.^{42,43}

Since bio-based carboxylic acids are viewed as high-value chemicals,⁴⁴ a monomer candidate was designed. Compound **12** is structurally similar to phthalic acid, the monomer of a widely versatile polymer Glyptal®.⁴⁵ The cyclobutane ring in **12** contains two carboxyl groups on adjacent carbons. These two groups can additionally be found on adjacent carbons on the benzene ring of phthalic acid.

Previously, our research group shows how photoreactions can be used to synthesize polycyclobutanes (PCBs), a polymer species centered around the repetition of the cyclobutane ring in the main body.^{46,47} In this study, the easy, inexpensive, and green synthesis of the 100% bio-based monomer **12** and a proof-of-concept non-petroleum dependent polycyclobutane are explored.

1.3 Double-stranded Polymers

The hydrogen-bonded double-stranded polymer was first found in nature as the double helical structure of deoxyribonucleic acid (DNA).⁴⁸ Then, a mimic of DNA was developed with peptide nucleic acid (PNA).⁴⁹ Instead of using ribosephosphate as the backbone of nucleic acids, PNA has the backbone made of a polyamide. Adenine-thymine and guanine-cytosine base pairs are used as hydrogen acceptors and donors to form the hydrogen bonds between two polyamide chains (Chart 1a). Other groups developed a similar double-stranded structure by coordinate bonds.⁵⁰ In this case, coordinate bonds between nitrogen and metals act as the binding force between two polymer chains (Chart 1b). Researchers believe that the study of double-stranded

molecules may help to develop gene therapeutic (antisense and antigene) drugs, and genetic diagnostics. But from another perspective, if cost-efficient ways to synthesize covalently bonded double-stranded polymers can be developed, these compounds may become good candidates for light and strong materials.

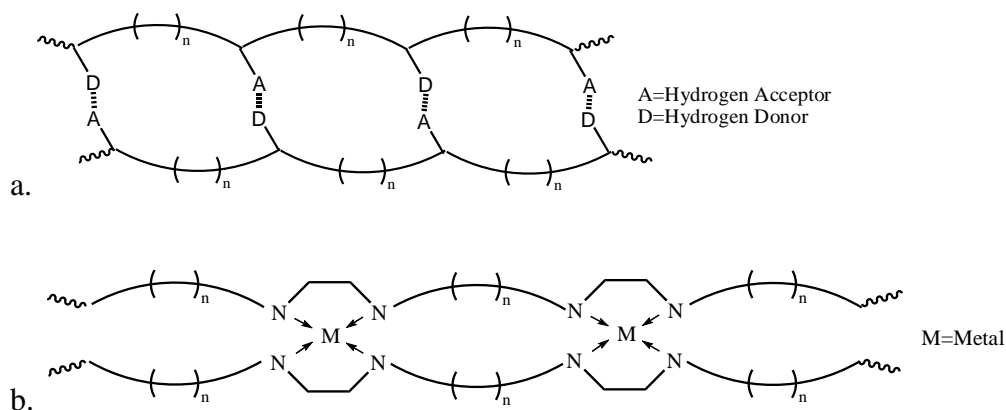


Chart 1. General structure of non-covalently bonded double-stranded polymers. 1a) Hydrogen-bonded double-stranded polymers. 1b) Metal-coordination bonded double-stranded polymers.

In this study, the two strands are designed to be anchored by a C-C single bond so that the width of the polymer chain is only extended by one covalent bond while the strength of the chain is enhanced. Every monomer has one C=C double bond at each end. Then [2+2] photocycloaddition is applied to form a cyclobutane ring between each monomer (Chart 2).

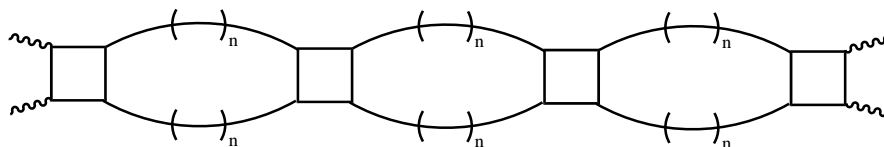


Chart 2. General structure of the proposed covalently bonded double-stranded polymers.

CHAPTER 2

STUDY OF THREE-FOLD SYMMETRIC CARBAMATES AS BUILDING BLOCKS FOR SUPRAMOLECULAR POLYMERS

2.1 Goals of the Study

Three-fold symmetric molecules with amide groups on each arm have been utilized as building blocks for column-like supramolecular polymers.⁵¹ As shown in Chart 3, many researchers believe that the hydrogen bonds on three arms of each molecule bind with a neighboring molecule to form a helix hydrogen-bonded network. However, in a previous study by our group, a sheet-like two dimensional supramolecular polymer was revealed.⁵² The goal of this research is to further explore other possible hydrogen-bonded networks and study the odd-even effect in some homologous series. Thus, a series of three-fold symmetric carbamates and inverted carbamates have been modified and synthesized. The general structure of these compounds is shown in Chart 4.

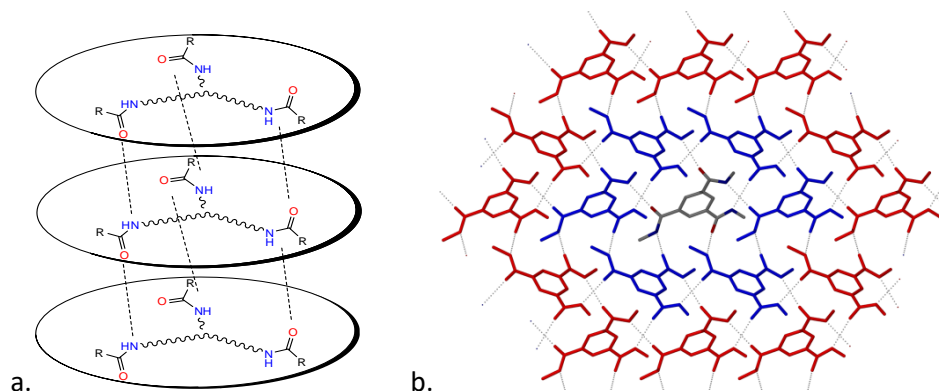


Chart 3. Column-like and sheet-like supramolecular polymers. a. The column-like supramolecular polymer and the generally proposed hydrogen-bonded network in other studies.⁵¹ b. A sheet-like supramolecular polymer with 2D hydrogen-bonded network.¹³

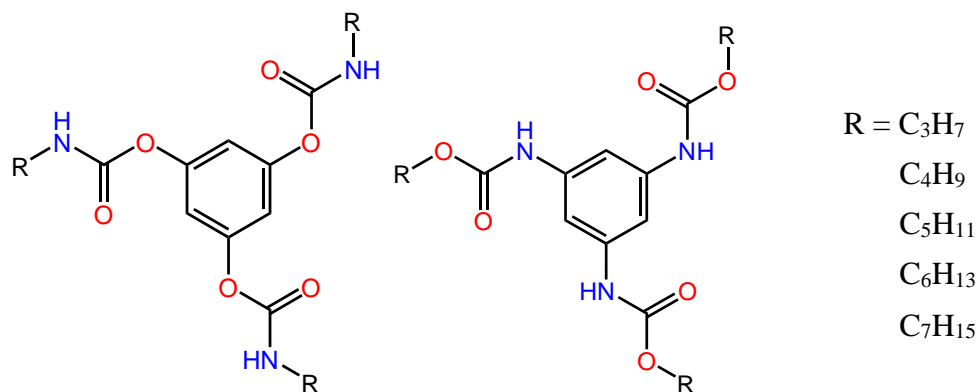
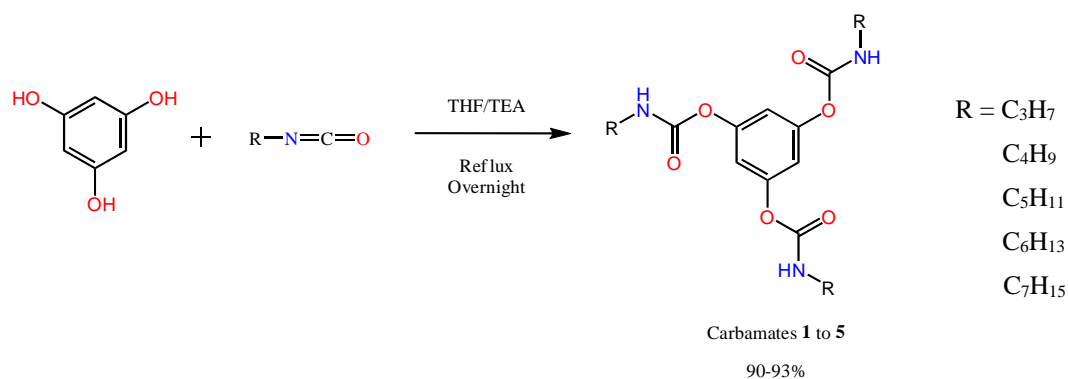


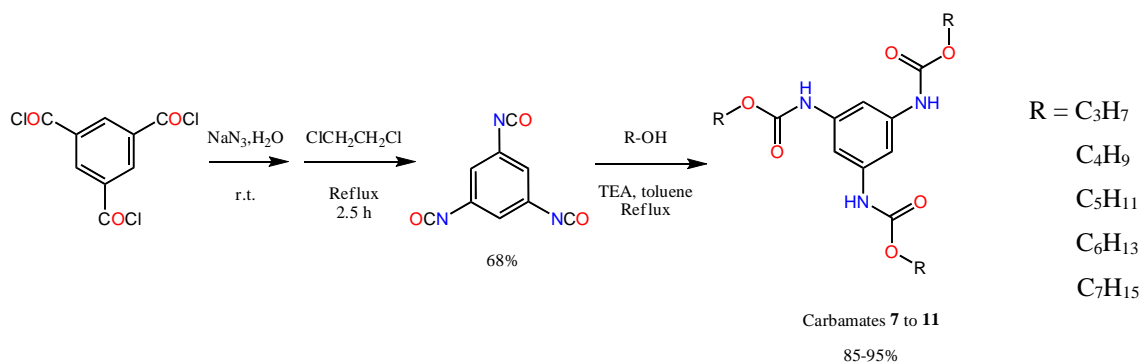
Chart 4. The general structure of the carbamates synthesized and studied in this work.

2.2 Synthesis of Three-fold Symmetric Carbamates

Carbamates **1-5** are readily synthesized from the reaction of phloroglucinol with 1-isocyanatopropane, 1-isocyanatobutane, 1-isocyanatopentane, isocyanatohexane, and 1-isocyanatoheptane, respectively (Scheme 1).⁵³ Carbamates **7-11** are the inverted carbamates **1-5**, which first require the synthesis of 1,3,5-triisocyanato-benzene.⁵⁴ Then the inverted carbamates are readily synthesized in good yield by reacting the corresponding primary alcohol with 1,3,5-triisocyanatobenzene (Scheme 2).



Scheme 1. Synthesis of carbamates **1-5**.



Scheme 2. Synthesis of carbamates **7-11**.

2.3 Self-assembly of Three-fold Symmetric Carbamates to Supramolecular Polymers

Carbamates **1-5** are soluble in a variety of organic solvents such as chloroform, ethyl acetate, DCM, acetone, acetonitrile, THF, and DMSO. The self-assembly behavior of carbamate **4** is used as an example and examined in various solvents. Evidence of intermolecular H-bonding can be seen in the ¹H NMR spectra (Figure 1).

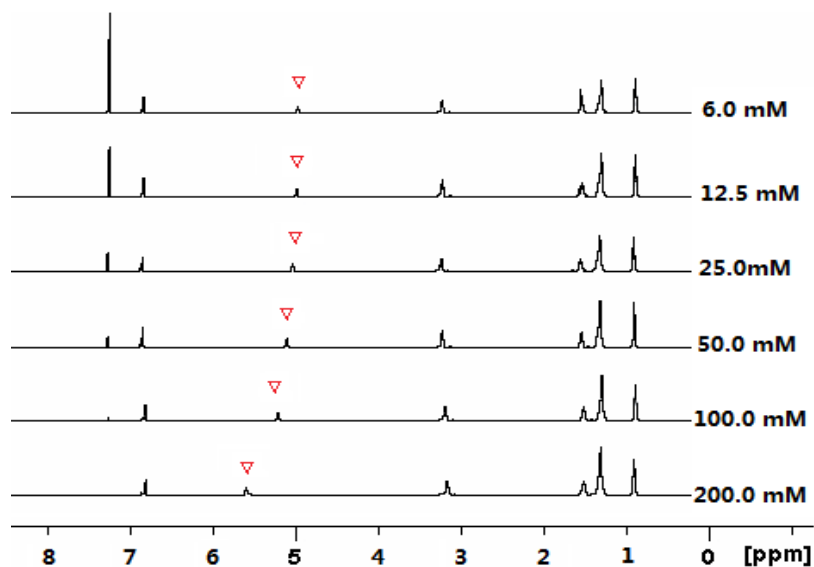


Figure 1. ¹H NMR spectra of carbamate **4** in CDCl₃ at different concentrations at room temperature.

As the concentration of the solution increases from 3.0 to 200.0 mM, the chemical shift of the amide proton gradually shifts downfield. Hydrogen bonding decreases the

electron density around the amide proton, thus moving its peak downfield. The possibility of forming intermolecular amide hydrogen bonding, $\text{-N-H}\cdots\text{O=C}$, is higher in a concentrated solution, and therefore the peak appears at downfield.

2.4 Hydrogen-bonded Network of Supramolecular Polymers from Carbamates

Since the inverted carbamates **7** to **11** do not form crystalline solids, only carbamates **1** to **5** are discussed in this section. A side-to-side comparison of the five carbamates reveals several interesting differences. The melting points (m.p.) of **2-5** are all around 130 °C, which is clearly lower than that of **1** (144 °C), although their molecular weights are higher. While the FT-IR spectra of **2-5** are nearly identical, they are different from that of **1**, especially in the stretching wavenumbers of the amide C=O (around 1700 cm^{-1}) and N-H bonds (around 3300 cm^{-1}). There are three peaks near 1700 cm^{-1} in the spectra of **2-5** but only two in the spectrum of **1** (Figure 2). Considering that the five carbamates contain the same functional groups, the IR spectral and m.p. differences indicate different types of hydrogen bonding patterns.

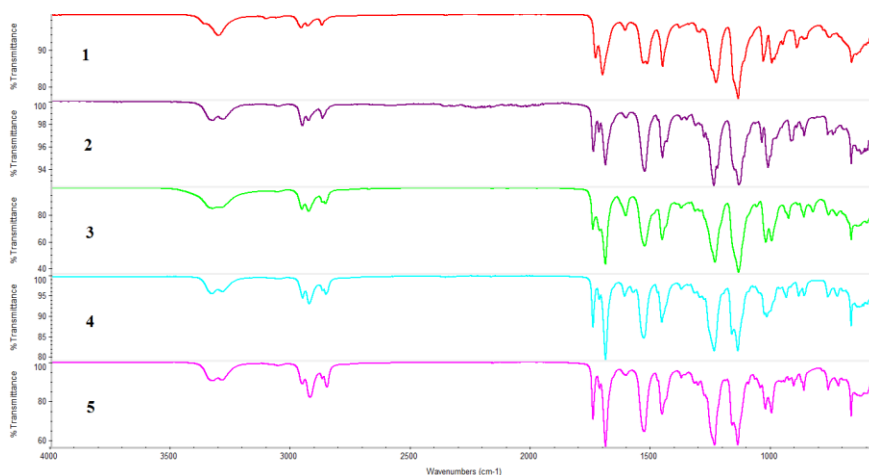


Figure 2. IR spectra of carbamates **1-5**.

Similar to **1**, high quality single crystals of **2-5** were obtained by slowly evaporating their acetonitrile solutions. On the one hand, the X-ray crystal structures show that 2D hydrogen bonded networks are present in the crystals of all five carbamates. The polar amide hydrogen bonded networks are sandwiched by two layers of non-polar alkyl chains forming sheet structures in all five cases. On the other hand, **2-5** adopt the same hydrogen bonding network but quite different from that of **1** (see Table 1 and Figures 2)

In Figure 3 left, the red dash lines represent the six hydrogens of each molecule **1** in the sheet. In Figure 3 right, the red dash lines represent the six hydrogens of each molecule **2**. Molecules **3-5** have similar pattern with molecule **2**. The red arrow shows the C=O moiety with two hydrogen bonds and the blue arrow shows the C=O group without hydrogen bonds.

Table 1. Crystal data of carbamates **1-5**.

Compound	1	2	3	4	5
Formula	C ₁₈ H ₂₇ N ₃ O ₆	C ₂₁ H ₃₃ N ₃ O ₆	C ₂₄ H ₃₉ N ₃ O ₆	C ₂₇ H ₄₅ N ₃ O ₆	C ₃₀ H ₅₁ N ₃ O ₆
Formula weight	381.43	423.57	465.66	507.75	549.84
Temperature/K	100	100	100	100	100
Space group	Fdd2, 16	P 2 ₁ /c	P 2 ₁ /c	P 2 ₁ /c	P 2 ₁ /c
Cell lengths/ Å					
a	13.4049(4)	17.4350(4)	18.6662(16)	21.2940(14)	24.3371(16)
b	48.9616(14)	13.8312(3)	14.1499(10)	13.8436(10)	13.6183(8)
c	12.2121(4)	9.7128(2)	9.7258(7)	9.8230(7)	9.7561(5)
Cell Angles/ °					
α	90	90	90	90	90
β	90	96.5590(10)	94.940(5)	91.467(4)	99.505(4)
γ	90	90	90	90	90
Cell volume	8015.11	2326.88	2559.28	2894.73	3189.07
Density/g·cm ⁻³	1.264	1.209	1.208	1.165	1.145

The hydrogen bonded backbone sheet of **5** is used as an example in this section since sheets of **2-4** are very similar to that of compound **5**. Carbamate **1** crystallizes in the

orthorhombic *Fdd2* space group and each molecule is connected to five neighbors through six intermolecular hydrogen bonds between N–H and C=O groups of the three carbamate groups (Figures 4a and b).

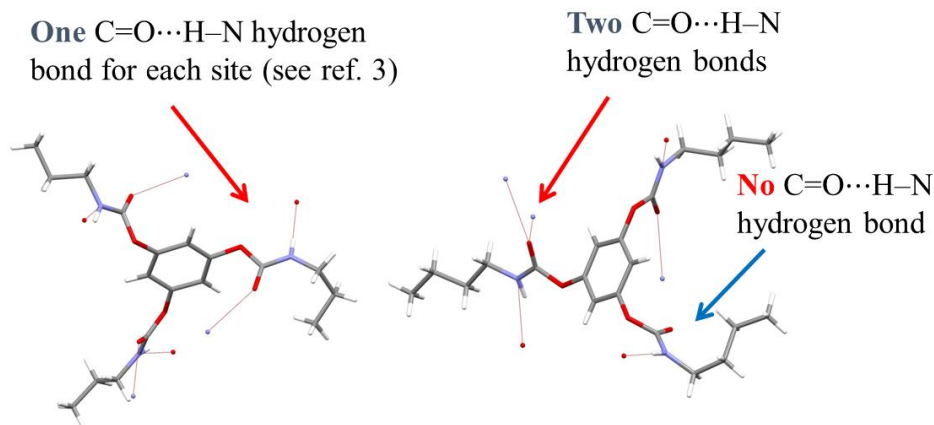


Figure 3. Comparison of the crystal structures of **1** and **2**.

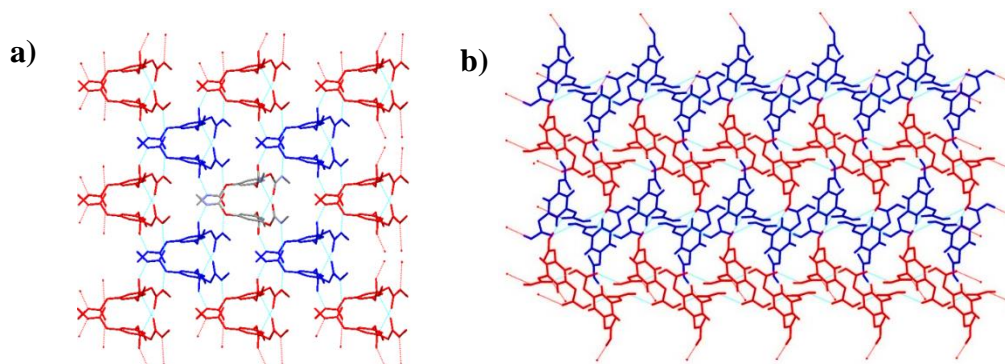


Figure 4. Comparison of hydrogen-bond networks. in **1** and **5**. a) Hydrogen bonded sheet backbone of **1**. b) hydrogen bonded sheet backbone of **5** (a representative of **2-5**). (Hydrogen atoms are omitted and the side chains are replaced with carbon atoms for simplicity. Neighboring hydrogen bonded ribbons are shown in two colors for clarity.)

Specifically, each carbamate molecule is connected to the one closest neighbor by two hydrogen bonds, forming a cyclic supramolecular dimer. Each dimer is held together with four neighbouring dimers by eight hydrogen bonds. The crystal structures consist of a supramolecular sheet extended in the crystallographic *ac* plane through a fully saturated

hydrogen bonded network. In contrast, carbamates **2-5** crystallize in the monoclinic $P2_1/c$ space group and each molecule is connected to four neighbors through six intermolecular hydrogen bonds, between the N-H and C=O groups of the three carbamates. The crystal structures consist of a supramolecular sheet extended in the crystallographic bc plane through an unsaturated hydrogen bonded network (Figure 3 left and 4b). In other words, one of the C=O groups (marked by the red arrow in Figure 3 right) forms two hydrogen bonds with two N-H groups of the two neighboring molecules while another C=O group (marked by the blue arrow in Figure 3 right) does not form a C=O \cdots H-N hydrogen bond.

The second difference between the crystals **1** and **2-5** is the packing of the sheets. One of the three n -propyl arms in crystal **1** lies within the plane of the hydrogen bonded network to fill up the space between the supramolecular dimers. There are grooves on the surface of the sheet formed by molecule **1**, so the neighboring sheets are packed like meshing gears to achieve close packing. In contrast, there is no space between the hydrogen bonded networks of the sheet formed by molecules **2-5** and all the non-polar alkyl chains point away from the polar hydrogen bonded networks. Although there are slightly periodic fluctuations, no gap or groove occurs on the surfaces of the sheets formed by molecule **2-5**.

A close examination of the sheets formed by molecules **2-5** reveals that each tricarbamate molecule connects with two neighbors by four amide hydrogen bonds leading to a supramolecular ribbon (Figure 5). The ribbons then are glued together side by side via the other two hydrogen bonds on each molecule. Evidently, the force holding the supramolecular ribbon together is stronger than that between the ribbons due to the number of hydrogen bonds being different.

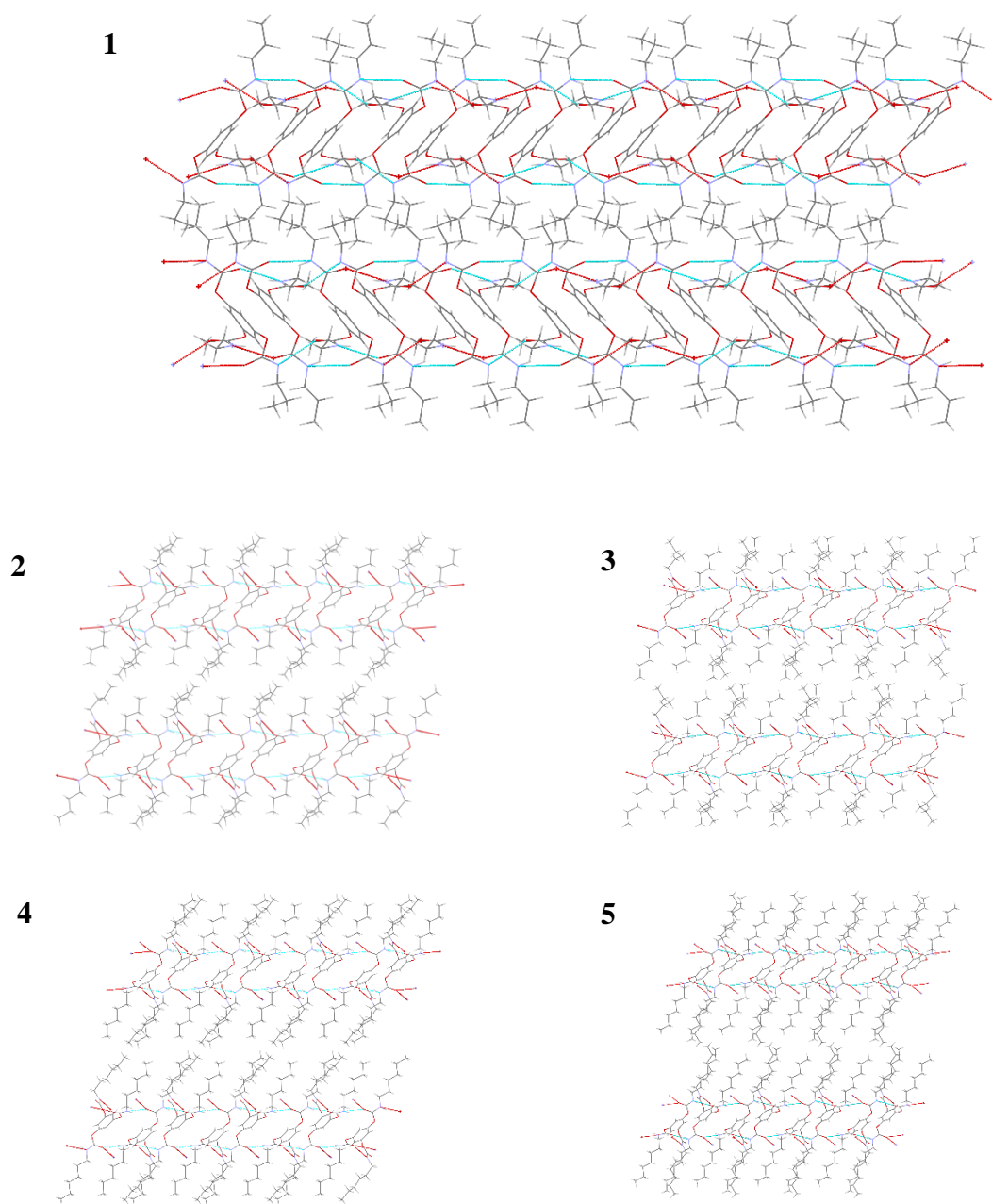


Figure 5. Crystal packing for two supramolecular polymer layers of carbamates **1-5**.

To understand the packing of the tricarbamate molecules, one can regard this new organic lamellar polymer as a hierarchical structure: the primary structure – a hydrogen bonded ribbon; the secondary structure – a supramolecular polymer sheet held together

by hydrogen bonding and the hydrophobic effect between peripheral non-polar alkyl chains; and the tertiary structure – a lamellar crystal based on London forces between the sheets.

2.5 Odd-even Effect of the Carbamates with a Similar H-bonded Network

Since compounds **2-5** possess similar hydrogen-bonded networks, the odd-even effect of them has been studied. Although their hydrogen-bonded networks from **2** to **5** are basically the same, there exists some conformational differences changing periodically. When one focuses on the unsaturated side chain, which is bound within the network through only one hydrogen bond, the shape of the side chain changes as the number change of sp^3 carbons on the side chain changes. If the number of carbons is even (compounds **2** and **4**), all the sp^3 carbons are in all-trans (zigzag) conformation. But when the number is odd (compounds **3** and **5**), the alkyl chain is twisted as shown in Figure 6. The twisted chain is derived from the gauche conformation of the carbon backbone. All four carbamates show gauche conformation when viewed along the α - β carbon axis (α carbon is the first sp^3 carbon next to nitrogen). But for the rest of the carbons in this arm, the situation is different. Compounds **2** and **4** do not display gauche conformation while **3** has two gauche conformations (Figure 6a and b) and **5** has one (Figure 6c). The difference in gauche count between **2** and **3** is two while that between **4** and **5** is one.

The second type of odd-even effect is found in the dihedral angle between the aromatic core and carbamate plane in the arm with three hydrogen bonds. Binding into the network by three hydrogen bonds, this arm has the greatest connection within the supramolecular network.

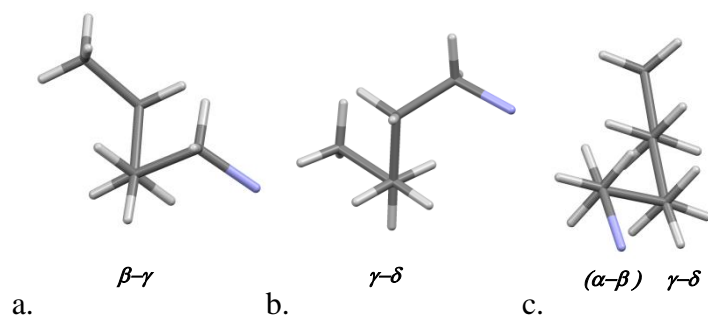


Figure 6. Side chain conformations in carbamates **3** and **5**. a) Gauche conformation in molecule **3**, view along β - γ axis. b) Gauche conformation for molecule **3**, view along γ - δ axis. c) Gauche conformation for molecule **5**, view along γ - δ axis.

The dihedral angles in **2**, **3**, **4** and **5** is 51.73° , 54.51° , 53.49° and 55.92° , respectively (Figure 7). The dihedral angle difference between **2** and **3** is 2.78° while that between **4** and **5** is 2.43° (Figure 8). For the other two arms, this effect is not observed, maybe partially due to the fact that the number of hydrogen bonds in either of these two arms is at least 30% weaker than that of the arm with three hydrogen bonds.

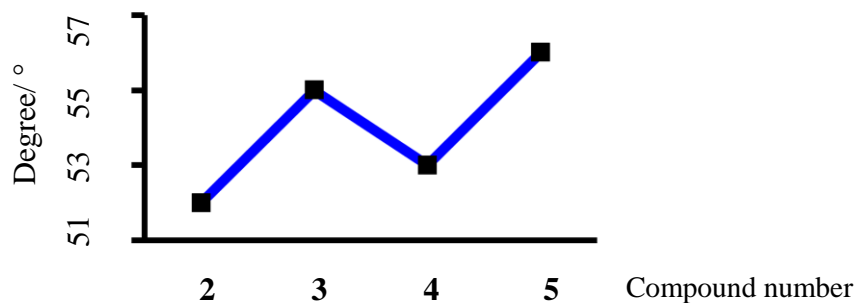


Figure 7. Dihedral angles between the aromatic core and the arm with three hydrogen bonds in carbamates **2-5**.

The third odd-even effect is reflected in the melting point. The melting points of compounds **2-5** are 130-132, 124-125, 130-131 and 127-128 $^\circ\text{C}$, respectively. The difference in melting points of **2** and **3** is 6.5°C while that of **4** and **5** is 3.0°C .

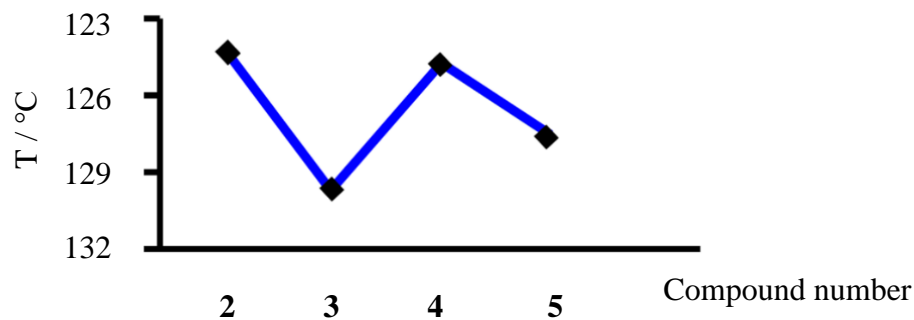


Figure 8. Melting points of carbamates 2-5.

It is believed that as the length of alkyl chain increases, the odd-even effect is supposed to decrease because the flexibility enables long chains to adopt a configuration that avoid steric problems. Consequently, the overall energy difference between two neighboring numbered molecules is gradually decreasing.

2.6 Organogelators Derived from Carbamates 7-11

Compounds 7-11 have the inverted carbamate group when compared to carbamates 1-5. Although these inverted carbamates do not form good crystalline solid for single-crystal XRD analysis, some of them form organic gels. Their high solubility makes it easy to test the gelation properties. The gelation capability of this group of tricarbamates were tested with different solvents. The result of gelation is shown in Table 2.

Table 2. Gelation capability of carbamates 7-11 in *n*-dodecane (20 g/L).

7	8	9	10	11
Suspension	Suspension	Partial gel	Partial gel	Solid gel

In a typical concentration of 20 g/L (2.6×10^{-2} M) in *n*-dodecane, with the increase of the alkyl side chain length, their solubility in *n*-dodecane increases accordingly. The partial organogels of **9** and **10** show high viscosity, but cannot pass the vial inversion test. As the alkyl chain length is further increased, the solid gels form quickly and hold their positions when the vials are turned upside down. As shown in Figure 9, organogel **11** lose about 5% of *n*-dodecane solvent during the vial inversion test, it is able to immobilize the solvent.



Figure 9. Carbamates **7-11** at 20 g/L (2.6×10^{-2} M) in *n*-dodecane.

Supramolecular polymers can potentially be used as organogelators. The gelation process of organogelators is thermo-reversible: small molecules self-assemble into three-dimensional supramolecular networks that entrap solvents by surface tension. Despite the fact that many efforts have been made to fully understand the mechanism and establish guidelines for the rationally design of organogelators, many novel organogelators have been found by serendipity rather than design.⁵⁵⁻⁵⁸ Models for supramolecular structures of

the aggregates have been proposed, but the true nature of the aggregation phenomenon is still under investigation.⁵⁹⁻⁶⁴

2.7 Conclusions

In this project, I study a new supramolecular polymer produced from three-fold symmetric tricarbamates with different alkyl side chains. A number of three-fold symmetric carbamates have been synthesized, characterized, and their self-assembly structures were examined. Their supramolecular structures are proved to be held together by hydrogen bonded network. Three different types of hydrogen bonded sites are found on these carbamate groups: unsaturated, saturated and oversaturated. Together with a number of our reported^{13,53} 2D saturated hydrogen bonded networks, the discovery of the unsaturated hydrogen bonded sheet further demonstrates the variety and adaptability of the sheet structures. The odd-even effect of those carbamates with similar hydrogen bonded networks is also observed in terms of the conformation of alkyl side chain, crystalline melting temperature, and dihedral angle between aromatic core and the arm with oversaturated hydrogen bond. Organogelators have been successfully made from the inverted carbamates, which are originally designed to make column-like supramolecular polymers. It turns out that the inverted carbamates with longer alkyl chain have better solubility and are more likely to form organic gels in *n*-dodecane.

CHAPTER 3

A POTENTIAL BUILDING BLOCK FOR FURFURAL-BASED POLYMERS

3.1 Goals of the Study

Since furfural is a commonly used bio-based chemical,⁶⁵⁻⁶⁷ I want to develop an easy, inexpensive, and green way to synthesize a dicarboxylic acid, which could be used as a polymer building block, from this aldehyde. The reaction to synthesize **12** was initially studied by Schmidt and provided a yield of 51% and reaction time was a month.³⁴ Besides the unreacted starting material, the main impurity was from the formation of oligomers. In the past decades, due to the low yield of **12** and long reaction time of this reaction,^{68,69} the follow-up development appeared to be impossible. Thus, few studies have been performed with **12**.⁴¹⁻⁴³ Our group recently developed the above-mentioned method to synthesize this 100% bio-based chemical with near quantitative yield.

Besides simple filtration, no follow-up purification work is needed. This breakthrough makes it possible to use **12** in a relatively easy and low-cost way. Meanwhile, the structural similarity (Chart 5) to phthalic acid, the monomer of the widely versatile polymer Glyptal[®], gave us a general idea about its applications.^{70,71} Thus, another furfural-based diol (1,5-pentanediol) and glycerol were chosen to combine with our monomer to make 100% bio-based polymers (Scheme 3).

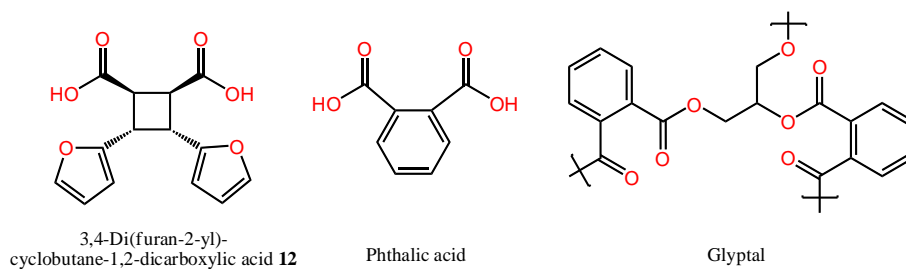
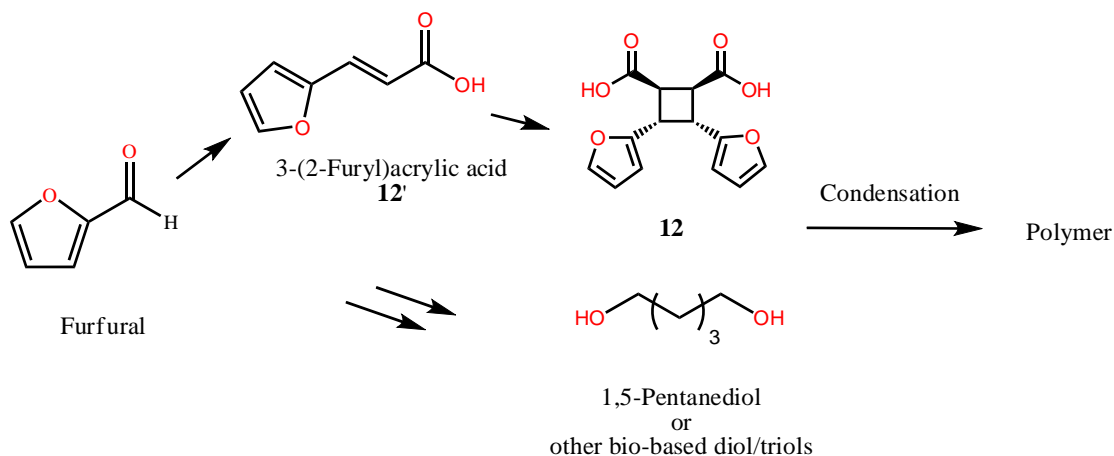


Chart 5. The structure of 3,4-di(furan-2-yl)cyclobutane-1,2-dicarboxylic acid **12**, phthalic acid, and glyptal.

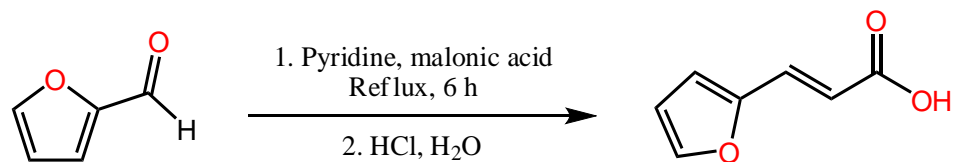


Scheme 3. General synthetic route about the furfural-based polymer in this study.

3.2 Synthesis and Characterization of the Furfural-derived Monomer

3.2.1 Synthesis of Monomer **12** and its Precursor **12'**

The synthesis of **12'** is shown in Scheme 4. A modification of Knoevenagel condensation is employed in which malonic acid was treated with commercially available furfural in the presence of pyridine. Thus, compound **12'** can be synthesized directly from furfural with high yields (>90%).⁷⁸ The distance between parallel C=C double bonds in 3-(2-furyl)acrylic acid (**12'**) crystals are 3.73 Å, which makes them good candidates for [2+2] photosynthesis (Figure 10).



Scheme 4. Synthesis of the furfural-based carboxylic acid **12'**.

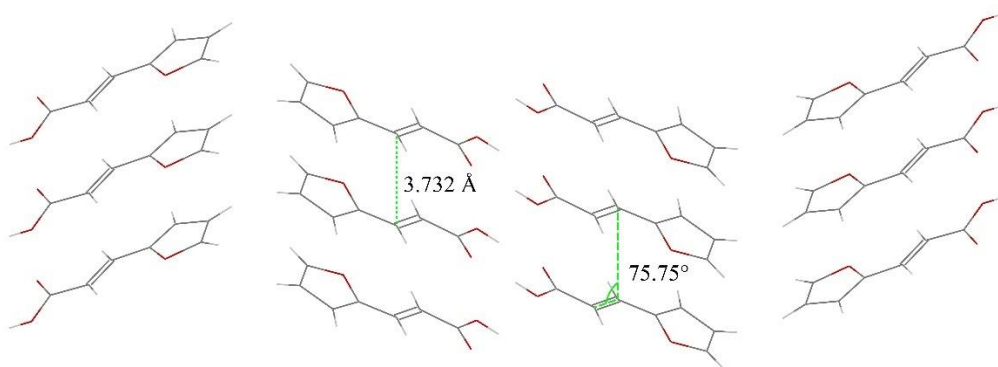


Figure 10. Crystal structure of 3-(2-furyl)acrylic acid **12'**.

Compound **12** is readily synthesized in multi-gram scale in solid state. The wavelength of UV irradiation source is the key to obtaining a high yield. The UV-Vis (Figure 11) spectra shows that the major absorption lies in the UV-A range. In solid state, it shows a broader peak than it does in the solution, and the peak shifts to longer wavelength range.

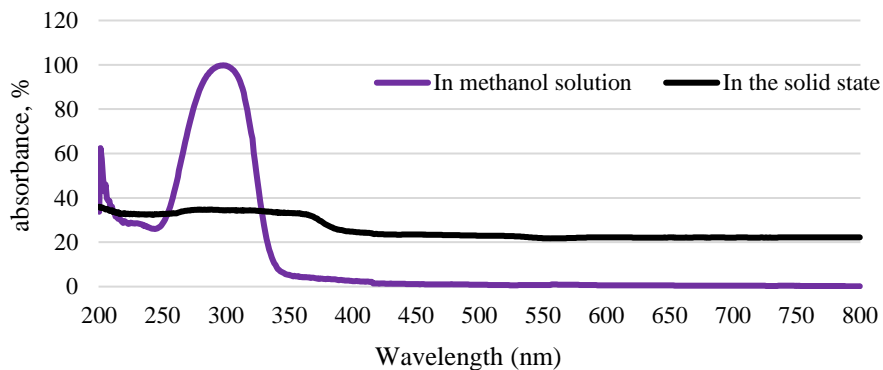
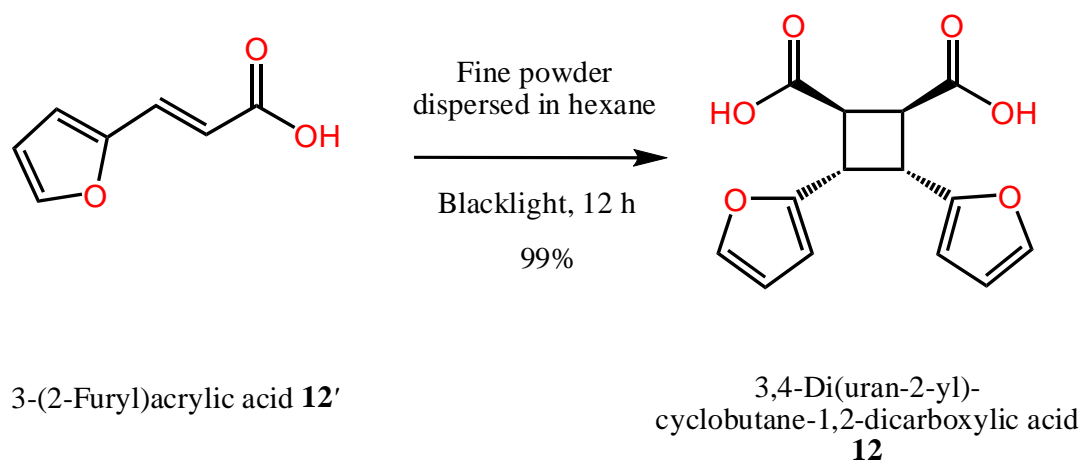


Figure 11. The UV-Vis spectra of **12** in the solid state and in MeOH solution.

When a mercury lamp is used as the irradiation resource, oligomers always occur. I assume that the C=C double bonds in the furan ring may absorb the low wavelength UV, which is emitted by the mercury lamp, then undergo [2+2] photoaddition between furan rings. Schmidt also observed this phenomenon when he applied irradiation from mercury lamp or sunlight to this crystalline solid.³⁹ However, I find that this side reaction can be inhibited when a blacklight, which emits long-wave (UV-A) ultraviolet light, is applied (Scheme 5).



Scheme 5. Synthesis of furfural-based monomer **12**.

Particle size is a key factor to the reaction time. While the dimerization within very fine powder of **12'** can be finished in a relatively short time (12 h), the ungrounded powder increases the reaction time dramatically.

3.2.2 Crystalline Structure of **12**

For the first time, to the best of our knowledge, the single crystal of **12** was obtained. A sheet-like crystal was formed by evaporating the solution in MeOH/DCM at room temperature. The crystal structure is shown in Figure 12.

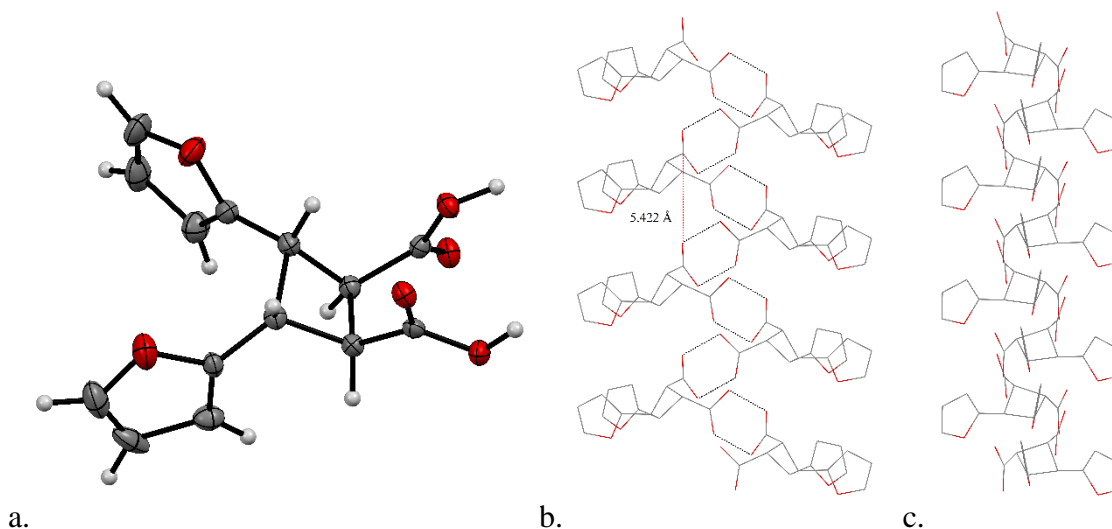


Figure 12. Image of **12** from single crystal X-ray diffraction.

The cyclobutane ring of **12** in solid state is not flat (Figure 12a); instead a 26° puckered conformation is adopted. This non-planar structure has been confirmed by ^1H NMR spectrum. Two peaks which are assigned to hydrogens on the cyclobutene ring at δ 4.05 and 3.68 ppm are split by each other, giving doublet of doublets. Two furan rings and two carboxyl groups are on opposite sides of the ring as the outcome of the solid-state [2+2] photoaddition. The front view of the repeating unit is presented in Figure 12b. Two carboxylic groups in a molecule are pointing to different directions, which forms a supramolecular helix supported by a hydrogen bond. The height of each spiro-circle is 5.42 Å. When watched from the side view (Figure 12c), the helix is more clear to see.

3.2.3 Photo, Thermal, and Chemical Stability of **12**

When I want to use **12** as a building block for polymers, researchers may have concerns on the ring strain of cyclobutanes. Particularly, is the ring stable enough to survive in polymerization or the working condition of its polymer? Theoretically, when a

cyclobutane ring is generated from two alkenes, the process is photo-allowed and thermally forbidden. The reversion process (ring opening) follows the same rule as well. Practically, after the examination, the cyclobutane ring is proved stable under sunlight and thermal condition. The ring formation usually happens at the longer wavelength UV due to the relatively large conjugated system. The ring opening usually occurs at lower wavelength UV range because of the disappearance of conjugation. Thus, when under the sunlight that contains all wavelength UV irradiation, no reverse reaction can happen.

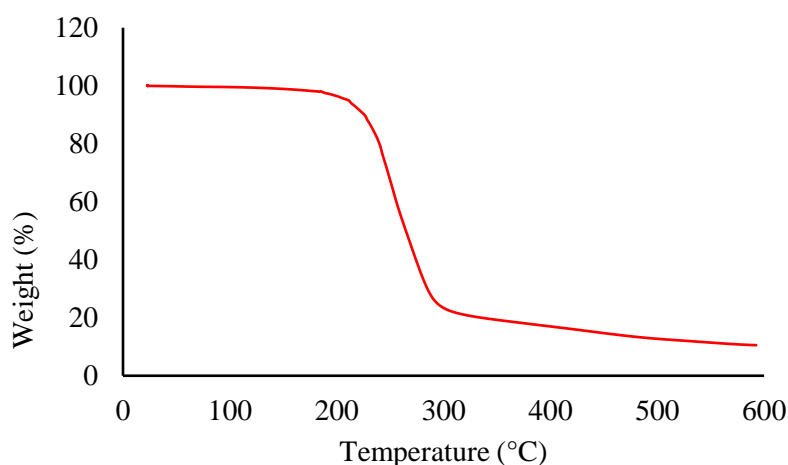


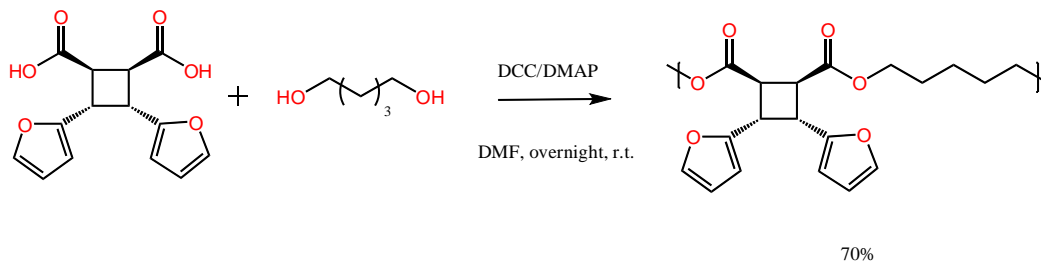
Figure 13. TGA curve of **12**.

As expected, the powder of **12** shows no change in ^1H NMR spectrum after exposure for 1 month to sunlight irradiation. The TGA curve shows no degradation below 200 °C (Figure 13). When monitored by ^1H NMR spectroscopy, the powder sample shows no degradation after 30 days of heating in the air at 100 °C. Acidic resistance of **12** is tested by adding 30 mg of fine powder of **12** to 30 mL of 6 M HCl aq. solution. The solution is stirred rapidly overnight. After filtration, the ^1H NMR test remains the same

with that of the original starting material. (All spectra involved in photo, thermal, and chemical stability are attached in the appendix).

3.3 Polymerization and Detection of **12**

Compound **12** contains two carboxyl groups that makes it a potential starting material for polyesters and polyamides. In particular, if bio-based diols or glycerol are introduced into the polymerization, then 100% bio-derived polymers can be made by this method. As a proof-of-concept, the condensation of **12** and 1,5-pentanediol was evaluated in this study. The Steglich esterification was carried out in DMF (Scheme 6).



Scheme 6. Synthesis of the polymer from **12** and 1,5-pentanediol.

^1H NMR (Figure 39) and $^{13}\text{C}\{^1\text{H}\}$ NMR spectra (Figure 40) in the appendix show the formation of the target polymer. Broad peaks occur at the position where the original peaks were located, indicating that the hydrogens or carbons now are still in a similar yet slightly different chemical environment. This may be due to the formation of polymer chains with different length or even the formation of some macrocyclic molecules.

3.4 Conclusions

In this study, a relatively inexpensive and green synthesis for a 100% bio-based monomer 3,4-di(furan-2-yl)cyclobutane-1,2-dicarboxylic acid has been developed. For

the first time its crystal structure is revealed. The monomer is photo, chemically and thermally stable. The monomer is stable under sunlight irradiation, after 1-month heating at 100 °C, and in 6 M HCl aq. solution. At last, a proof-of-concept non-petroleum dependent polymer is successfully synthesized.

CHAPTER 4

BUILDING BLOCKS FOR DOUBLE-STRANDED POLYMERS

4.1 Goals of the Study

Strong and light materials (SLIM) are highly desirable in engineering plastics.⁷²⁻⁷⁴ However, the challenge lies in enhancing the strength of a polymer without simply increasing the physical dimension or sacrificing its flexibility.^{75,76}

Our goal is to synthesize a linear polymer with double-stranded chains. The two strands will be linked by a C-C single bond so that the strength of the polymer is enhanced. To achieve this goal, a three-step strategy has been proposed (Chart 6).

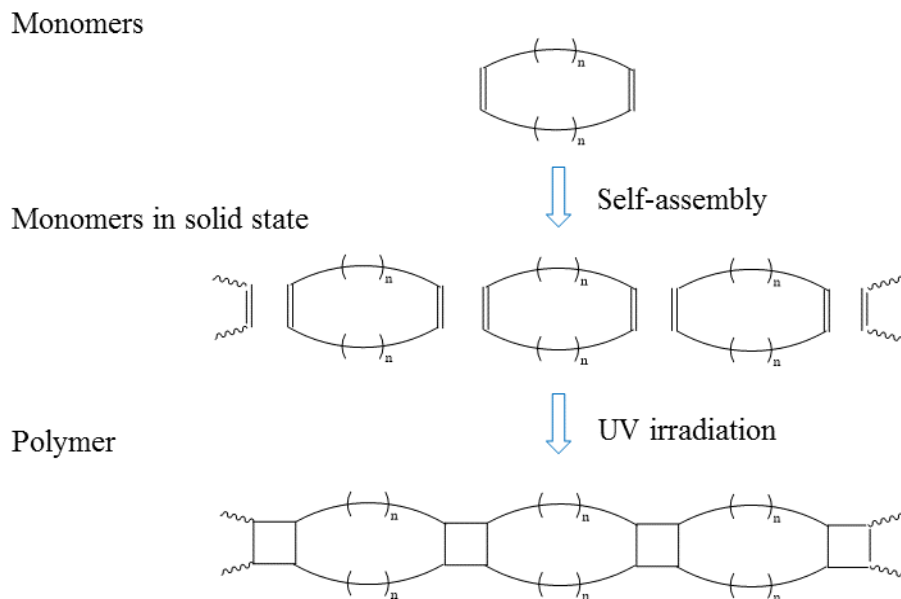


Chart 6. The proposed three-step preparation for double-stranded polymers.

The goal of the first step is to synthesize a cyclic monomer with a C=C bond at each end of the molecule. The second step is to apply intermolecular interactions for self-assembling the monomer. When desirable crystalline packing is obtained, the third step is to generate cyclobutane rings between each neighboring C=C bond by solid-state [2+2] photocycloaddition to form the target polymer.

4.2 Synthesis of the Monomers

Since our target molecule is symmetric, three possible synthetic routes have been proposed (Chart 7). The first one is to cut the target molecule horizontally (Route A). Then the next step is to synthesize a linear molecule with two terminal alkenes. Following this, an alkene metathesis reaction is needed to form the cyclic target molecule.

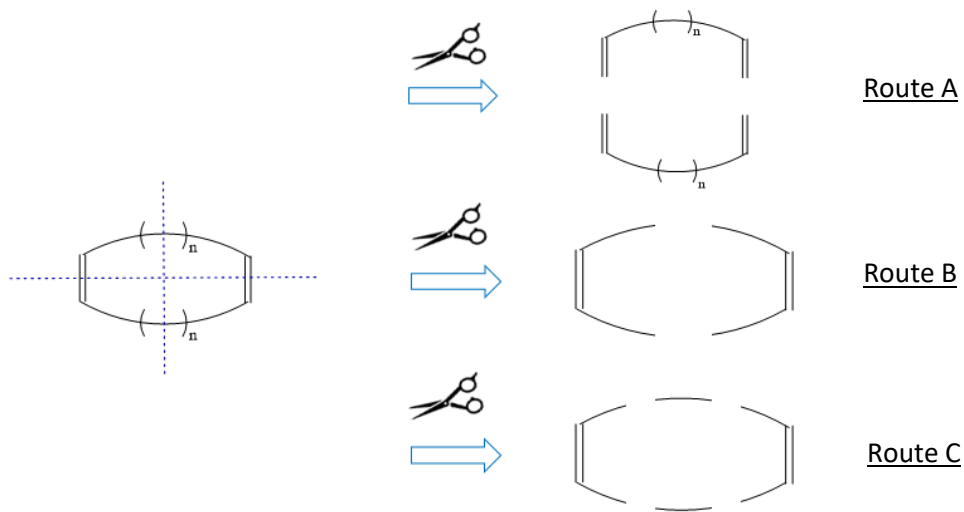


Chart 7. General designs of the monomer synthesis for the double-stranded polymers.

The second route is to cut the target vertically (Route B). The two identical pieces should be capable of reacting with each other to form the target cyclic monomer. C-C coupling is also an option.

The third plan is to cut the target molecule vertically into three parts (Route C). In this plan, a symmetric diacid with a C=C bond in the middle can be used as one of the starting materials. A diol molecule can be used as the other. Thus, a simple condensation reaction is all that is needed to assemble the target polymer. Considering the cost of raw materials and ease of implementation, Route C was chosen.

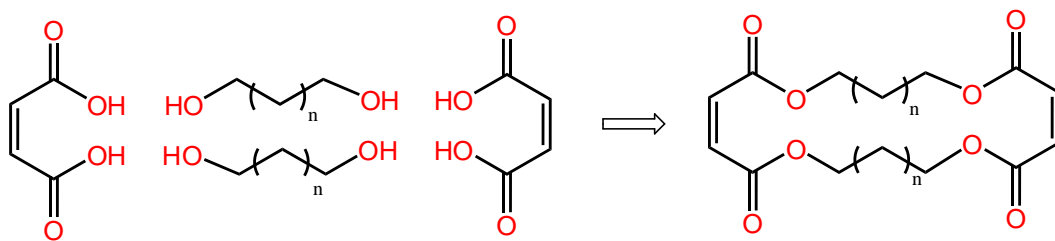
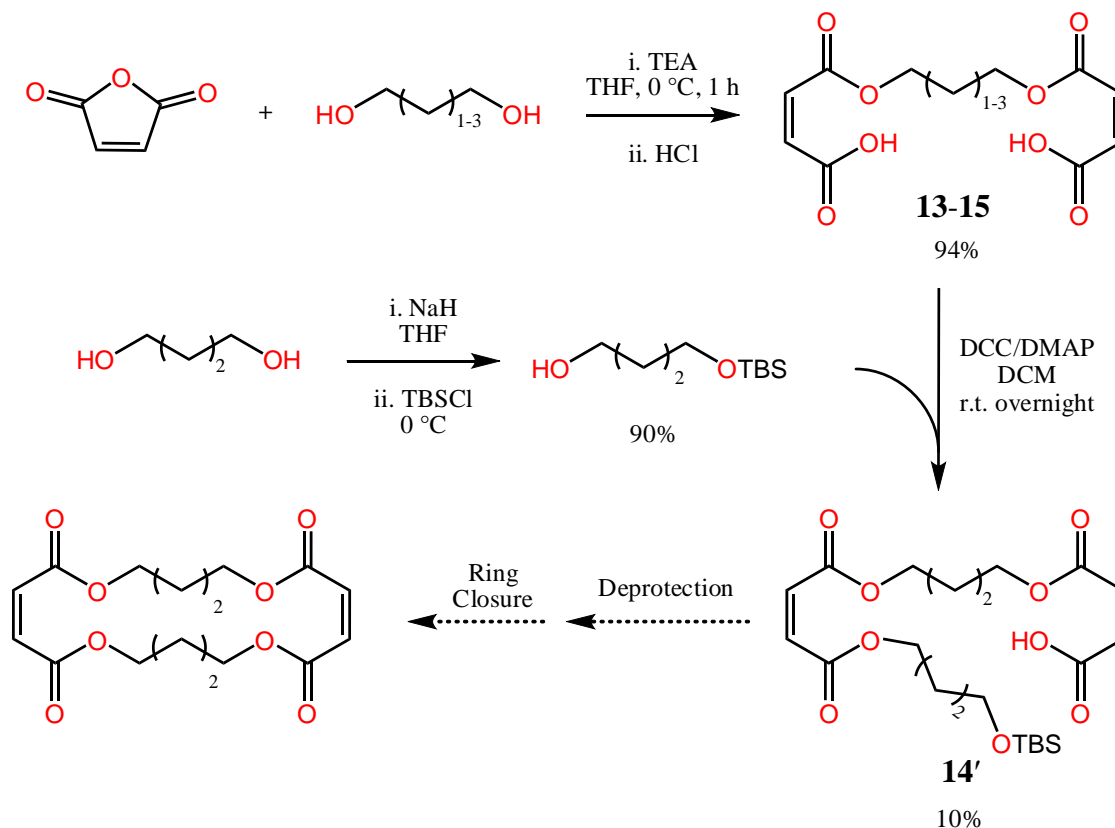


Chart 8. The starting materials chosen for monomers.

As shown in Chart 8, maleic acid or maleic anhydride are selected as the starting diacids. 1,3-Propanediol, 1,4-butanediol, and 1,5-pentanediol are chosen as the starting diols for monomer synthesis.

To synthesize the monomer, three different synthetic routes have been tried. In Route 1 (Scheme 7), maleic anhydride reacts with article diol to get the cis,cis-diacids **13-15**, which are different in alkyl chain length in the middle. One of the two hydroxy groups in 1,4-butanediol needs to be protected with a TBS group. Then the monoprotected 1,4-butanediol is reacted with **14** by Steglich esterification to afford

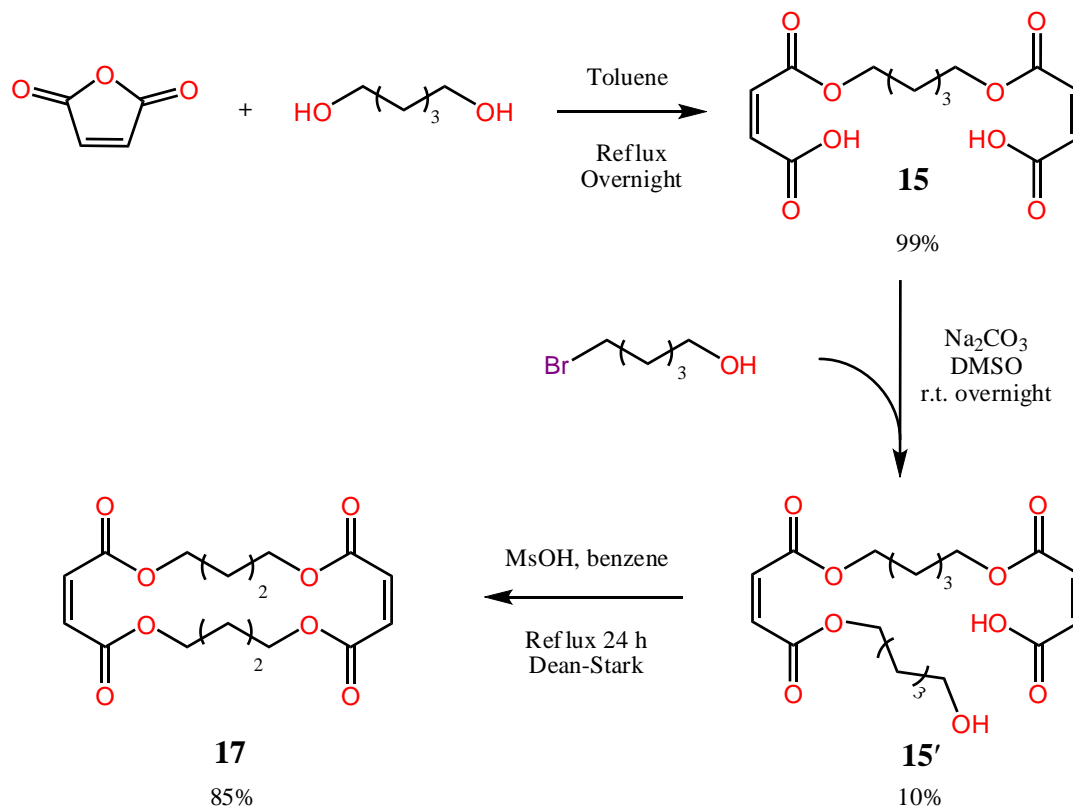
compound **14'** with 10% yield. Considering that a deprotection and a ring closure reaction are needed, and the yield is not satisfying, this synthetic route has been abandoned.



Scheme 7. Synthetic Route 1 of double-stranded polymers from cyclic monomers.

The second route (Scheme 8) develops the synthesis of **13-15**. Instead of using TEA as a catalyst and base, maleic anhydride and diols are reacted directly with reflux in benzene overnight. With this modification, the yield increases by 5% and the process is simplified. The diols are replaced with 5-bromopentan-1-ol. It reacts with **15** to give (Z)-4-{5-[(Z)-4-(5-bromopentyloxy)-4-oxobut-2-enoyloxy]pentyloxy}-4-oxobut-2-enoic acid (**15'**) in 10% yield. Compound **15'** undergoes the ring closure reaction by losing a molecule of water. MsOH is used as the catalyst and a Dean-Stark apparatus is applied to remove water. The key to this reaction is to maintain a low concentration of **15'**.

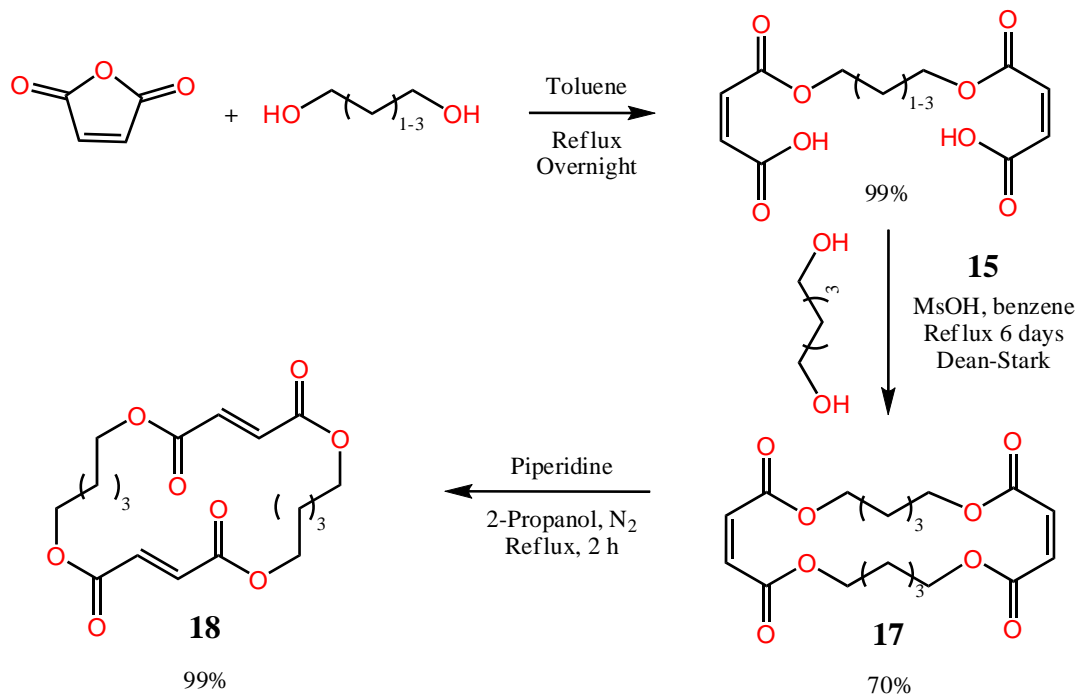
Otherwise, a linear polymer would form in a large amount and significantly lower the yield for our target molecule. After refluxing the mixture for 24 h, compound **17** is isolated in 85% yield.



Scheme 8. Synthetic Route 2 of double-stranded polymers from cyclic monomers.

The synthetic route has been further explored in another attempt (Scheme 9). The synthesis of **17** from **15** is successfully simplified to a single step. When starting materials are added into the reaction every hour, compound **17** can be synthesized during a period of six days. Recrystallization is used to purify the product **17** with a 70% yield. Each oxygen atom connected to the alkyl chain in compound **17** has two lone pairs of electrons, when the two oxygen atoms are close to each other, they may encounter steric problems preventing them from staying in the same plane. This may cause problems in

the self-assembly process, so its trans-trans isomer **18** was synthesized. The isomerization can be performed in a single step as shown in Scheme 9.



Scheme 9. Synthetic Route 3 of double-stranded polymers from cyclic monomers.

4.3 Self-assembly of the Monomers

The next step after the synthesis of **17** is to obtain the desirable crystal packing of the monomers. Based on Schmidt's rule,⁷⁷ if two C=C bonds are expected to react in solid state, they should be parallel and within a distance of 4.2 Å. In our case, if a polymer chain is expected to form, the C=C bond on the 'beginning' side should match the rule with the C=C bond on the 'ending' side in the neighboring molecule as shown in Chart 9.

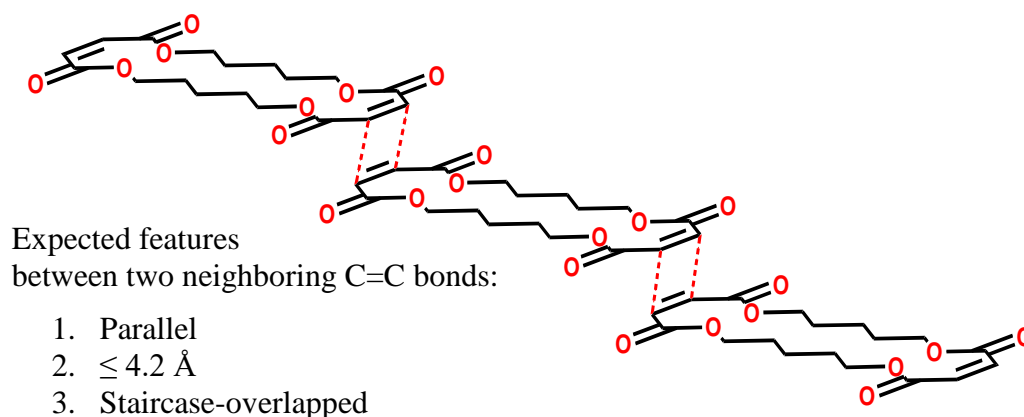


Chart 9. The crystal packing expected to form a polymer.

Both crystalline compounds **17** and **18** are obtained in good quality from a series of solvents by evaporation. The single crystal structure of **17** was examined by SCXRD. Evaporating the solution of **17** in THF, ethyl acetate, CH_3CN , and $\text{CH}_2\text{Cl}_2/\text{MeOH}$ affords crystals with the same packing (Figure 14).

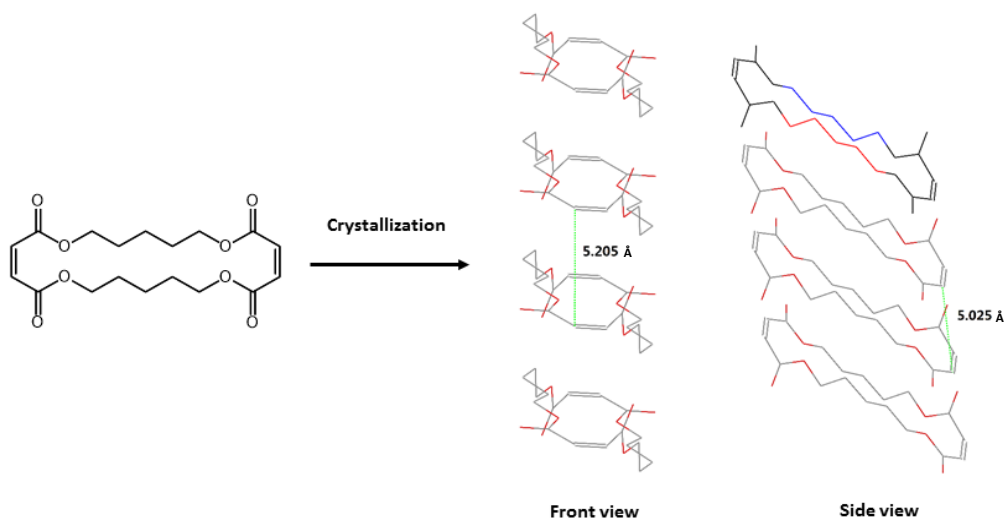


Figure 14. Single crystal structure of **17**.

The distance between two neighboring C=C bonds is 5.025 \AA , which is too far away for the [2+2] photocycloaddition to occur. The staircase overlap does not match the

criteria either. As predicted, the two oxygen atoms connected to the alkyl chain face a steric problem staying on the same plane. Consequently, one of the alkyl chains in the molecule is tilted. Given these facts, the molecule **17** in this packing is not suitable for our designed polymerization.

Samples for powder XRD tests are obtained from recrystallization in ethyl acetate and used directly without further treatment. This spectrum basically matches the powder pattern calculated by the Mercury software based on the data of the single crystal structure of **17** (Figure 15). The unmatched peaks around 10.3° and 14.3° may belong to other crystalline forms of this compound.

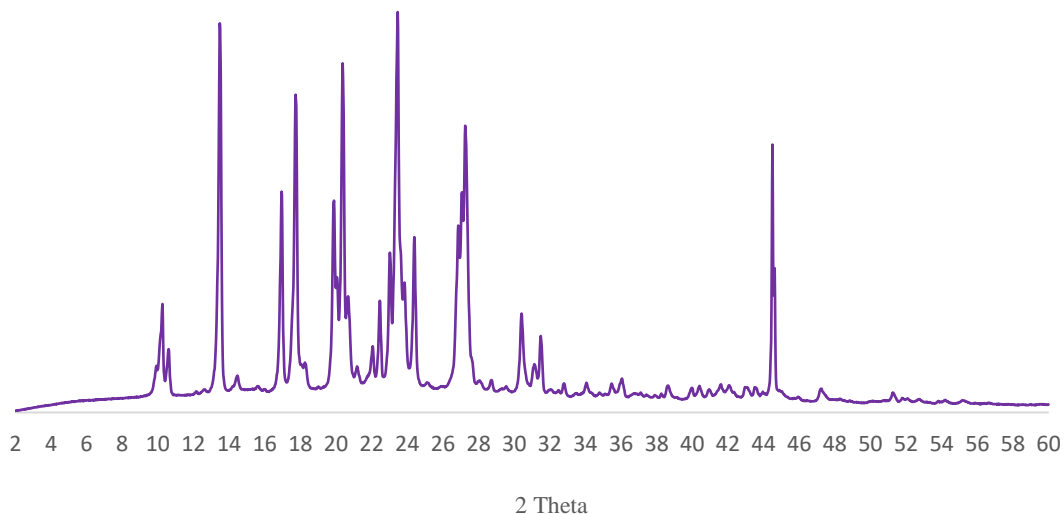


Figure 15. Powder XRD of **17**.

The single crystal structure of **18** was examined by SCXRD and solved (Figure 16). The same packing has been found in the crystals that are grown from the solution of THF, EA, and $\text{CH}_2\text{Cl}_2/\text{MeOH}$.

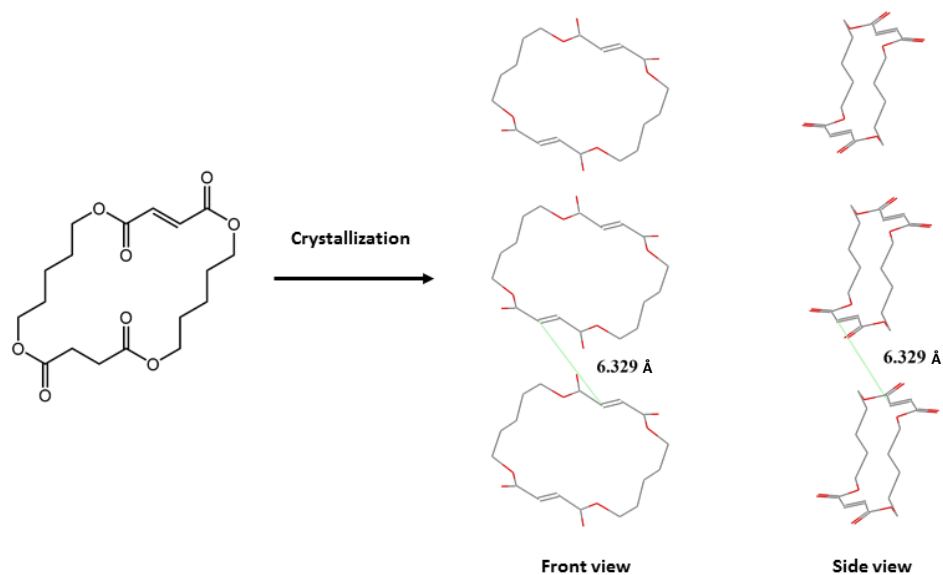


Figure 16. Single crystal structure of **18**.

The distance between two neighboring C=C bonds is 6.329 Å, which is greater than 4.2 Å. Although the two double bonds are parallel to each other, their orbitals do not have overlap. As predicted, there are no longer any steric problems associated with the oxygen atoms because of their trans position. Due to the large conjugation, the C=C bond lies in a planar environment. Usually, a flat section is required for two molecules to get close in crystalline form. Thus, at least this is a good sign for further modification. However, the molecule **18** in this packing is not suitable for our designed polymerization.

The sample for powder XRD test was obtained by cooling down 2-propanol in the cis-trans isomerization step. The powder was detected directly without further treatment. The spectrum matches the theoretical prediction very well, which also indicates that the crystal form shown above is the dominating form for compound **18**. The powder XRD spectrum is shown in Figure 17.

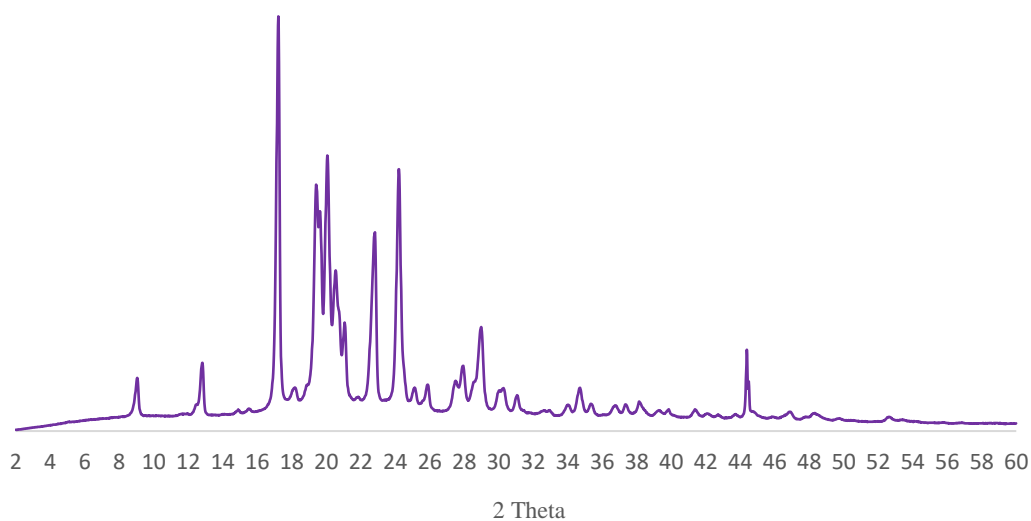
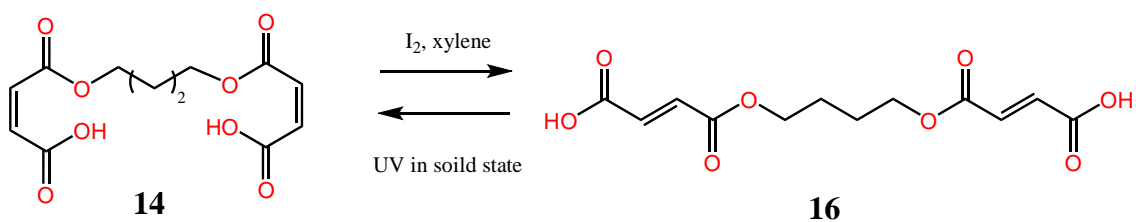


Figure 17. Powder XRD of **18**.

4.4 Cis-trans Isomerization of the Monomers

The cis-trans isomerization has been found in both our monomers and their precursors. The reaction of **14** is shown in Scheme 10. I_2 is used as a catalyst to convert the cis conformation to trans. Xylene is used as the solvent for reflux. It has a relatively high boiling point at 138 °C, which allows the isomerization to occur. When benzene is used with reflux overnight, there is no reaction. Different from the thermoreaction in solution, the backward reaction in the solid state from **16** to **14** is observed after mercury lamp UV irradiation for 6 h.



Scheme 10. Cis-trans isomerization of **14**.

The cis to trans isomerization is clean and provides a quantitative yield. All the peaks of the hydrogens in the cis isomer shift downfield when it is converted to the trans isomer (Figure 18). The trans to cis isomerization happens under photo-condition. An approximate yield of 90% was obtained (Figure 19). The main impurity is identified to be the unreacted cis isomer **14**.

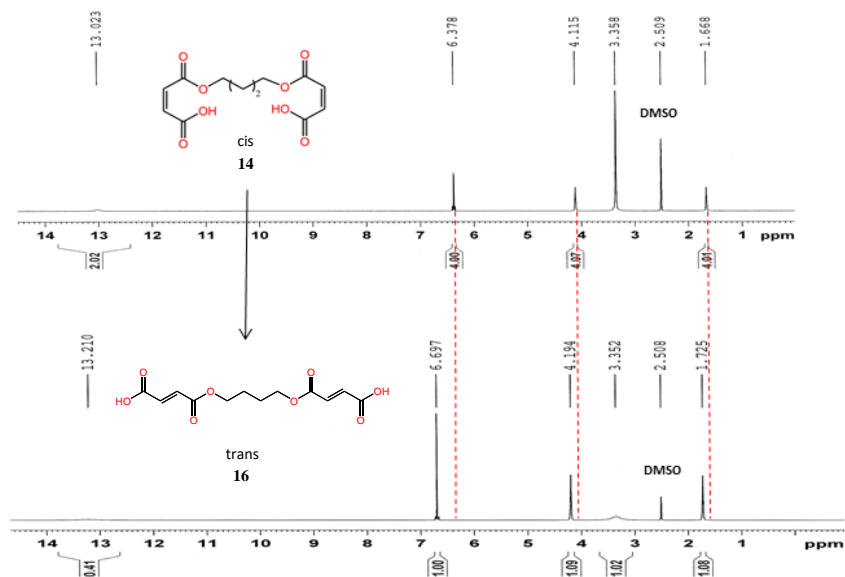


Figure 18. ^1H NMR (CDCl_3) spectra of **14** and **16**.

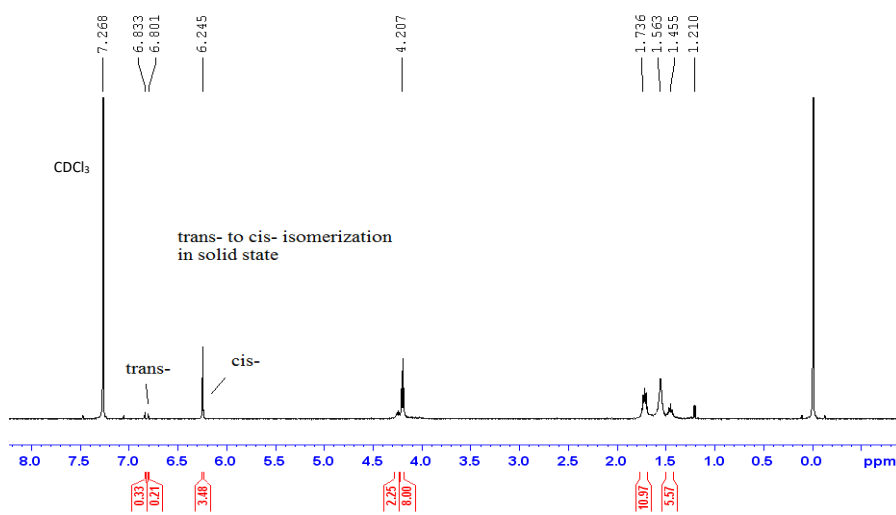
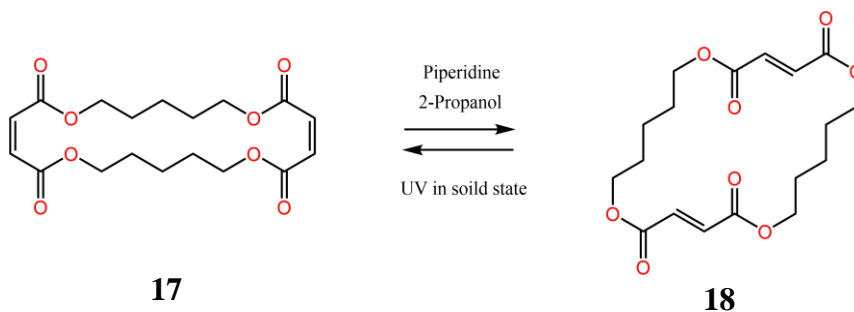


Figure 19. ^1H NMR (CDCl_3) spectrum of **16** after UV irradiation.

Similar to the result of **14** and **16**, the isomerization between **17** and **18** is achieved in a very good yield (Scheme 11 and Figure 20). More than 90% of **17** can be recovered from a single cis to trans and trans to cis cycle. In this case, the combination of I₂ and xylene does not work. Instead, piperidine and 2-propanol should be used.



Scheme 11. Cis-trans isomerization of **17**.

This isomerization happens in both solution (cis to trans) and solid state (trans to cis). In the solid-state reaction, I find the product half-melted after UV irradiation even though the reaction temperature is significantly lower than its melting point.

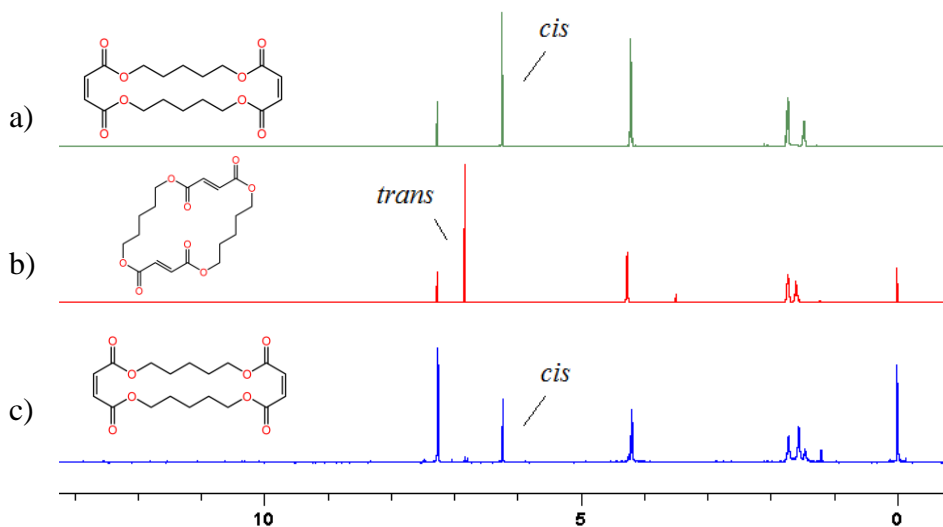


Figure 20. ¹H NMR spectra of the compounds **17** and **18** in cis to trans and trans to cis isomerization. a) The cis isomer **17**. b) The crude product of the trans isomer **18** obtained after cis to trans isomerization in solution. c) The crude product of cis isomer **17** from trans to cis isomerization in the solid state.

A possible explanation is that when some trans molecules on the surface are converted to cis molecules, the crystal is no longer pure. The appearance of cis isomers in the crystalline lattice disrupts the repeating pattern of forces that hold the solid together. This allows for part of the solid to melt at temperature in the photoreactors. The melted mixture of cis and trans isomers possibly further react to form a cross-linked polymer.

4.5 Synthesis of the Polymers

The polymerization has been tried in solution. The selection of solvent relies on the UV spectra of the cis isomer **17** and trans isomer **18** (Figure 21). A solvent is usually preferred when it does not absorb UV light within the range that the isomers do. Based on the UV absorbance spectra of common solvents, hexane is selected.

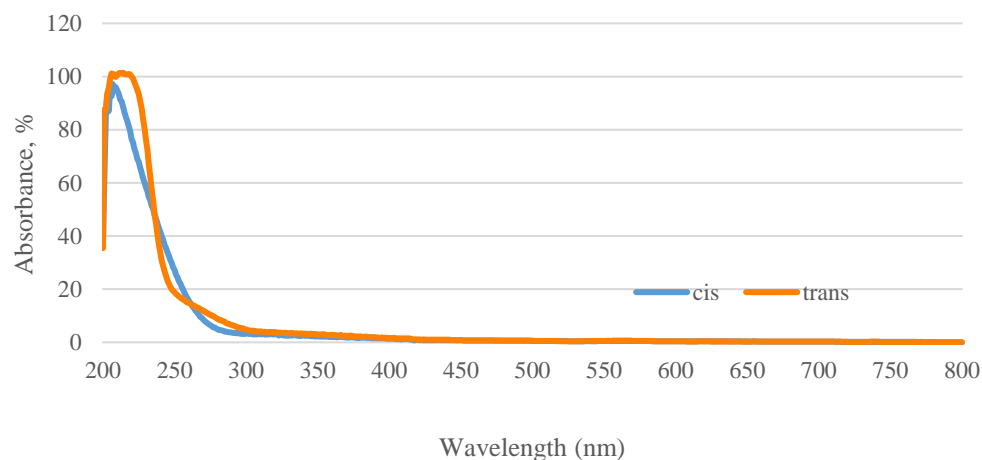


Figure 21. UV spectra of the cis isomer **17** and trans isomer **18** in hexane.

A saturated hexane solution of **17** was left under mercury lamp UV irradiation overnight with argon protection. A white solid formed at the bottom of the flask. The fluffy solid was not soluble in common organic solvents including acetone, acetonitrile,

benzene, MeOH, EtOH, chloroform, DCM, diethyl ether, hexane, EA, THF, DMSO, DMF and water. There is no peak in the NMR spectrum due to the poor solubility. To increase the productivity, a 5 g scale reaction was performed by making a slurry of **17** in hexane. The product image is shown in Figure 22.

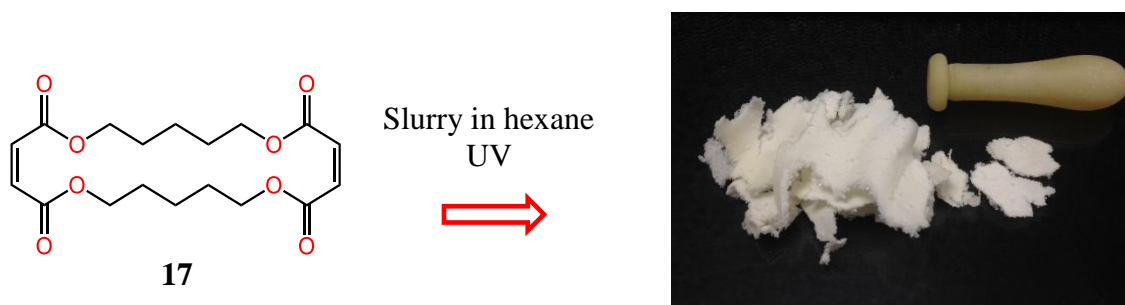


Figure 22. The image of product obtained from polymerization trial.

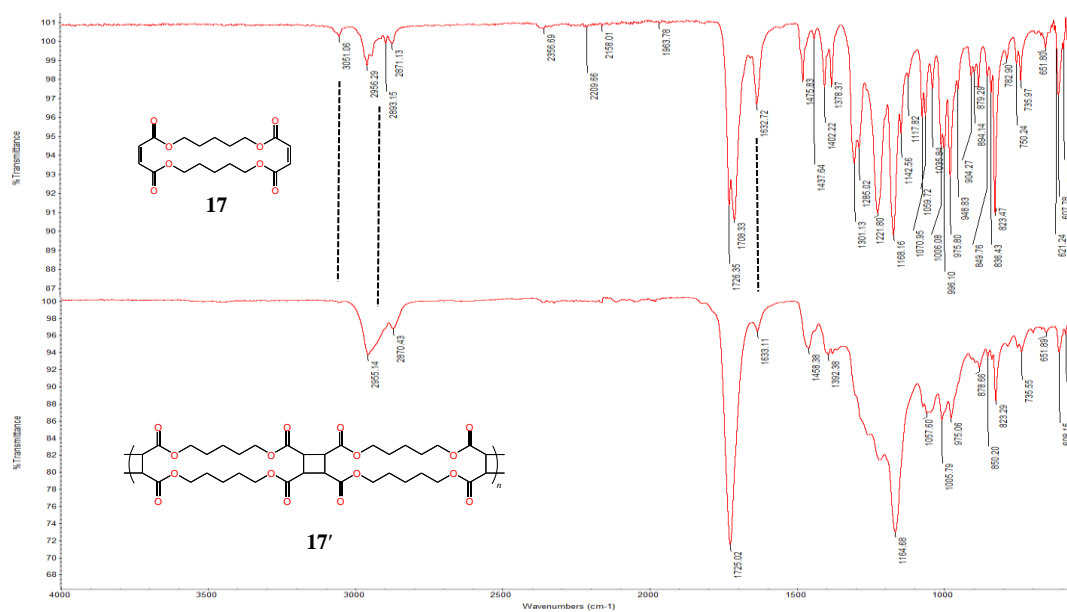


Figure 23. IR spectra of monomer **17** and its polymer **17'**.

After polymerization, the peak at 3051 cm^{-1} , which is assigned to vinylic C-H stretching in molecule **17**, is not shown in the spectrum of **17'** (Figure 23). Meanwhile,

peaks from alkane C-H stretching ($2870\text{-}2960\text{ cm}^{-1}$) become broader and the peaks from C=C bond stretching at 1632 cm^{-1} become smaller than those in the spectrum of **17**. These changes indicate the disappearance of C=C bond and the formation of new C-C bonds.

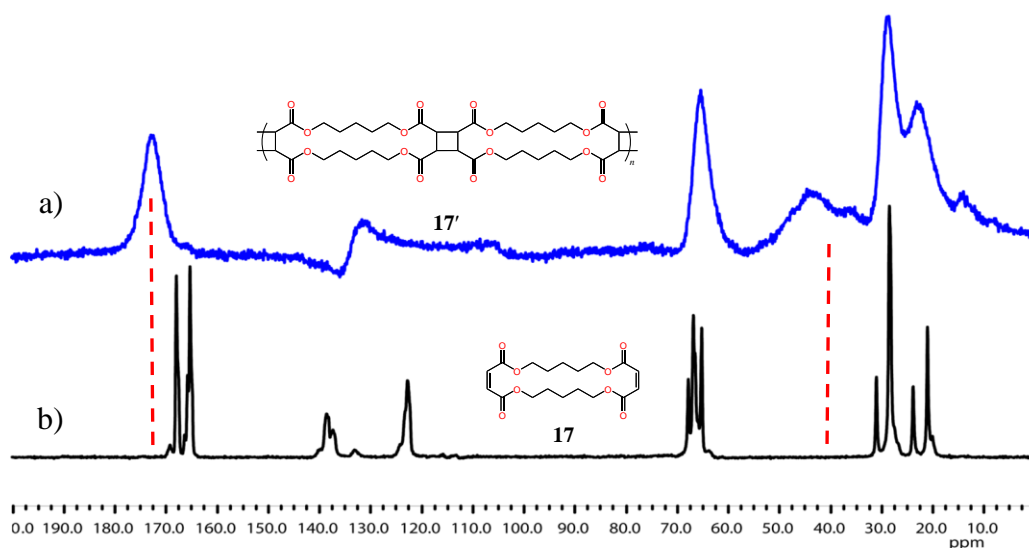


Figure 24. Solid state $^{13}\text{C}\{^1\text{H}\}$ NMR spectra of monomer **17** and polymer **17'**. a) The spectrum of polymer **17'**. b) The spectrum of monomer **17**.

The result from solid state $^{13}\text{C}\{^1\text{H}\}$ NMR spectra further support the conclusion drawn from IR spectra. The peaks from the carbons in C=O bonds, which are adjacent to C=C bonds, shift downfield from 165-167 ppm to around 173 ppm after polymerization. This change signifies a loss of conjugation, in this case, due to the [2+2] photoaddition. The rise of a new peak in Figure 24a around 40 ppm suggests the creation of sp^3 carbons. It agrees with the formation of cyclobutane rings during the polymerization.

4.6 Conclusions

1,6,12,17-Tetraoxacyclodocosa-3,14-diene-2,5,13,16-tetraone **17**, a functional symmetric building block for a double-strand polymer is successfully synthesized. The

key for reaction is to maintain a low concentration for the ring closure step. This cis isomer can be easily converted to the trans isomer with a yield of 99%. These novel building blocks and their intermediates have been thoroughly characterized by UV-Vis, FT-IR, NMR, powder XRD, and single crystal XRD. The proof-of-concept polymerization has been tried and the formation of a double-strand polymer is confirmed by IR and solid-state $^{13}\text{C}\{^1\text{H}\}$ NMR spectra.

CHAPTER 5

EXPERIMENTAL SECTION

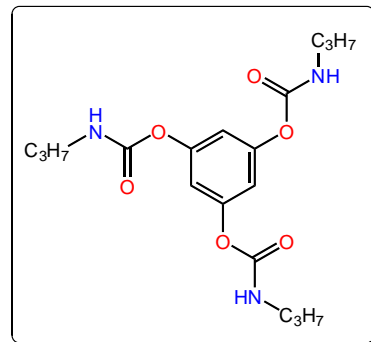
5.1 General Procedure and Instrumentation

All starting materials were obtained commercially and used as received. All moisture-sensitive reactions were run under argon. THF was distilled from CaH₂ before use. Analytical TLC was performed on silica G TLC plates w/UV254 (Sorbent Technologies). Column chromatography was carried out on silica with 230-400 mesh particle size. ¹H and ¹³C{¹H} NMR data were collected on a Bruker ADVANCE 500 MHz spectrometer and processed with its self-bond software. Proton and carbon chemical shifts were reported in ppm downfield from tetramethylsilane (TMS) or using the resonance of corresponding deuterated solvent as an internal standard. ¹H NMR data were reported as follows: chemical shift (ppm), s = singlet, d = doublet, t = triplet, q = quartet, dd = doublet of doublets, m = multiplet, coupling constant (Hz), and integration. IR spectra were acquired on a Thermo Scientific Nicolet iS5 FT-IR spectrometer. Electrospray ionization mass spectra (ESI-MS) were obtained on a Time-of-Flight MS SYNAPT G2/Si spectrometer (Waters Co., USA). UV-Vis spectra were recorded on a Beckman DU400 UV/vis spectrometer. Calorimetric curves were recorded on a Perkin Elmer Jade DSC at a ramping rate 10 °C/min. Heat flow was recorded from both the first heating and cooling curve. X-ray powder diffraction spectra were collected at room temperature in a 2θ range of 3°~35° at a scanning rate of 3° min⁻¹.

5.2 Synthetic Procedures

5.2.1 Synthesis of Benzene-1,3,5-triyl tris(propylcarbamate) **1**

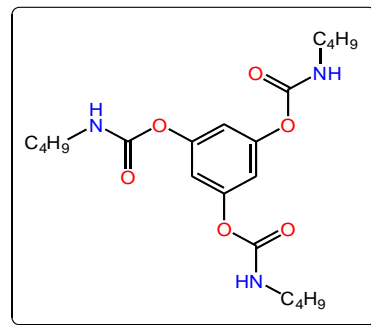
A flame-dried 50 mL round bottom flask equipped with a magnetic stir bar was charged with 1-isocyanatopropane (1.06 g, 12.5 mmol) and 5 drops of triethylamine (catalyst) in 10 mL of THF. The mixture was stirred at room temperature for 5 minutes.



Phloroglucinol (470 mg, 3.75 mmol) in 5 mL of THF was added from a dropping funnel with a rough rate of 1 drop/s. Then the solution was refluxed overnight. The mixture was concentrated in a rotavapor and precipitated in 100 mL of ice cold water. The solid product was filtered and air-dried.⁵³ The titled compound **1** (m.p. 96-98 °C) was obtained as a white solid (1.35 g, 94%). ¹H NMR (CDCl₃, 500 MHz) δ 0.95 (t, J = 7.0 Hz, 9H), 1.59 (m, 8H), 3.22 (m, 8H), 5.06 (t, J = 6.5 Hz 3H), 6.86 (s, 3H); ¹³C{¹H} NMR (CDCl₃, 125 MHz) δ 11.6, 23.4, 43.3, 112.3, 151.8, 154.2; IR (Nujol, ν , cm⁻¹) 3306, 3108, 2960, 2934, 2875, 1734, 1705, 1612, 1520, 1455, 1385, 1301, 1232, 1141, 1035, 1000, 955, 896, 866, 759, 668.

5.2.2 Synthesis of Benzene-1,3,5-triyl tris(butylcarbamate) **2**

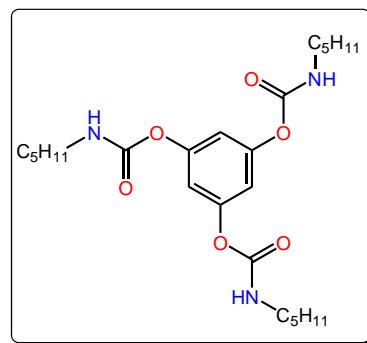
A flame-dried 50 mL round bottom flask equipped with a magnetic stir bar was charged with 1-isocyanatobutane (1.19 g, 12 mmol) and 5 drops of triethylamine (catalyst) in 10 mL of THF. The mixture was stirred at room temperature for 5 minutes.



Phloroglucinol (500 mg, 4 mmol) in 5 mL of THF was added from a dropping funnel with a rough rate of 1 drop/s. Then the solution was refluxed overnight. The mixture was concentrated in a rotavapor and precipitated in 100 mL of ice cold water. The solid product was filtered and air-dried.⁵³ The titled compound **2** (m.p. 118-120 °C) was obtained as a white solid (1.60 g, 93%). ¹H NMR(CDCl₃, δ, ppm): 0.95 (t, *J* = 7.4 Hz, 9H), 1.38 (m, 6H), 1.54 (m, 6H), 3.24 (m, 6H), 5.04 (s, 3H), 6.85 (s, 3H); ¹³C{¹H} NMR (CDCl₃, δ, ppm): 14.1, 20.2, 32.2, 41.3, 112.2, 151.8, 154.1; IR (Nujol, ν, cm⁻¹) 3331, 3289, 2955, 2931, 2871, 2231, 2020, 1744, 1720, 1693, 1607, 1530, 1455, 1375, 1355, 1317, 1283, 1241, 1137, 1042, 1015, 920, 865, 767, 745, 669.

5.2.3 Synthesis of Benzene-1,3,5-triyl tris(pentylcarbamate) **3**

A flame-dried 50 mL round bottom flask equipped with a magnetic stir bar was charged with 1-isocyanatopentane (1.36 g, 12 mmol) and 5 drops of triethylamine (catalyst) in 10 mL of THF. The mixture was stirred at room temperature for 5 minutes. Phloroglucinol

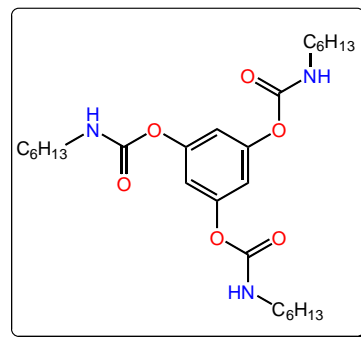


(500 mg, 4 mmol) in 5 mL of THF was added from a dropping funnel with a rough rate of 1 drop/s. Then the solution was refluxed overnight. The mixture was concentrated in a rotavapor and precipitated in 100 mL of ice cold water. The solid product was filtered and air-dried. The titled compound **3** (m.p. 124-125 °C) was obtained as a white solid (1.73 g, 93%). ¹H NMR (CDCl₃, 500 MHz) δ 0.91 (t, *J* = 6.5 Hz 9H), 1.34 (m, 12H), 1.58 (m, 6H), 3.24 (m, 6H), 5.01 (t, *J* = 6.5 Hz 3H), 6.85 (s, 3H); ¹³C{¹H} NMR (CDCl₃, 125 MHz) δ 14.4, 22.7, 29.3, 29.8, 41.6, 112.5, 151.8, 154.2; IR (Nujol, ν, cm⁻¹) 3334,

3291, 2958, 2929, 2859, 1745, 1719, 1693, 1606, 1530, 1456, 1377, 1320, 1237, 1140, 1063, 1025, 1002, 930, 867, 763, 731, 670.

5.2.4 Synthesis of Benzene-1,3,5-triyl tris(hexylcarbamate) **4**

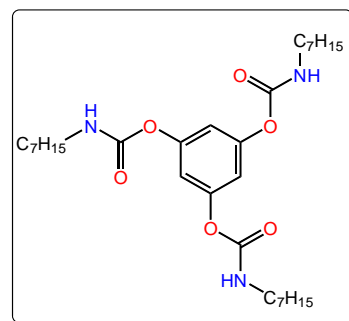
A flame-dried 50 mL round bottom flask equipped with a magnetic stir bar was charged with 1-isocyanatohexane (1.13 g, 9 mmol) and 5 drops of triethylamine (catalyst) in 10 mL of THF. The mixture was stirred at room temperature for 5 minutes. Phloroglucinol



(380 mg, 3 mmol) in 5 mL of THF was added from a dropping funnel with a rough rate of 1 drop/s. Then the solution was refluxed overnight. The mixture was concentrated in a rotavapor and precipitated in 100 mL of ice cold water. The solid product was filtered and air-dried.⁵⁵ The titled compound **4** (m.p. 130-131 °C) was obtained as a white solid (1.4 g, 93%). ¹H NMR(CDCl₃, δ, ppm): 0.90 (t, *J* = 7.0 Hz, 9H), 1.28 – 1.44 (m, 18H), 1.65 (t, *J* = 7.1, 6H), 3.23 (m, 6H), 5.05 (s, 3H), 6.85 (s, 3H). ¹³C{¹H} NMR (CDCl₃, δ, ppm): 14.4, 23.0, 26.8, 30.2, 31.8, 41.6, 112.2, 151.8, 154.2. IR (Nujol, ν, cm⁻¹) 3332, 3290, 2954, 2927, 2858, 1745, 1719, 1693, 1613, 1578, 1534, 1458, 1240, 1167, 1142, 1021, 940, 888, 866, 767, 727, 670, 635, 565.

5.2.5 Synthesis of Benzene-1,3,5-triyl tris(heptylcarbamate) **5**

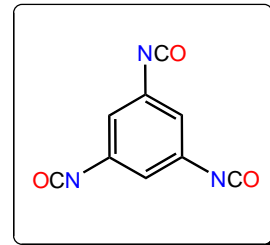
A flame-dried 50 mL round bottom flask equipped with a magnetic stir bar was charged with 1-isocyanatoheptane (1.27 g, 9 mmol) and 5 drops of triethylamine (catalyst) in 10 mL of THF. The mixture was



stirred at room temperature for 5 minutes. Phloroglucinol (380 mg, 3 mmol) in 5 mL of THF was added from a dropping funnel with a rough rate of 1 drop/s. Then the solution was refluxed overnight. The mixture was concentrated in a rotavapor and precipitated in 100 mL of ice cold water. The solid product was filtered and air-dried. The titled compound **5** (m.p. 127-128 °C) was obtained as a white solid (1.5 g, 91%). ¹H NMR (CDCl₃, 500 MHz) δ 0.90 (t, *J* = 7.0 Hz 9H), 1.32 (m, 24H), 1.56 (m, 6H), 3.25 (m, 6H), 5.01 (t, *J* = 5.5 Hz 3H), 6.86 (s, 3H); ¹³C{¹H} NMR (CDCl₃, 125 MHz) δ 14.5, 23.0, 27.1, 29.3, 30.2, 30.6, 32.2, 41.7, 112.4, 151.8, 154.3; IR (Nujol, ν, cm⁻¹) 3329, 3290, 3058, 2956, 2924, 2873, 2853, 1745, 1718, 1693, 1608, 1531, 1457, 1377, 1308, 1238, 1142, 1027, 1002, 909, 867, 765, 723, 670, 630.

5.2.6 Synthesis of 1,3,5-Triisocyanatobenzene **6**

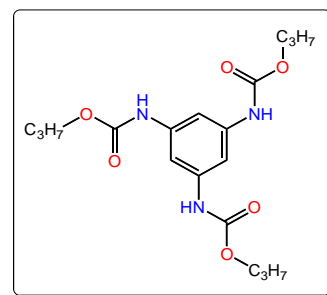
1,3,5-Triisocyanatobenzene was synthesized by following the procedure of M. C. Davis with modification.⁶⁴ A 500-mL round bottomed flask equipped with magnetic stirbar was charged with 35 mL of H₂O and 10.73 g sodium azide (165 mmol, 3.3 equiv). The mixture was stirred at room temperature until all solid dissolved. The flask was stirred in an ice bath while a solution of 13.2 g 1,3,5-tribenzenecarbonyl chloride (50 mmol, 1.0 equiv) in 150 mL of 1, 2-dichloroethane was added by addition funnel over 30 min. The cooling bath was removed, and the mixture was stirred at room temperature. After 2.5 hours, the formation of 1,3,5-benzenetricarbonyl triazide was completed. The organic phase was washed once with 25 mL of 1, 2-dichloroethane. The organic phase was dried over anhydrous MgSO₄ for 15 min. The drying agent was removed by filtration through filter paper into a 500 mL round-bottomed flask equipped a magnetic stir bar.



The mixture was refluxed for 2.5 h. The solvent was rotary evaporated, leaving 7.5 g (77%) of white solid as a crude product. The crude was recrystallized in *n*-hexane to give the title compound as needle white crystal 5.1 g (68%). ^1H NMR (CDCl_3 , 500 MHz) δ 6.68 (s, 3H); $^{13}\text{C}\{^1\text{H}\}$ NMR (CDCl_3 , 125 MHz) δ 135.9, 125.7, 118.8.

5.2.7 Synthesis of Tripropanyl *N',N'',N'''*-benzene-1,3,5-tricarbamate **7**

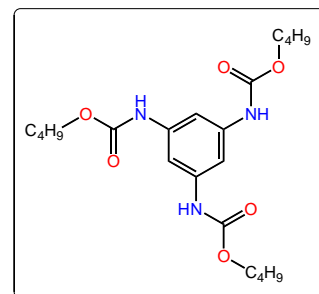
A flame-dried 100 mL round-bottomed flask equipped with a magnetic stir bar was charged *n*-propanol 0.8 g (13.2 mmol, 3.3 equiv.) and 1,3,5-triisocyanatobenzene 0.80 g (4 mmol, 1.0 equiv.) in 25 mL of dry toluene. Three drops of



Et_3N was added to the above solution as a catalyst. The reaction mixture was refluxed overnight and monitored by TLC. Evaporation of solvent afforded a yellowish oil, which was then purified by column chromatography with an eluent of ethyl acetate/hexane = 1/9 to afford the titled compound **7** (1.36 g, yield: 85 %, m.p.: 93-94 °C) as white powder. ^1H NMR (acetone- d_6 , 500 MHz) δ 0.95 (t, 9H), 1.65 (m, 6H), 4.04 (q, 6H), 7.32 (s, 3H), 9.52 (s, 3H); $^{13}\text{C}\{^1\text{H}\}$ NMR (acetone- d_6 , 125 MHz) δ 10.5, 22.3, 40.0, 65.8, 104.0, 139.9, 154.0; IR (Nujol, v, cm^{-1}): 3293, 3108, 2967, 1696, 1621, 1550, 1461, 1437, 1277, 1234, 1216, 1099, 854, 770; $[\text{M}+\text{H}^+]$ calculated for $\text{C}_{18}\text{H}_{27}\text{O}_6\text{N}_3$, 382.1973, Found, 382.1978.

5.2.8 Synthesis of Tributyl *N',N'',N'''*-benzene-1,3,5-tricarbamate **8**

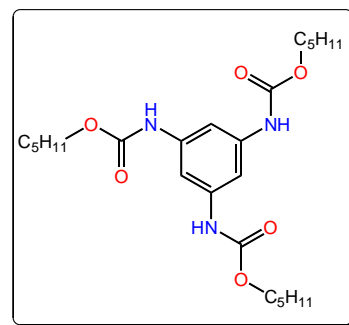
A flame-dried 100 mL round-bottomed flask equipped with a magnetic stir bar was charged *n*-butanol 0.98 g (13.2 mmol, 3.3 equiv.) and 1,3,5-triisocyanatobenzene 0.80 g (4 mmol, 1.0 equiv.) in 25 mL of dry toluene. Three drops



of Et₃N was added to the above solution as a catalyst. The reaction mixture was refluxed overnight and monitored by TLC. Evaporation of solvent afforded a yellowish honey, which was further purified by silica gel column chromatography with an eluent of ethyl acetate/hexane gradient = 1/9 to afford the titled compound **8** (1.6 g, yield: 90 %, m.p.: 83-84 °C) as white powder. ¹H NMR (acetone-*d*₆, 500 MHz) δ 0.93 (t, 9H), 1.39 (m, 6H), 1.60 (m, 6H), 4.05 (q, 3H), 7.29 (s, 3H), 9.51 (s, 3H); ¹³C{¹H} NMR (acetone-*d*₆, 125 MHz) δ 14.0, 19.0, 31.1, 64.1, 104.2, 140.0, 154.1; IR (Nujol, ν, cm⁻¹): 3296, 3108, 2959, 2873, 1694, 1618, 1552, 1433, 1235, 1092, 98, 853, 770. [M+H⁺] calculated for C₂₁H₃₃O₆N₃, 424.2442, Found, 424.2448.

5.2.9 Synthesis of Tripentyl *N',N'',N'''*-benzene-1,3,5-tricarbamate **9**

A flame-dried 100 mL round-bottomed flask equipped with a magnetic stir bar was charged *n*-pentanol 1.16 g (13.2 mmol, 3.3 equiv.) and 1,3,5-trisocyanatobenzene 0.80 g (4 mmol, 1.0 equiv.) in 25 mL of

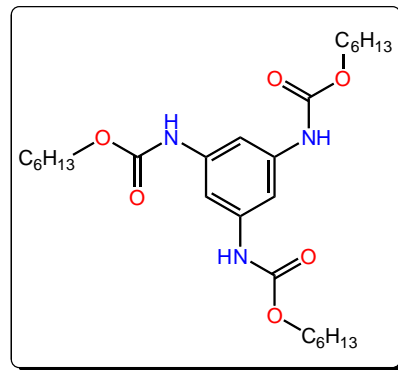


dry toluene. Three drops of Et₃N was added to the above solution as a catalyst. The reaction mixture was refluxed overnight and monitored by TLC. Evaporation of solvent afforded a yellowish oil, which was further purified by silica gel column chromatography with an eluent of ethyl acetate/hexane gradient = 1/9 to afford the titled compound **9** (1.76 g, yield: 90 %, m.p.: 103-104 °C) as white powder. ¹H NMR (CDCl₃, 500 MHz) δ 0.91-0.93 (t, 9H), 1.35-1.37 (m, 12H), 1.65-1.68 (m, 6H), 4.13-4.15 (q, 6H), 6.73 (s, 3H), 7.28 (s, 3H); ¹³C{¹H} NMR (CDCl₃, 125 MHz) δ 14.4, 22.7, 28.4, 28.9, 65.9, 103.5, 139.7, 153.9; IR (Nujol, ν, cm⁻¹): 3312, 2956, 2932, 2871, 1686, 1615, 1546, 1501, 1274,

1238, 1216, 1093, 766, 680; [M+H⁺] calculated for C₂₄H₃₉O₆N₃, 466.2912, Found, 466.2917.

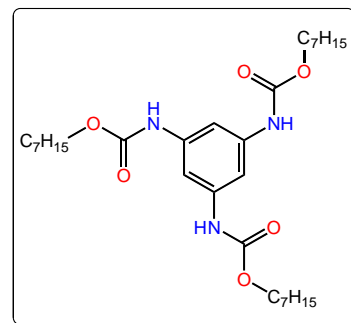
5.2.10 Synthesis of Trihexyl *N',N'',N'''*-benzene-1,3,5-tricarbamate **10**

A flame-dried 100 mL round-bottomed flask equipped with a magnetic stir bar was charged *n*-hexanol 1.35 g (13.2 mmol, 3.3 equiv.) and 1,3,5-trisocyanatobenzene 0.80 g (4 mmol, 1.0 equiv.) in 25 mL of dry toluene. Three drops of Et₃N was added to the above solution as a catalyst. The reaction mixture was refluxed overnight and monitored by TLC. Evaporation of solvent afforded a yellowish honey, which was further purified by silica gel column chromatography with an eluent of ethyl acetate/hexane gradient = 1/9 to afford the titled compound **10** (2.0 g, yield: 94 %, m.p.: 103-104 °C) as white powder. ¹H NMR (CDCl₃, 500 MHz) δ 0.89 (t, 9H), 1.30-1.38 (m, 18H), 1.61-1.66 (m, 6H), 4.11-4.14 (q, 6H), 6.92 (s, 3H), 7.30 (s, 3H); ¹³C{¹H} NMR (CDCl₃, 125 MHz) δ 14.0, 22.6, 25.5, 28.9, 31.5, 65.5, 103.2, 139.4, 153.7; IR (Nujol, v, cm⁻¹) 3299, 2927, 2859, 1685, 1613, 1544, 1433, 1215, 1092, 985, 863, 767, 678; [M+H⁺] calculated for C₂₇H₄₅O₆N₃, 508.3381, Found, 508.3387.



5.2.11 Synthesis of Triheptyl *N',N'',N'''*-benzene-1,3,5-tricarbamate **11**

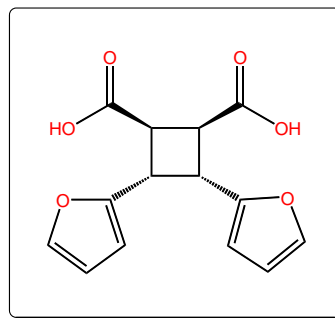
A flame-dried 100 mL round-bottomed flask equipped with a magnetic stir bar was charged *n*-heptanol 1.53 g (13.2 mmol, 3.3 equiv.) and 1,3,5-trisocyanatobenzene 0.80 g (4 mmol, 1.0 equiv.) in 25 mL of



dry toluene. Three drops of Et₃N was added to the above solution as a catalyst. The reaction mixture was refluxed overnight and monitored by TLC. Evaporation of solvent afforded a yellowish honey color, which was further purified by silica gel column chromatography with an eluent of ethyl acetate/hexane gradient = 1/9 to afford the titled compound **11** (2.2 g, yield: 95 %, m.p.: 100-101 °C) as white powder. ¹H NMR (CDCl₃, 500 MHz) δ 0.91 (t, 9H), 1.32(m, 24H), 1.68 (m, 6H), 4.16(q, 6H), 6.71 (s, 3H), 7.29 (s, 3H); ¹³C{¹H} NMR (CDCl₃, 125 MHz) δ 14.5, 23.0, 26.2, 29.3, 29.4, 32.1, 65.9, 103.5, 139.7, 153.9; IR (Nujol, ν, cm⁻¹) 3302, 2954, 2921, 2853, 1685, 1613, 1544, 1454, 1433, 1214, 1093, 766, 680; [M+H⁺] calculated for C₃₀H₅₁O₆N₃, 550.3851, Found, 550.3856.

5.2.12 Synthesis of 3,4-di(furan-2-yl)cyclobutane-1,2-dicarboxylic acid **12**

The photosynthesis was carried out in an open top quartz tube. 2 g of crystalline 3-(2-furyl)acrylic acid (Alfa Aesar, 99%) was grinded to fine power. The acid was suspended in 100 mL of hexane in the flask with

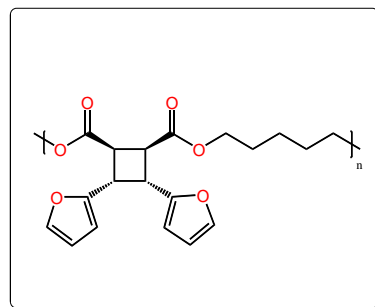


magnetic stirring. The continuously stirred suspension was under UV irradiation of eight 11-watt black lights for 12 hours. The powder clustered on the inside wall of the tube was cleaned occasionally during the reaction. The slurry was then filtered and the white solid (1.9 g, m.p. 170-171 °C) was obtained. The crude product was determined as the titled compound. ¹H NMR (DMSO-*d*₆, 500 MHz) δ 3.68 (dd, 2H), 4.05 (dd, 2H), 6.11 (d, *J* = 3.5 Hz 2H), 6.26 (dd, 2H), 7.41 (d, *J* = 2.5 Hz H), 12.56 (s, 2H); ¹³C{¹H} NMR (DMSO-*d*₆, 125 MHz) δ 38.0, 43.0, 107.3, 110.8, 142.4, 153.5, 173.6; IR (Nujol, ν, cm⁻¹) 2960, 2922, 2853, 2162, 2050, 1695, 1596, 1504, 1417, 1350, 1319, 1281, 1259, 1224, 1198,

1183, 1167, 1147, 1129, 1075, 1012, 996, 959, 883, 862, 822, 799, 728, 687, 666, 618, 597.

5.2.13 Preparation of Polymer from **12** and 1,5-Pentanediol

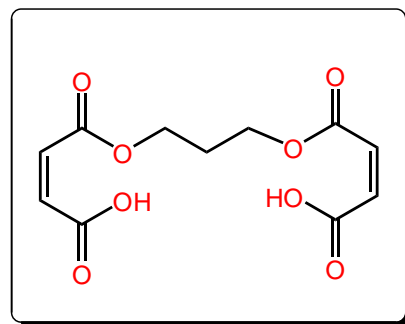
12 (1.9 g, 6.88mmol), *N,N*-dicyclohexyl-carbodiimide (3.14 g, 15.12 mmol, 2.2 equiv), and 4-(*N,N*-dimethylamino)pyridine (80 mg) were added to a solution of 1,5-pentanediol (715.5 mg, 6.88 mmol, 1 equiv) in 40



mL of dry DMF at room temperature with magnetic stirring for 3 hours. The solution was filtrated. 100 mL of water was added into the filtrate and collected the precipitate as a paste. The paste was dissolved in 50 mL of DCM. By adding diethyl ether to the DCM solution, dicyclohexylurea can be further removed as precipitate by following filtration. After removing solvent, the sticky oil-like liquid was obtained and tested by NMR.

5.2.14 Synthesis of (2*Z*,2'*Z*)-4,4'-[propane-1,3-diylbis(oxy)]bis(4-oxobut-2-enoic acid) **13**

A flame-dried 250 mL round bottom flask equipped with a magnetic stir bar was charged with maleic anhydride (9.8 g, 100 mmol) and 1,3-propanediol (3.8 g, 50 mmol) in 200 mL of toluene. The mixture was stirred and refluxed overnight. The

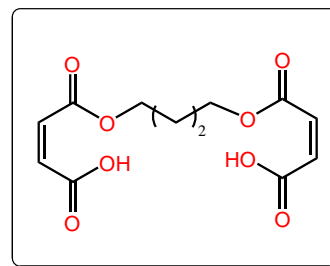


solution was cooled down and recrystallized in ice bath. The solid product was filtered and dried. The titled compound **13** (m.p. 93.0-94.6 °C) was obtained as a white solid (13.5 g, 99%). ¹H NMR (DMSO-*d*₆, 500 MHz) δ 1.95 (m, 2H), 4.17 (t, *J* = 6.5 Hz 4H),

6.38 (s, 2H) 6.39 (s, 2H), 13.05 (s, 2H); IR (Nujol, ν , cm^{-1}) 3054, 2977, 2944, 2905, 2606, 1721, 1695, 1642, 1474, 1440, 1380, 1365, 1323, 1262, 1233, 1207, 1169, 1134, 1101, 1029, 993, 965, 919, 879, 853, 811, 777, 723, 709, 682, 668, 614, 593.

5.2.15 Synthesis of (2Z,2'Z)-4,4'-[butane-1,4-diylbis(oxy)]bis(4-oxobut-2-enoic acid) **14**

A dry 250 mL round bottom flask equipped with a magnetic stir bar was charged with maleic anhydride (9.8 g, 100 mmol) and 1,3-butanediol (4.5 g, 50 mmol) in 200 mL of toluene. The mixture was stirred and refluxed overnight.

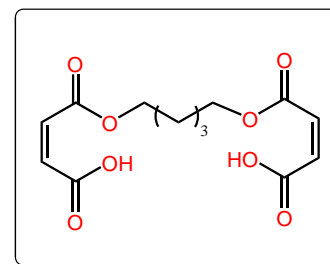


The solution was cooled down in ice bath. The solid product was filtered and dried. The titled compound **14** (m.p. 119.5-120.4 °C) was obtained as a white solid (14.1 g, 99%).

^1H NMR (DMSO- d_6 , 500 MHz) δ 1.67 (m, 4H), 4.12 (t, $J = 5.0$ Hz H), 6.37 (s, 2H), 6.38 (s, 2H) 13.02 (s, 2H); ^1H NMR (CDCl_3 , 500 MHz) δ 1.80 (m, 4H), 4.25 (m, 4H), 6.25 (d, $J = 12.5$ Hz 2H), 6.42(d, $J = 12.5$ Hz 2H); $^{13}\text{C}\{^1\text{H}\}$ NMR (DMSO- d_6 , 125 MHz) δ 24.9, 64.3, 129.3, 131.9, 165.6, 167; IR (Nujol, ν , cm^{-1}) 3045, 2969, 2866, 2780, 2578, 1948, 1714, 1695, 1644, 1474, 1450, 1431, 1393, 1358, 1327, 1309, 1273, 1254, 1225, 1168, 1049, 1029, 1009, 983, 920, 860, 813, 760, 709, 668, 610.

5.2.16 Synthesis of (2Z,2'Z)-4,4'-[pentane-1,5-diylbis(oxy)]bis(4-oxobut-2-enoic acid) **15**

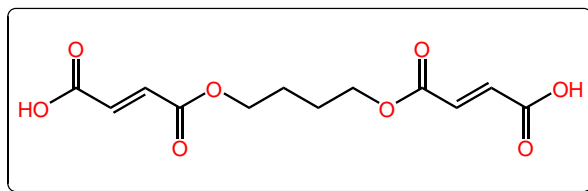
A dry 250 mL round bottom flask equipped with a magnetic stir bar was charged with maleic anhydride (9.8 g, 100 mmol) and 1,3-pentanediol (5.2 g, 50 mmol) in 200 mL of toluene. The mixture was stirred and refluxed overnight.



The solution was cooled down and recrystallized in ice bath. The solid product was filtered and dried. The titled compound **15** (m.p. 86.1-87.2 °C) was obtained as a white solid (15.2 g, 99%). ¹H NMR (DMSO-*d*₆, 500 MHz) δ 1.38 (t, *J* = 8.0 Hz 2H), 1.62 (m, 4H), 4.09 (t, *J* = 6.0 Hz 4H), 6.37 (s, 2H), 6.38 (s, 2H), 13.00 (s, 2H); ¹³C{¹H} NMR (DMSO-*d*₆, 125 MHz) δ 20.6, 26.3, 63.2, 127.7, 130.2, 164.2, 165.4; IR (Nujol, ν, cm⁻¹) 3059, 2940, 2900, 2876, 2858, 2619, 2530, 1717, 1700, 1643, 1479, 1430, 1372, 1357, 1271, 1252, 1206, 1170, 1067, 1042, 976, 916, 886, 819, 738, 685, 595, 576.

5.2.17 Synthesis of (2*E*,2'*E*)-4,4'-[butane-1,4-diylbis(oxy)]bis(4-oxobut-2-enoic acid) **16**

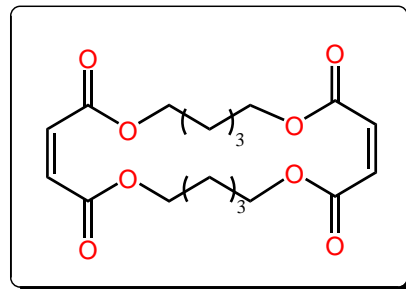
A flame-dried 50 mL round bottom flask equipped with a magnetic stir bar was charged with **14** (0.7 g) and



I₂ (0.1 g) in 35 mL of xylene. The mixture was stirred and refluxed overnight with N₂ protection. The solution was cooled down and recrystallized in an ice bath. The solid product was filtered and dried. The titled compound (m.p. 179.2-180.1 °C) was obtained as a white solid (0.7 g, 100%). ¹H NMR (DMSO-*d*₆, 500 MHz) δ 1.72 (m, 4H), 4.19 (t, *J* = 5.5 Hz 4H), 6.698 (s, 2H) 6.700 (s, 2H), 13.24 (s, 2H); ¹³C{¹H} NMR (DMSO-*d*₆, 125 MHz) δ 25.0, 64.8, 132.9, 135.0, 164.9, 166.1; IR (Nujol, ν, cm⁻¹) 3079, 2962, 2878, 2675, 2542, 1712, 1682, 1632, 1557, 1466, 1428, 1306, 1281, 1263, 1218, 1168, 1042, 992, 955, 934, 914, 900, 889, 777, 755, 735, 659.

5.2.18 Synthesis of (3Z,14Z)-1,6,12,17-tetraoxacyclodocosa-3,14-diene-2,5,13,16-tetraone **17**

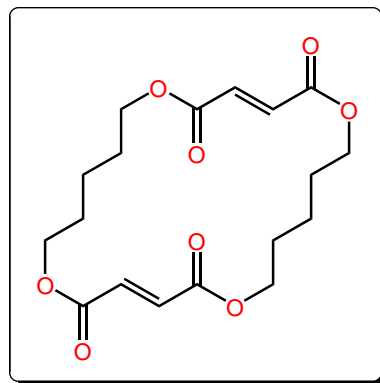
A flame-dried 4 L round bottom flask equipped with a magnetic stir bar was charged with **15** (200 mg, 0.67 mmol) and 1,5-pentanediol (70 mg, 0.67 mmol) in 3 L of benzene. The mixture was stirred and refluxed



with a Dean-Stark apparatus to remove water. The same amount of **15** and 1,5-pentanediol was added to the solution every hour (there's a no-operation gap of 8 hours between each day). The water was removed from Dean-Stark apparatus every 4 hours. After 6 days, the solution was cooled down and solvent was removed under vacuum. 200 mL of ethyl ether was added to the residue and the mixture was stirred then sonicated for 20 min. The solid product was filtered and dried. After recrystallization in EA, the titled compound **17** (m.p. 122.9-124.7°C) was obtained as a white solid (18 g, 71%). ¹H NMR (CDCl₃, 500 MHz) δ 1.48 (m, 4H), 1.73 (m, 8H), 4.21 (t, *J* = 6.5 Hz H), 6.24(s, 4H); ¹H NMR (DMSO-*d*₆, 500 MHz) δ 1.35 (m, 4H), 1.62 (m, 8H), 4.10 (d, *J* = 4.5 Hz 8H), 6.46 (d, *J* = 4.5 Hz 4H); ¹³C{¹H} NMR (CDCl₃, 125 MHz) δ 21.9, 28.0, 64.9, 129.7, 165.3; IR (Nujol, v, cm⁻¹) 3051, 2956, 2893, 2871, 2357, 2210, 2158, 1964, 1726, 1708, 1633, 1476, 1438, 1402, 1378, 1301, 1285, 1222, 1168, 1143, 1118, 1071, 1060, 1036, 1006, 996, 976, 949, 904, 894, 879, 850, 836, 823, 783, 750, 736, 652, 621, 608, 591.

5.2.19 Synthesis of (3*E*,14*E*)-1,6,12,17-tetraoxacyclodocosa-3,14-diene-2,5,13,16-tetraone **18**

A flame-dried 50 mL round bottom flask equipped with a magnetic stir bar was charged with **17** (0.51 g) and piperidine (0.5 mL, catalyst) in 20 mL of 2-propanol. The mixture was stirred and refluxed for 1.5 h. The solution was cooled down in ice bath. The solid product was filtered and dried. The titled compound **18** (m.p. 98.7-



100.0 °C) was obtained as a white solid (0.5 g, 99%). CDCl₃: ¹H NMR (CDCl₃, 500 MHz) δ 1.59 (m, 4H), 1.74 (m, 8H), 4.27 (t, *J* = 6.0 Hz 8H), 6.83 (s, 4H); ¹³C{¹H} NMR (CDCl₃, 125 MHz) δ 23.9, 28.8, 65.3, 134.2, 165.3; IR (Nujol, ν, cm⁻¹) 3073, 3000, 2964, 2923, 2867, 2844, 1714, 1645, 1469, 1456, 1432, 1385, 1357, 1304, 1266, 1255, 1237, 1196, 1177, 1098, 1069, 1043, 990, 976, 960, 907, 871, 842, 804, 770, 748, 731, 655, 607, 583.

5.2.20 Synthesis of a Double-stranded Polymer from **17**

A flame-dried 500 mL quartz tube equipped with a magnetic stir bar was charged with **17** (5 g) in 400 mL of hexane. The mixture was stirred under mercury lamp UV irradiation with argon protection overnight. The fluffy white solid was scraped off the inside surface of the tube. It was dried under vacuum. The product of this reaction was obtained as a white solid (4.9 g, 98%). IR (Nujol, ν, cm⁻¹) 2955, 2870, 1725, 1633, 1458, 1392, 1165, 1058, 1006, 975, 879, 850, 823, 736, 652, 608, 585.

APPENDIX

SELECTED SPECTRA

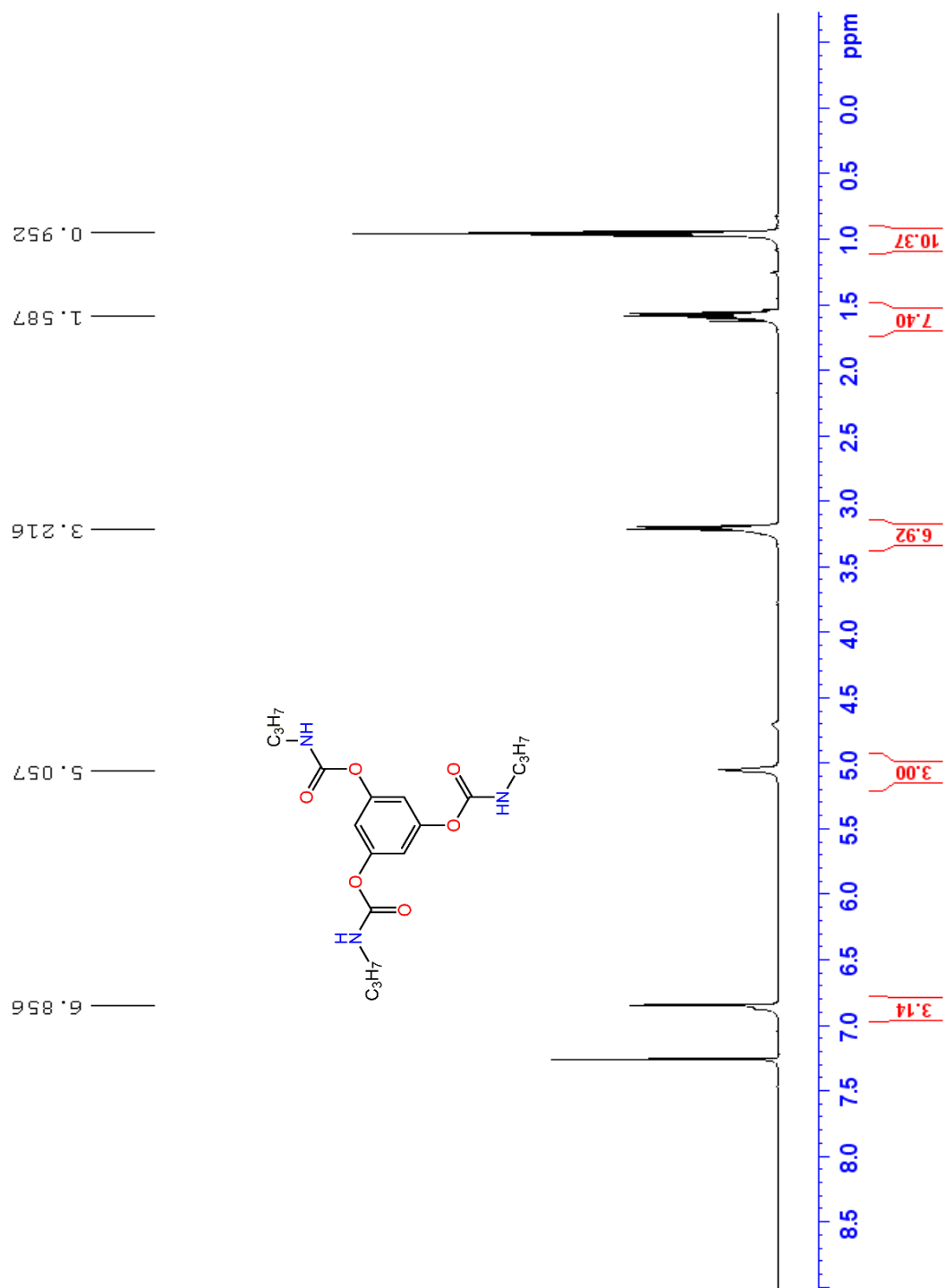


Figure 25. ¹H NMR spectrum of benzene-1,3,5-triyl tris(propylcarbamate) **1** in CDCl₃.

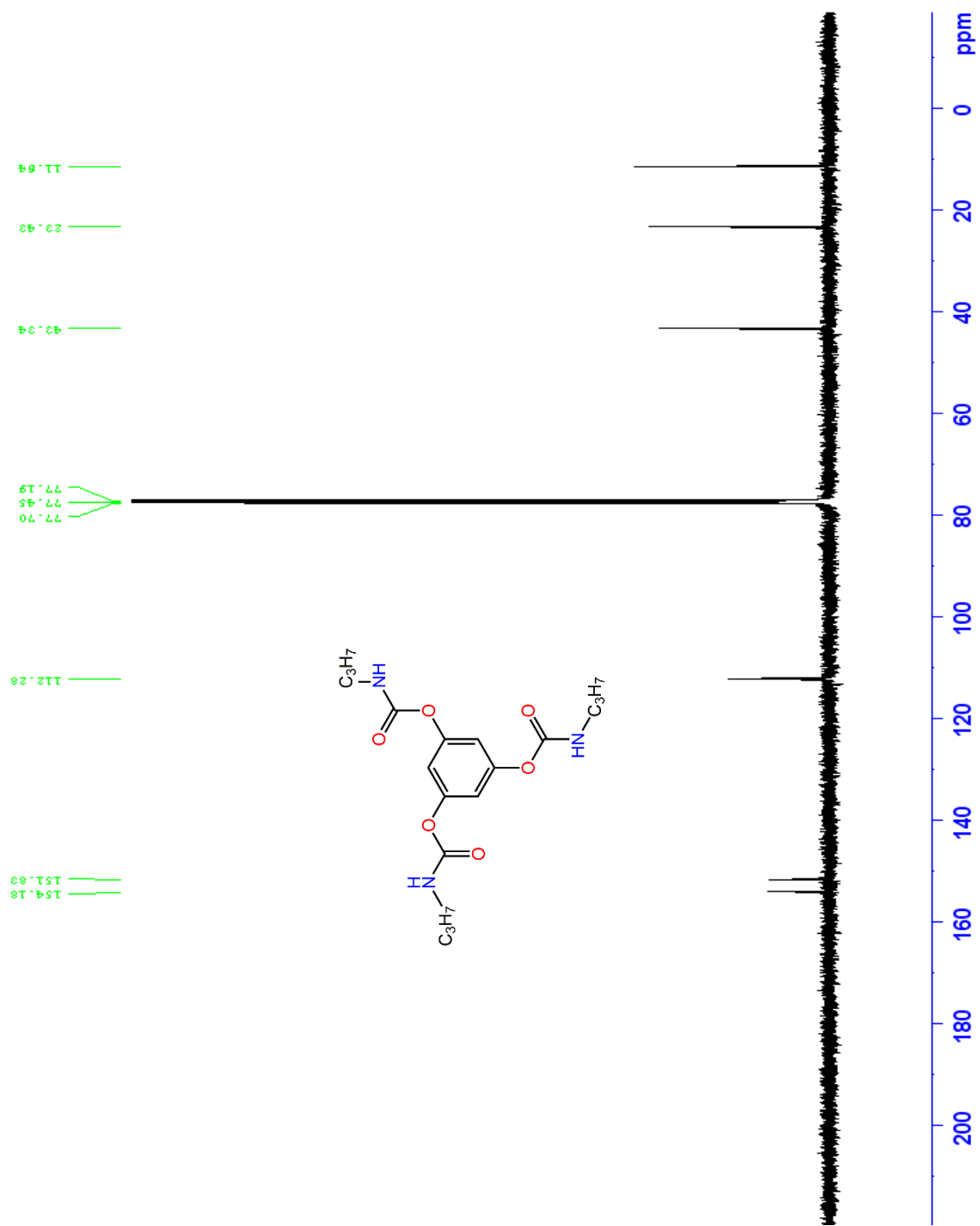


Figure 26. $^{13}\text{C}\{^1\text{H}\}$ NMR spectrum of benzene-1,3,5-triyl tris(propylcarbamate) **1** in CDCl_3 .

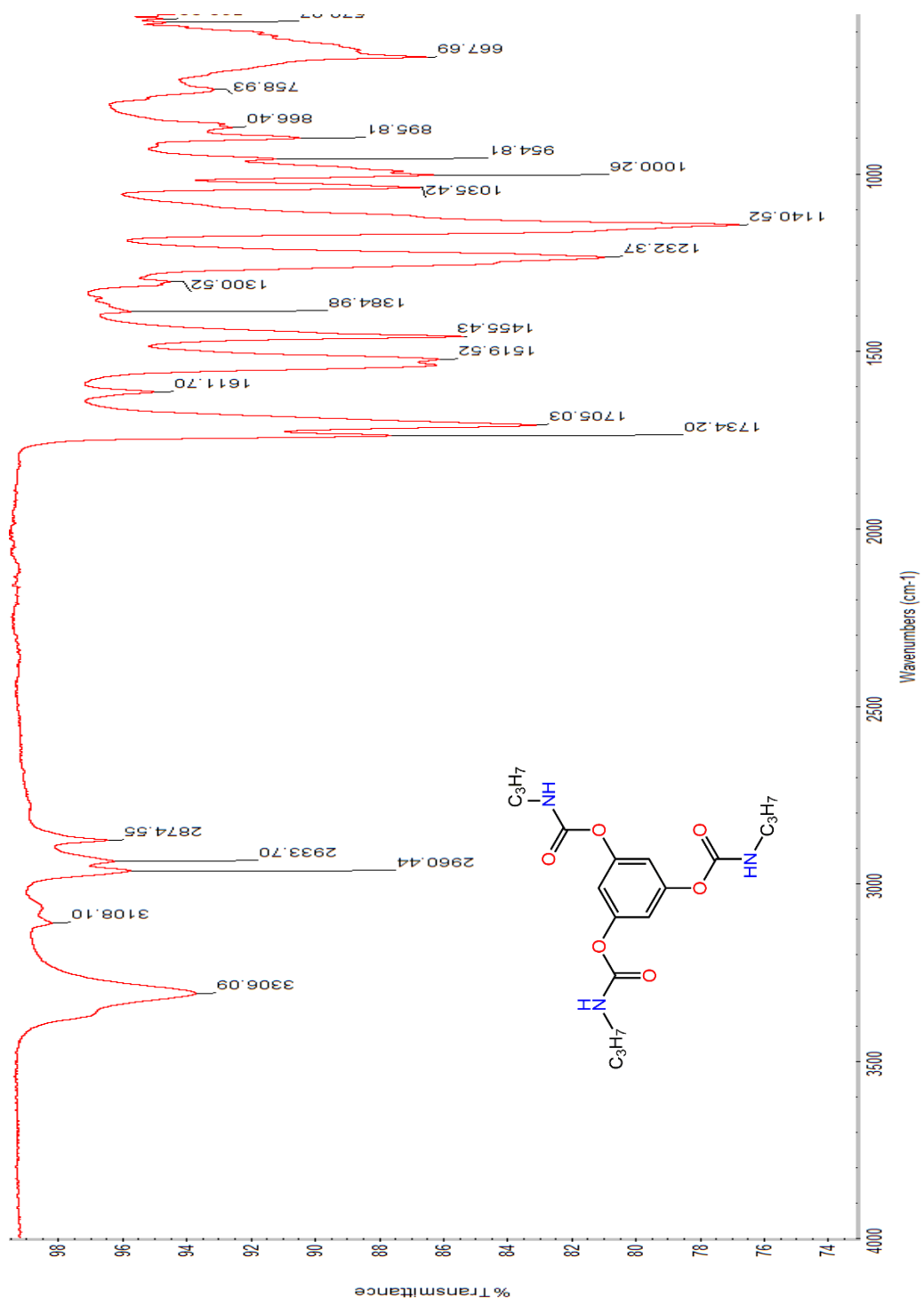


Figure 27. IR spectrum of benzene-1,3,5-triyl tris(propylcarbamate) **1**.

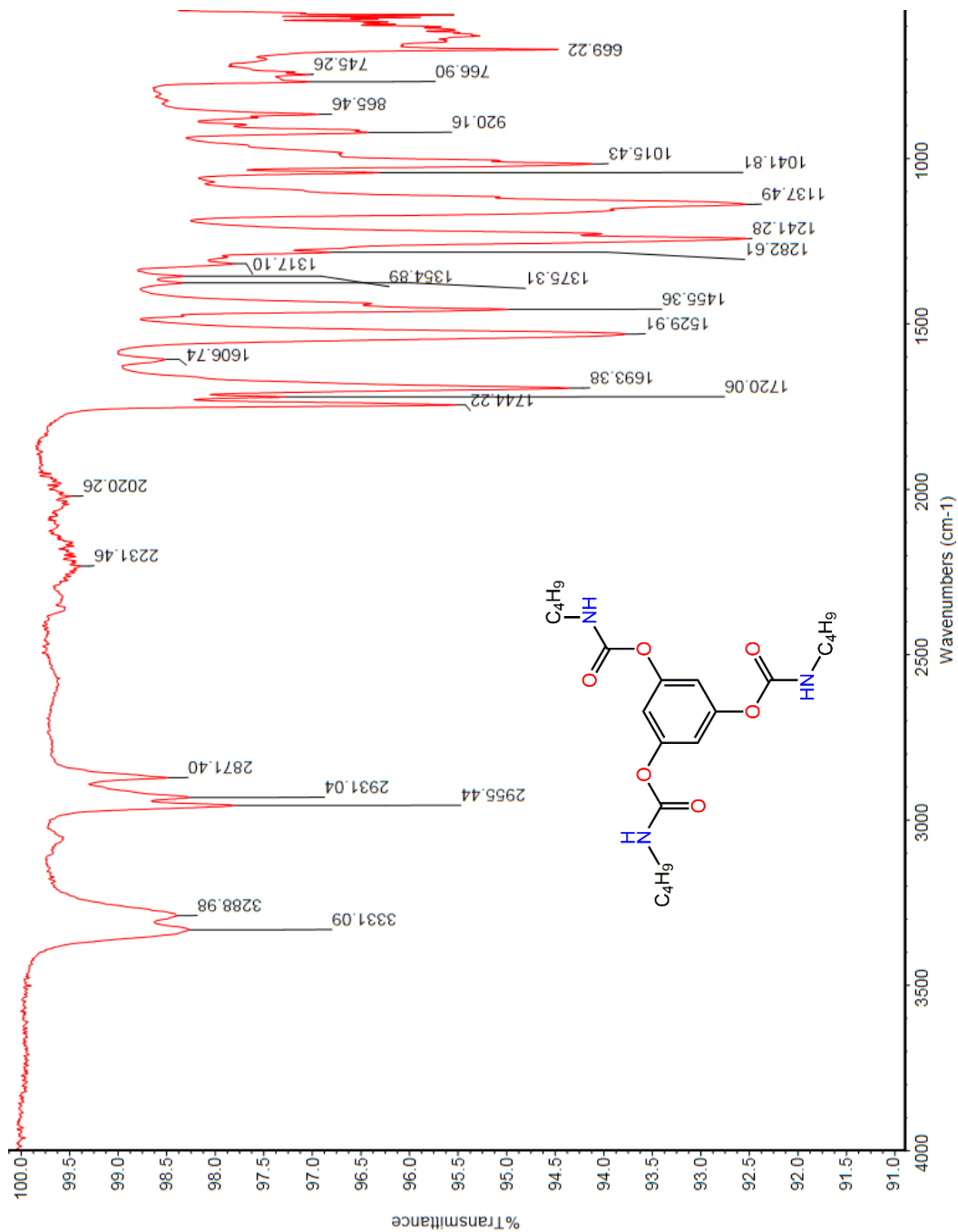


Figure 28. IR spectrum of benzene-1,3,5-triyl tris(butylcarbamate) 2.

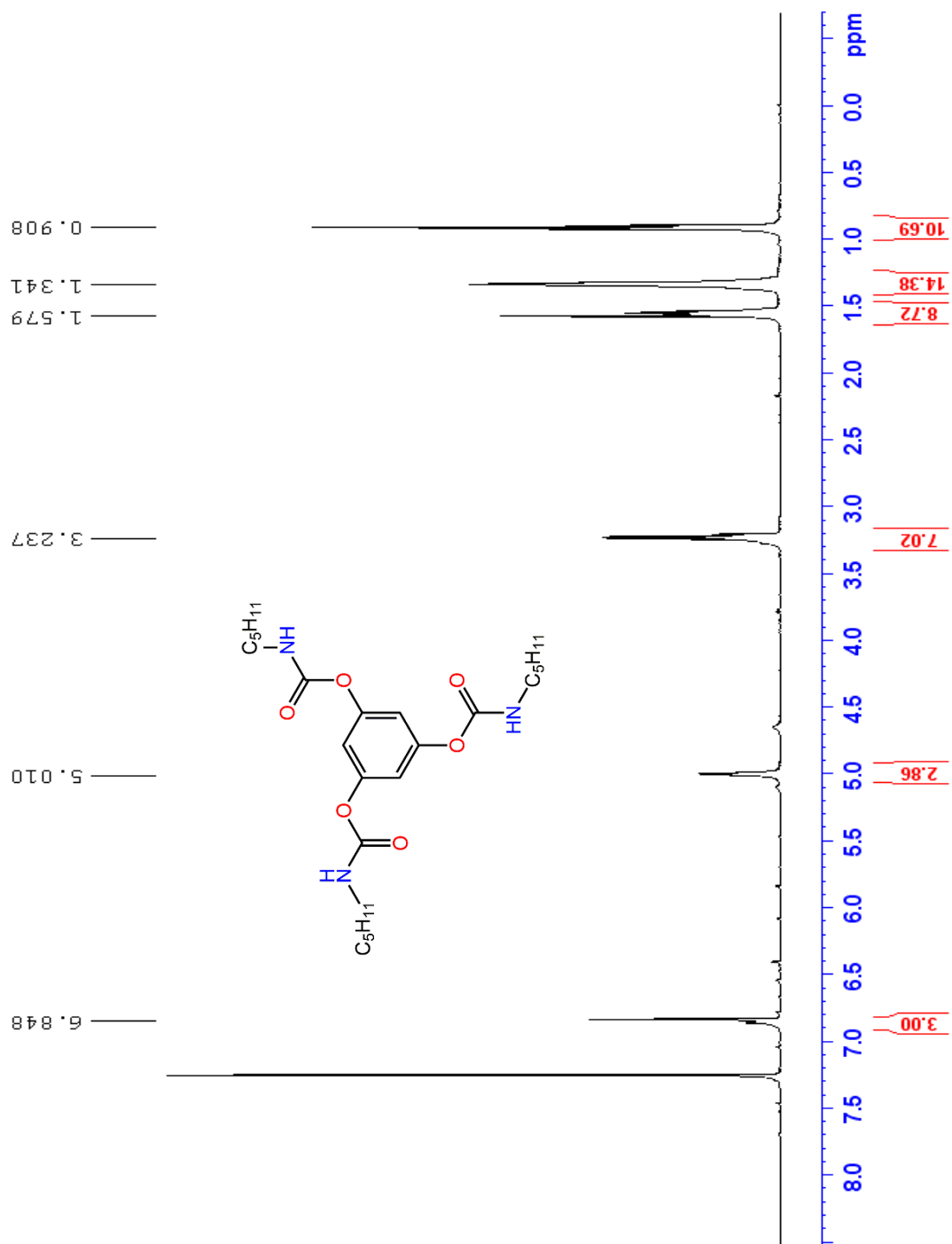


Figure 29. ¹H NMR spectrum of benzene-1,3,5-triyl tris(pentylcarbamate) **3** in CDCl₃.

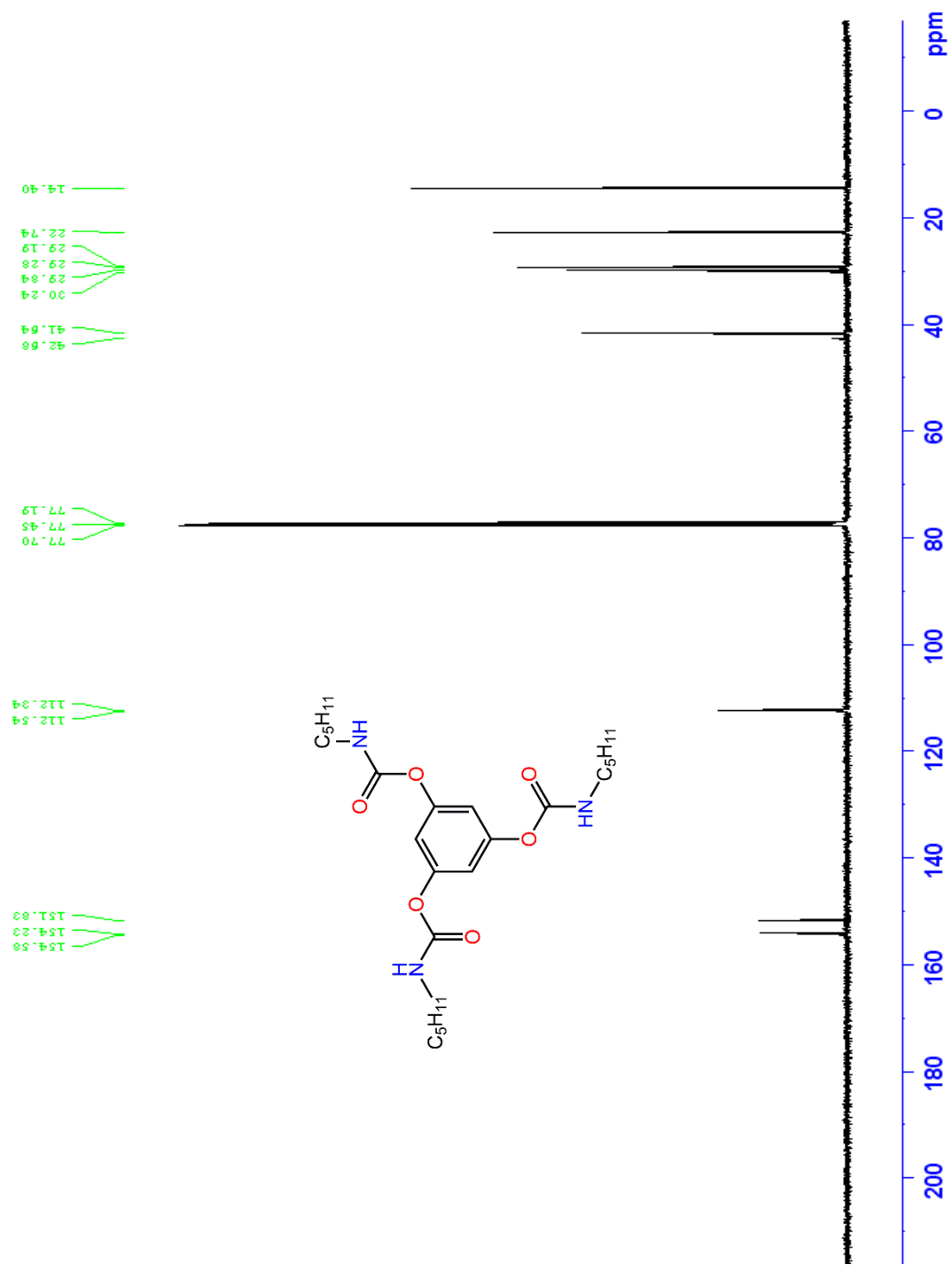


Figure 30. $^{13}\text{C}\{^1\text{H}\}$ NMR spectrum of benzene-1,3,5-triyl tris(pentylcarbamate) **3** in CDCl_3 .

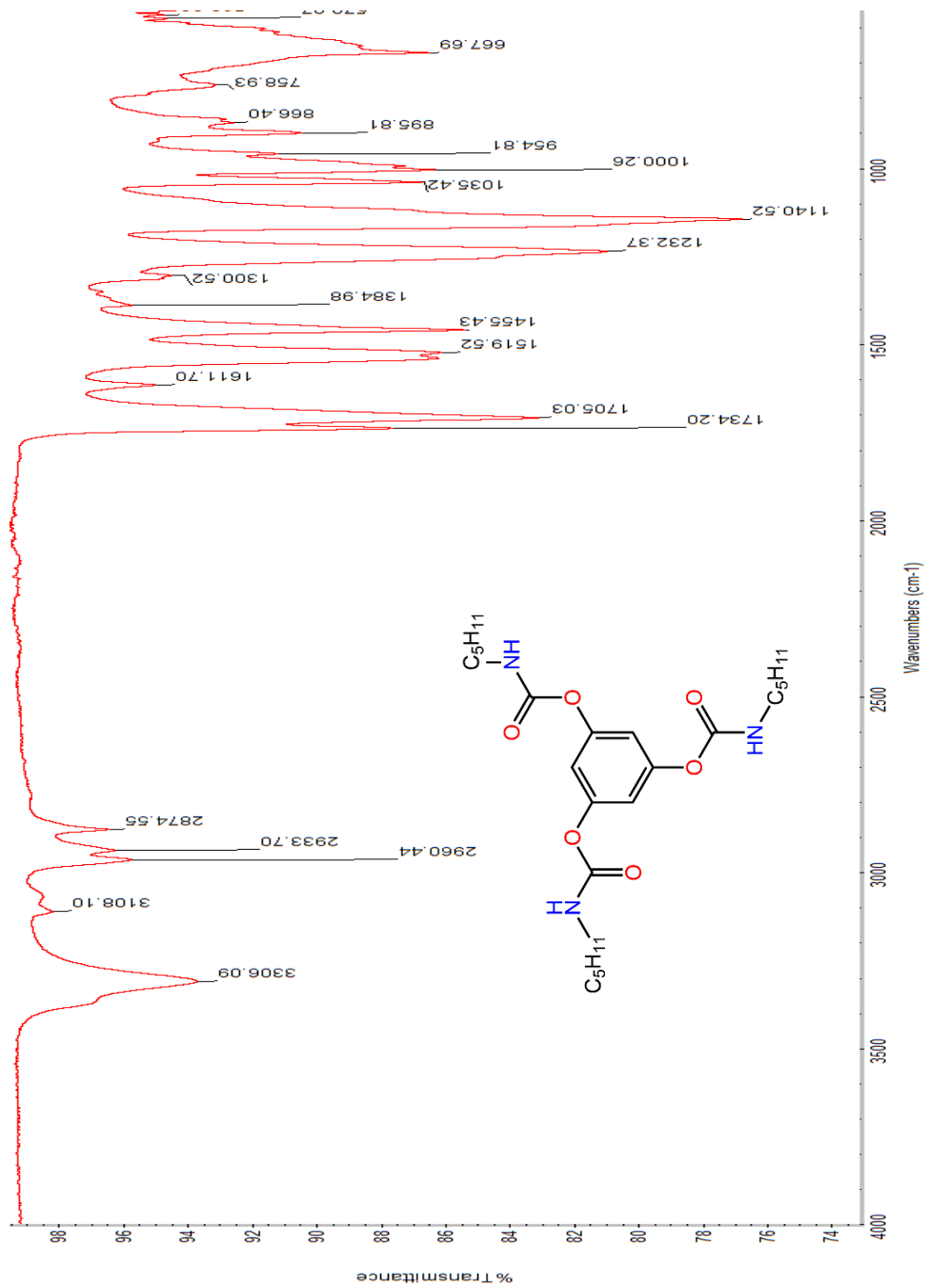


Figure 31. IR spectrum of benzene-1,3,5-triyl tris(pentylcarbamate) **3**.

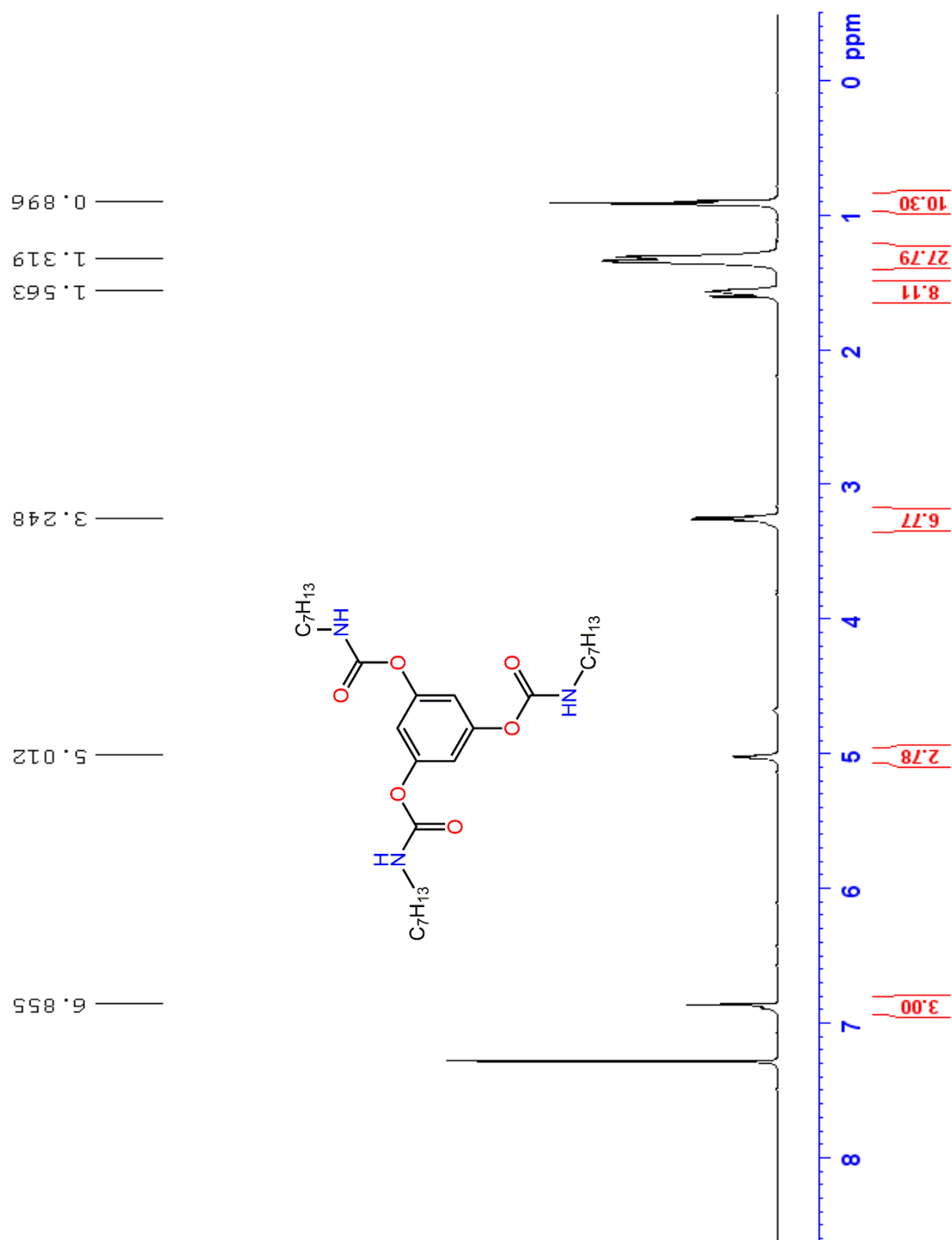


Figure 32. ^1H NMR spectrum of benzene-1,3,5-triyl tris(heptylcarbamate) **5** in CDCl_3 .

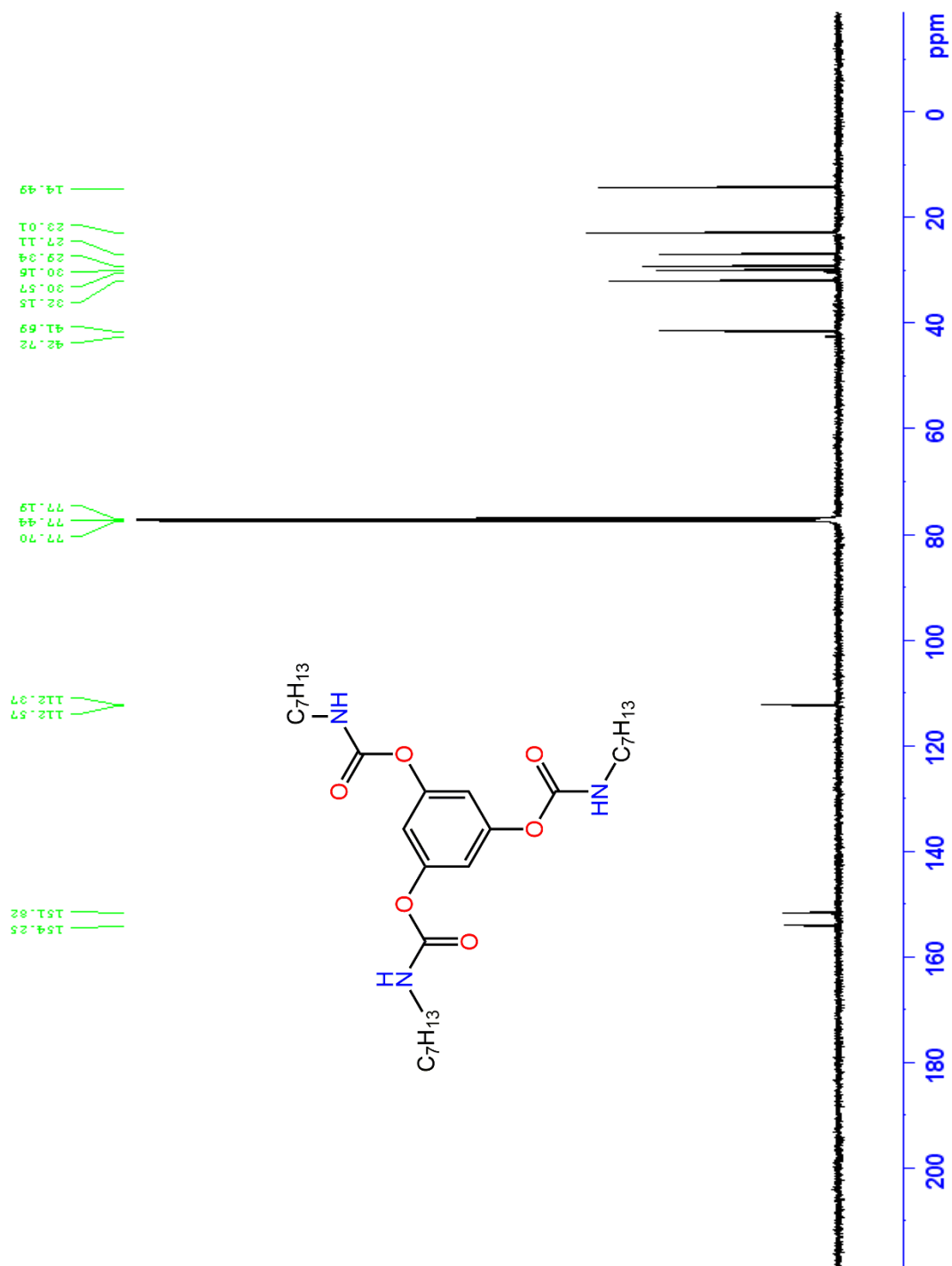


Figure 33. $^{13}\text{C}\{^1\text{H}\}$ NMR spectrum of benzene-1,3,5-triyl tris(heptylcarbamate) **5** in CDCl_3 .

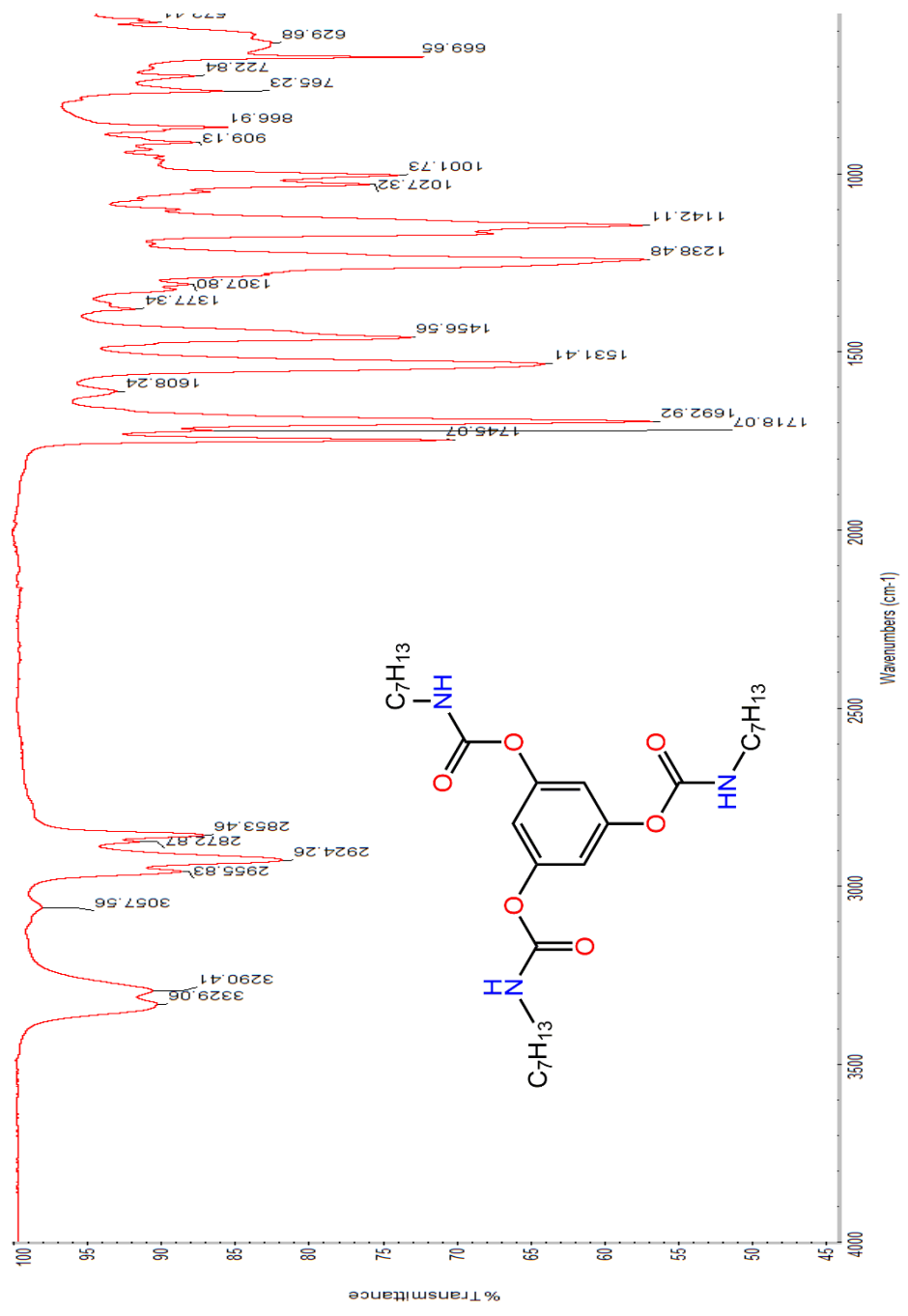


Figure 34. IR spectrum of benzene-1,3,5-triyl tris(heptylcarbamate) **5**.

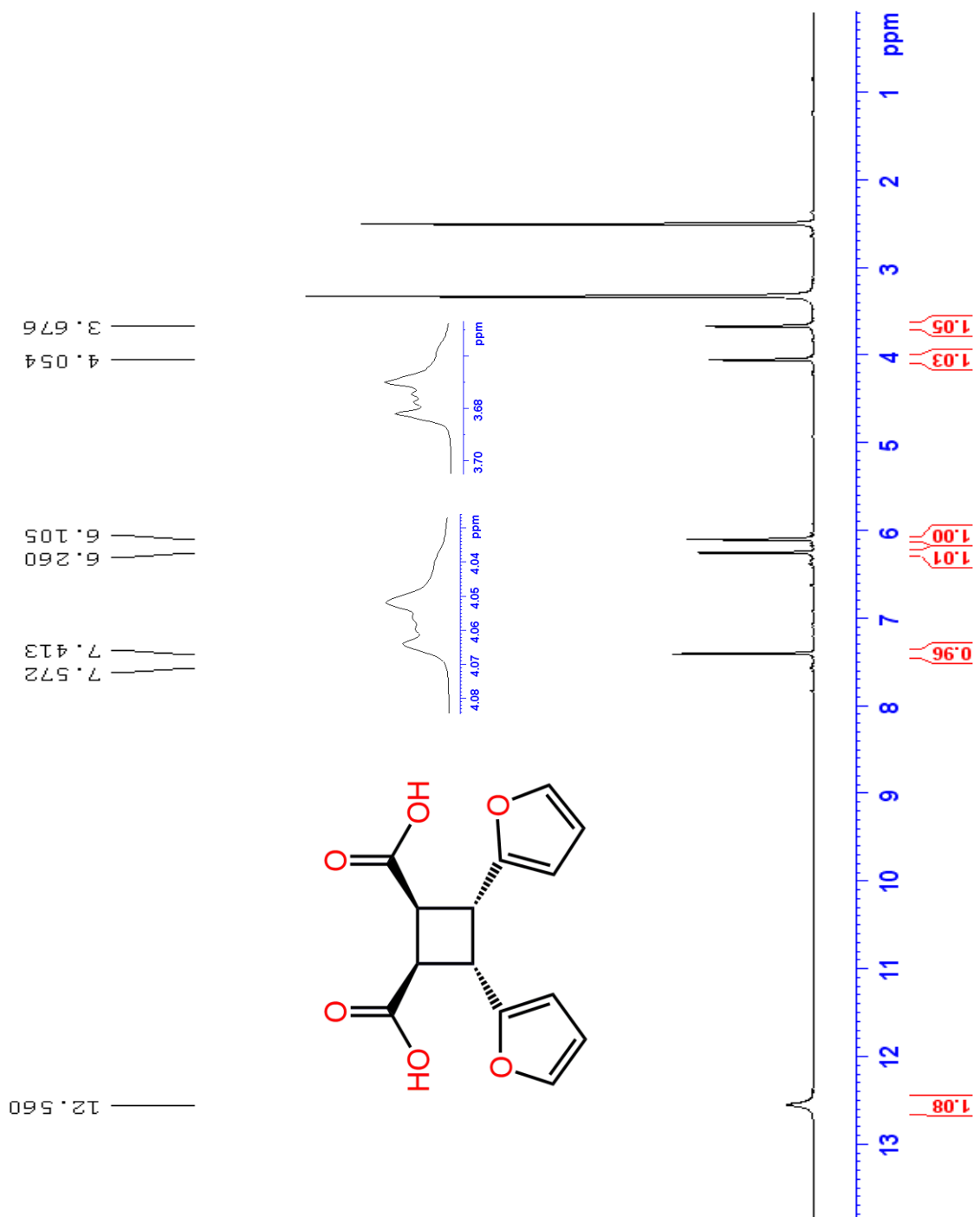


Figure 35. ^1H NMR spectrum of 3,4-di(furan-2-yl)cyclobutane-1,2-dicarboxylic acid **12** in $\text{DMSO-}d_6$.

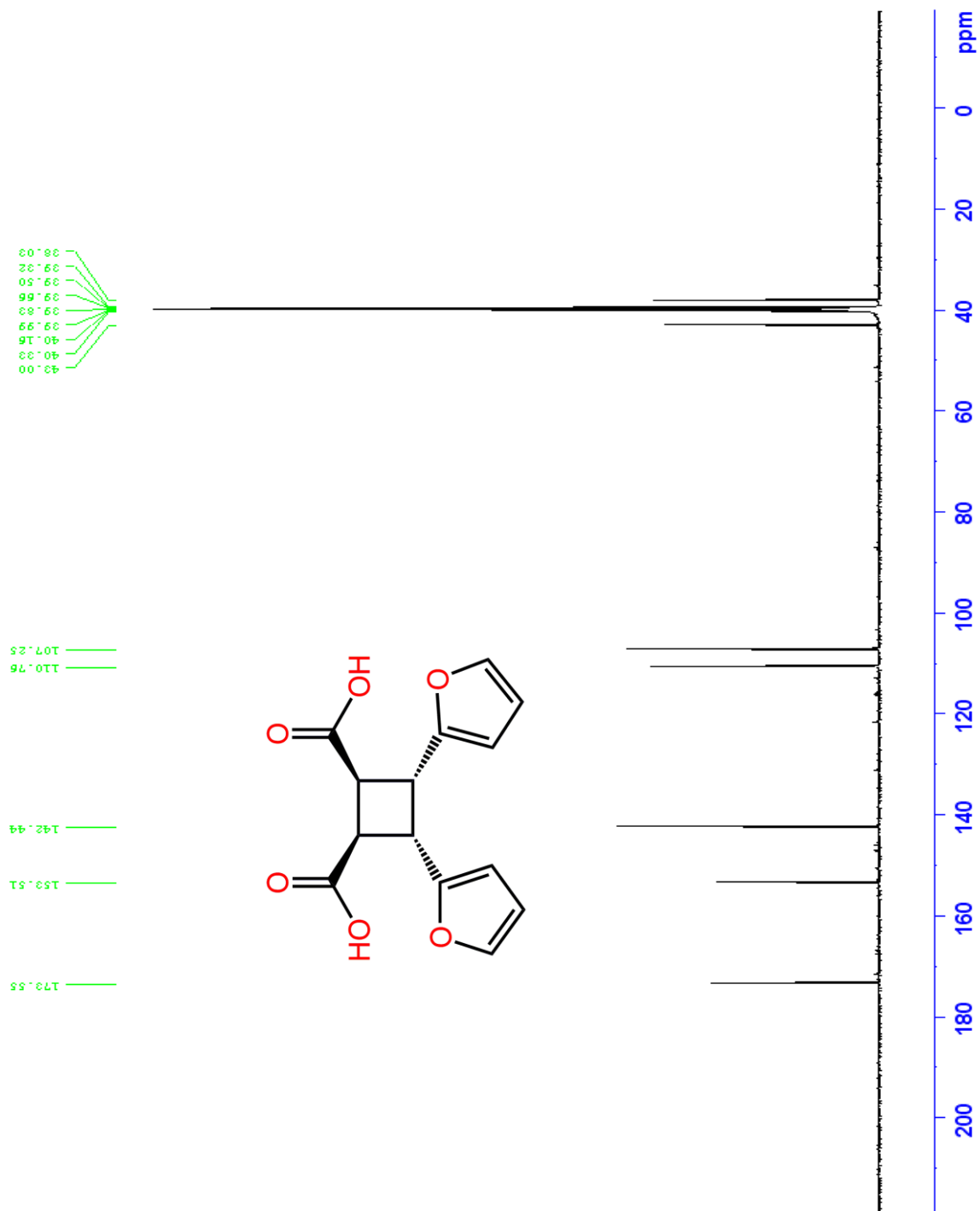


Figure 36. $^{13}\text{C}\{^1\text{H}\}$ NMR spectrum of 3,4-di(furan-2-yl)cyclobutane-1,2-dicarboxylic acid **12** in $\text{DMSO-}d_6$.

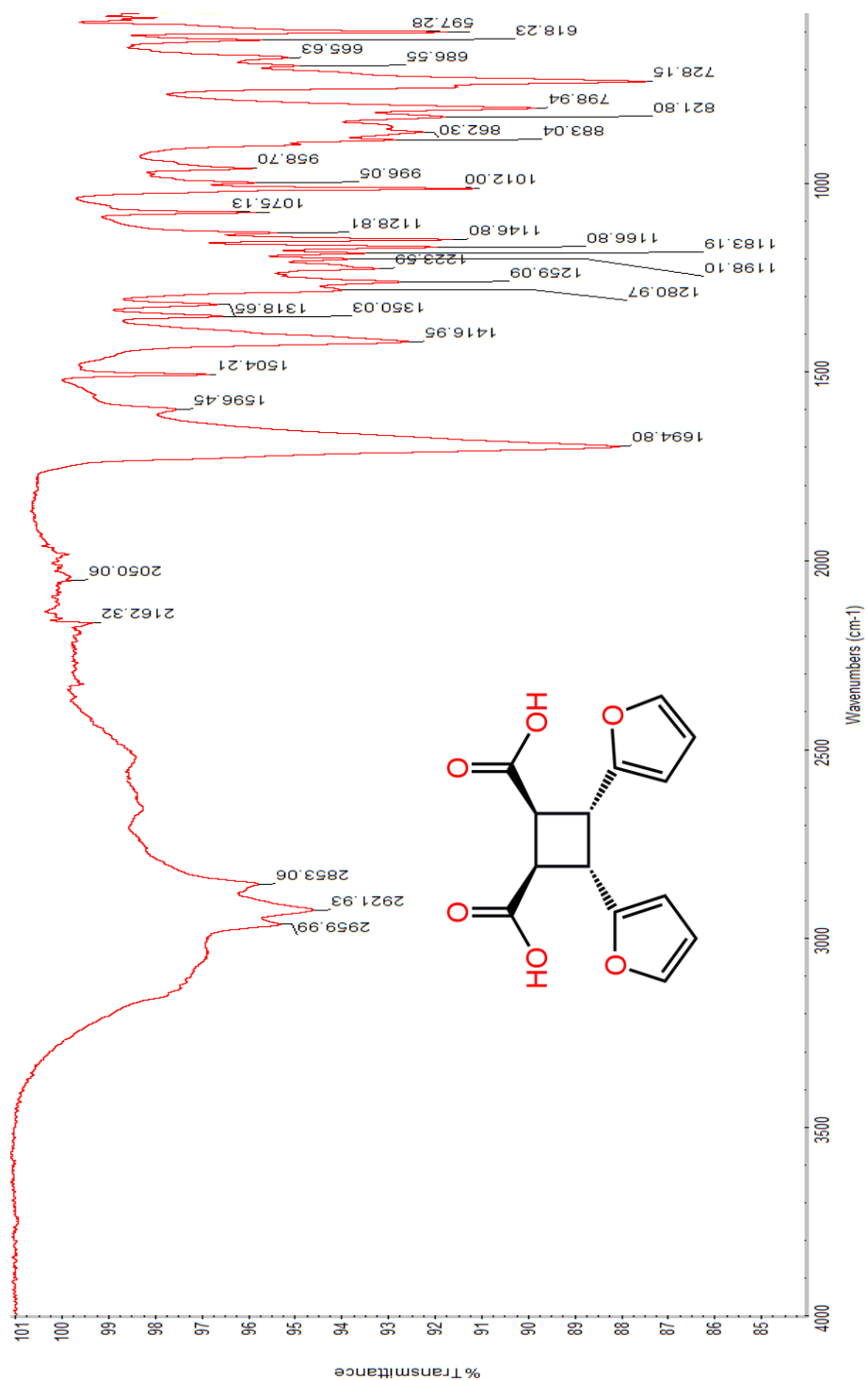


Figure 37. IR spectrum of 3,4-di(furan-2-yl)cyclobutane-1,2-dicarboxylic acid **12**.

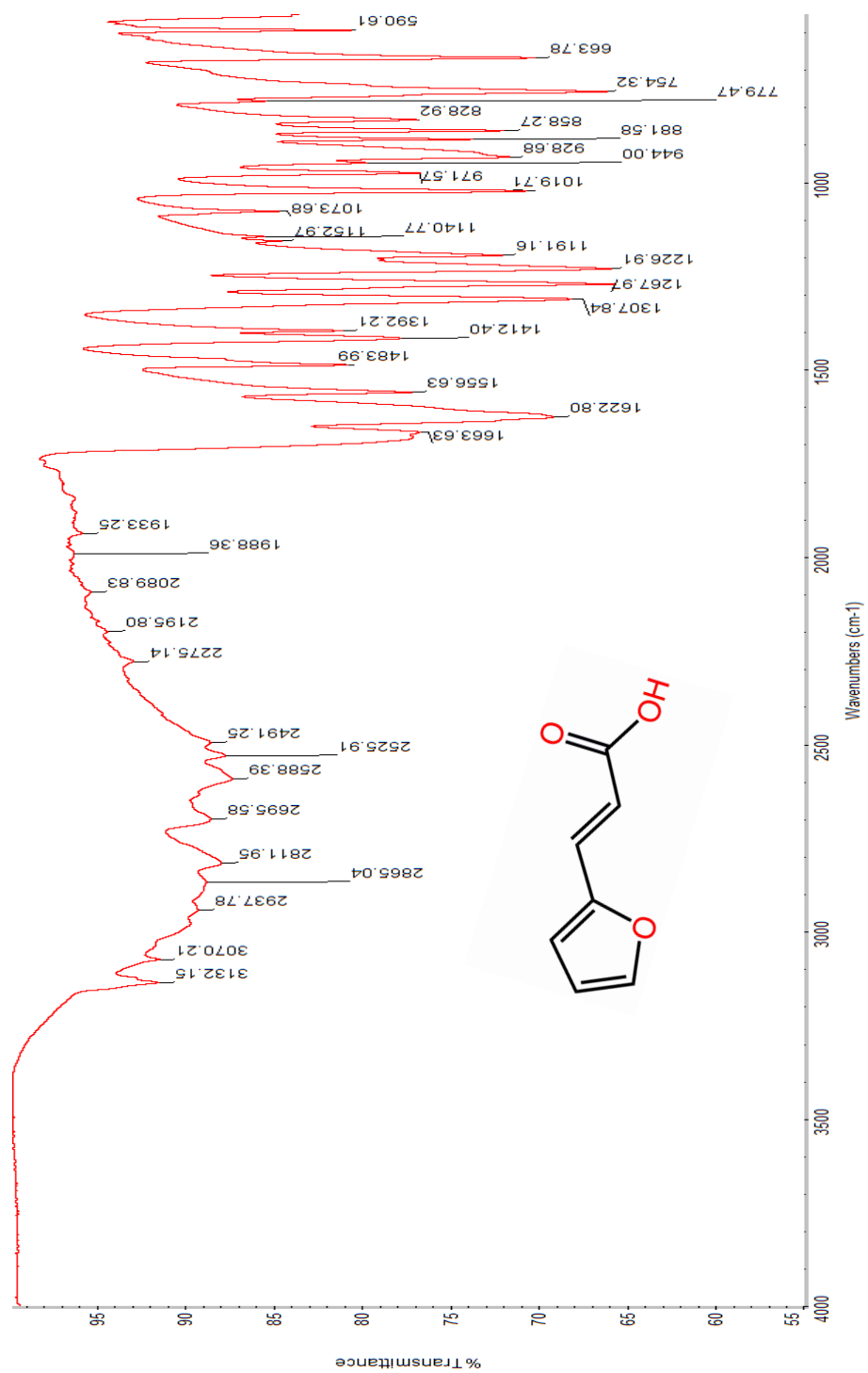


Figure 38. IR spectrum of 3-(2-furyl)acrylic acid **12'**.

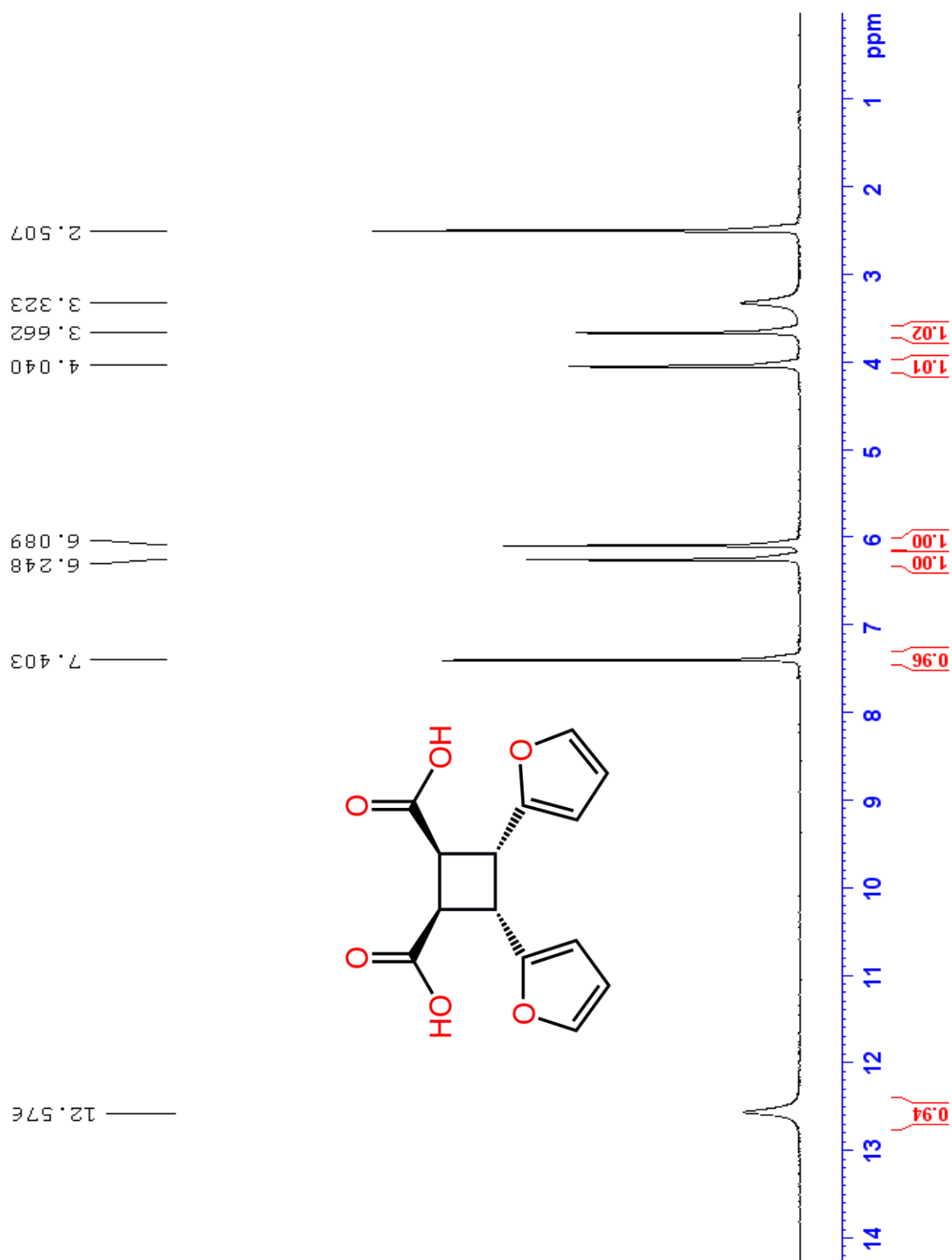


Figure 39. ^1H NMR ($\text{DMSO-}d_6$) spectrum of 3,4-di(furan-2-yl)cyclobutane-1,2-dicarboxylic acid **12** after 6 M HCl (aq.) treatment overnight.

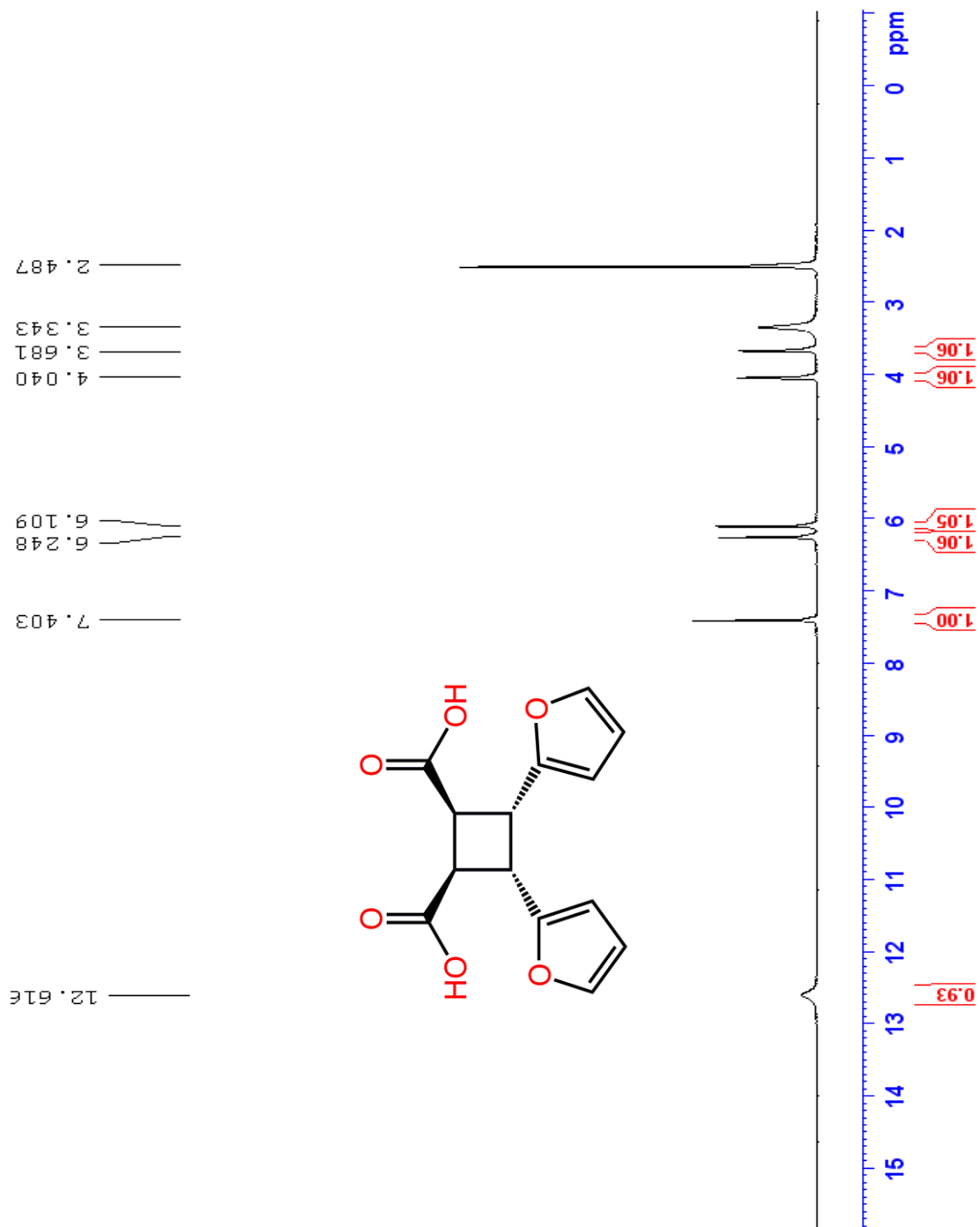


Figure 40. ¹H NMR (DMSO-*d*₆) spectrum of 3,4-di(furan-2-yl)cyclobutane-1,2-dicarboxylic acid **12** after 1 month heat treatment at 100 °C.

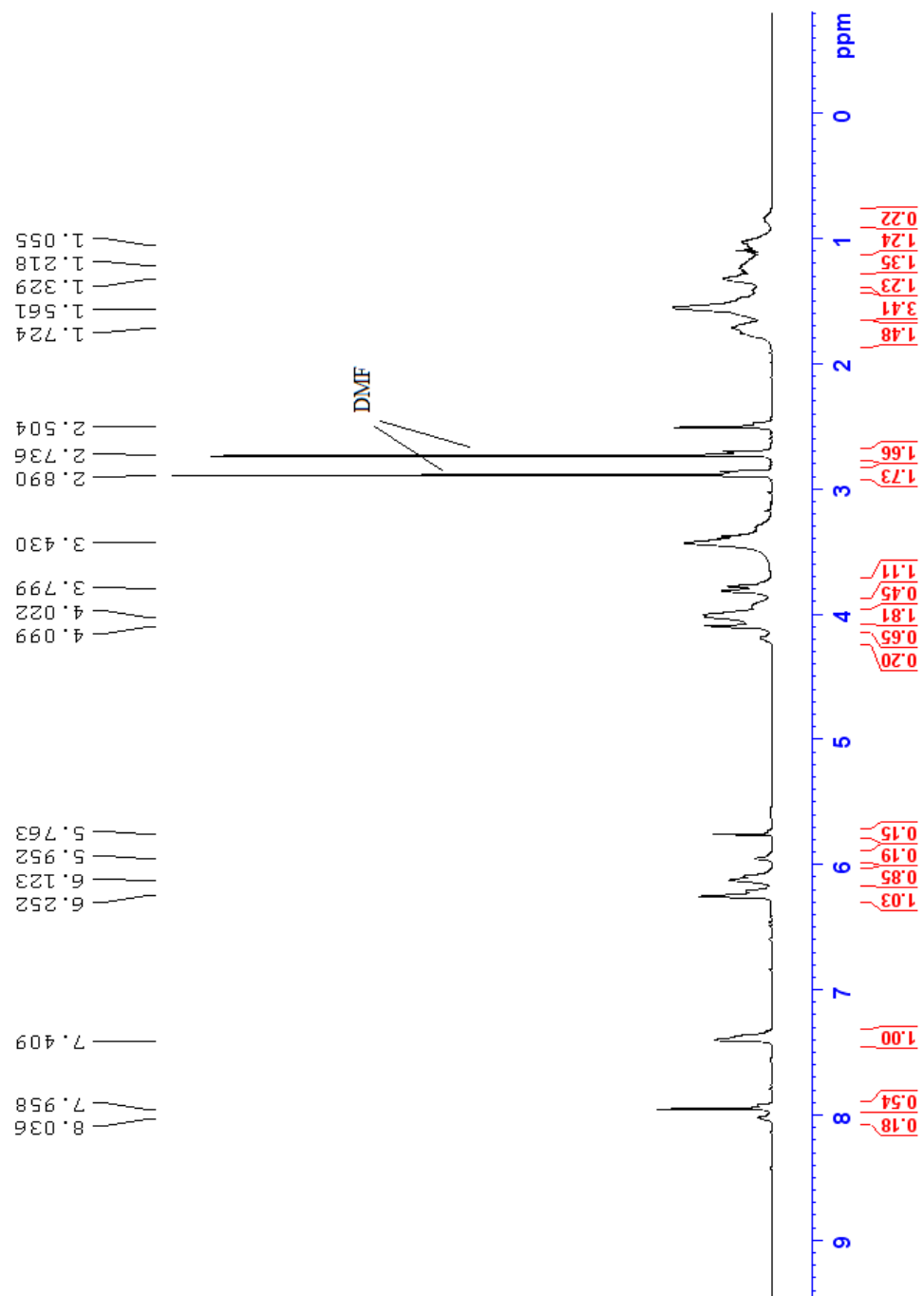


Figure 41. ^1H NMR ($\text{DMSO-}d_6$) spectrum of the polymer product obtained from 3,4-di(furan-2-yl)cyclobutane-1,2-dicarboxylic acid **12** and 1,5-pentanediol.

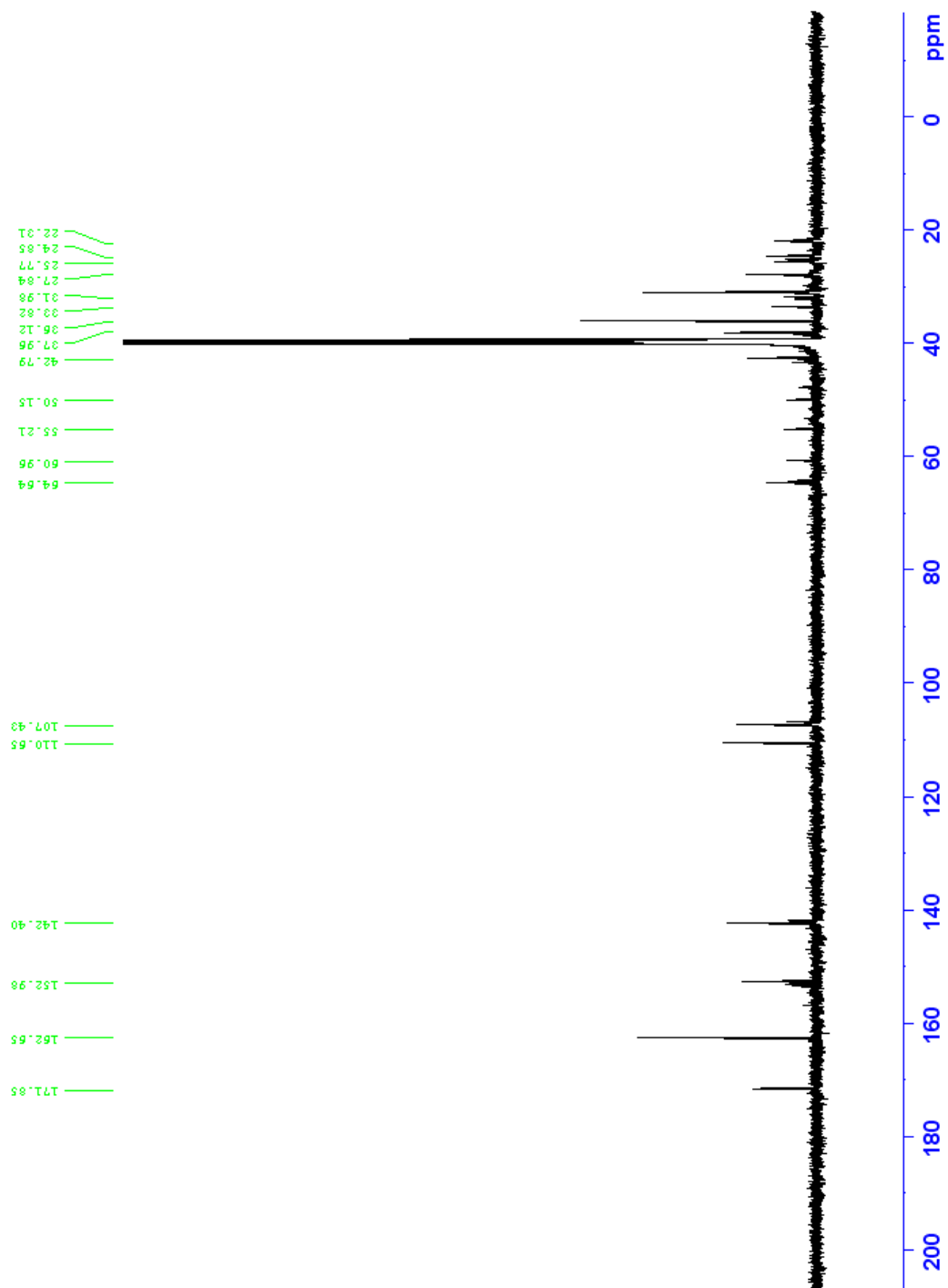


Figure 42. $^{13}\text{C}\{^1\text{H}\}$ NMR ($\text{DMSO-}d_6$) spectrum of the polymer product from 3,4-di(furan-2-yl)cyclobutane-1,2-dicarboxylic acid **12** and 1,5-pentanediol.

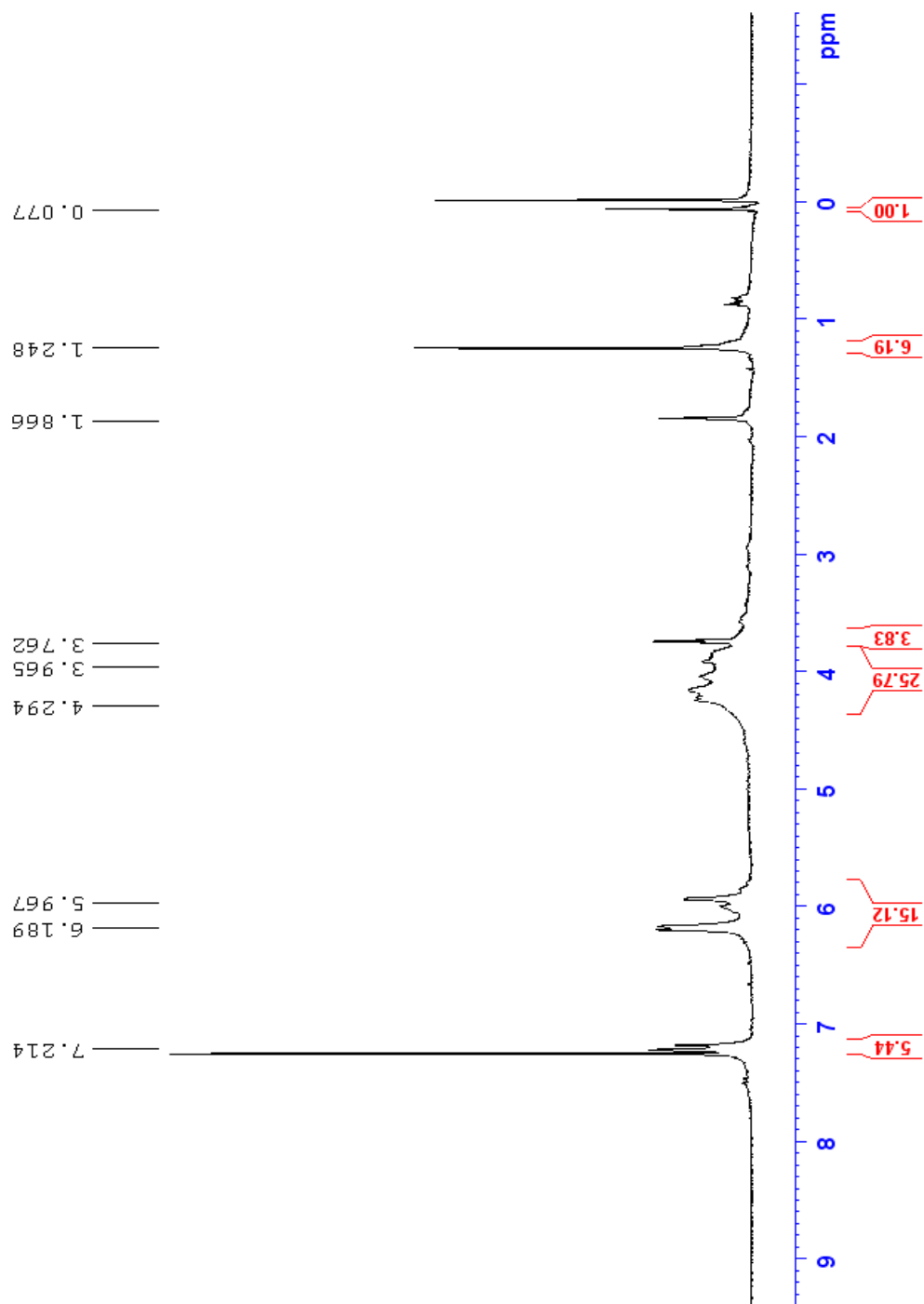


Figure 43. ^1H NMR (CDCl_3) spectrum of the polymer product prepared from 3,4-di(furan-2-yl)cyclobutane-1,2-dicarboxylic acid **12** and glycerol.

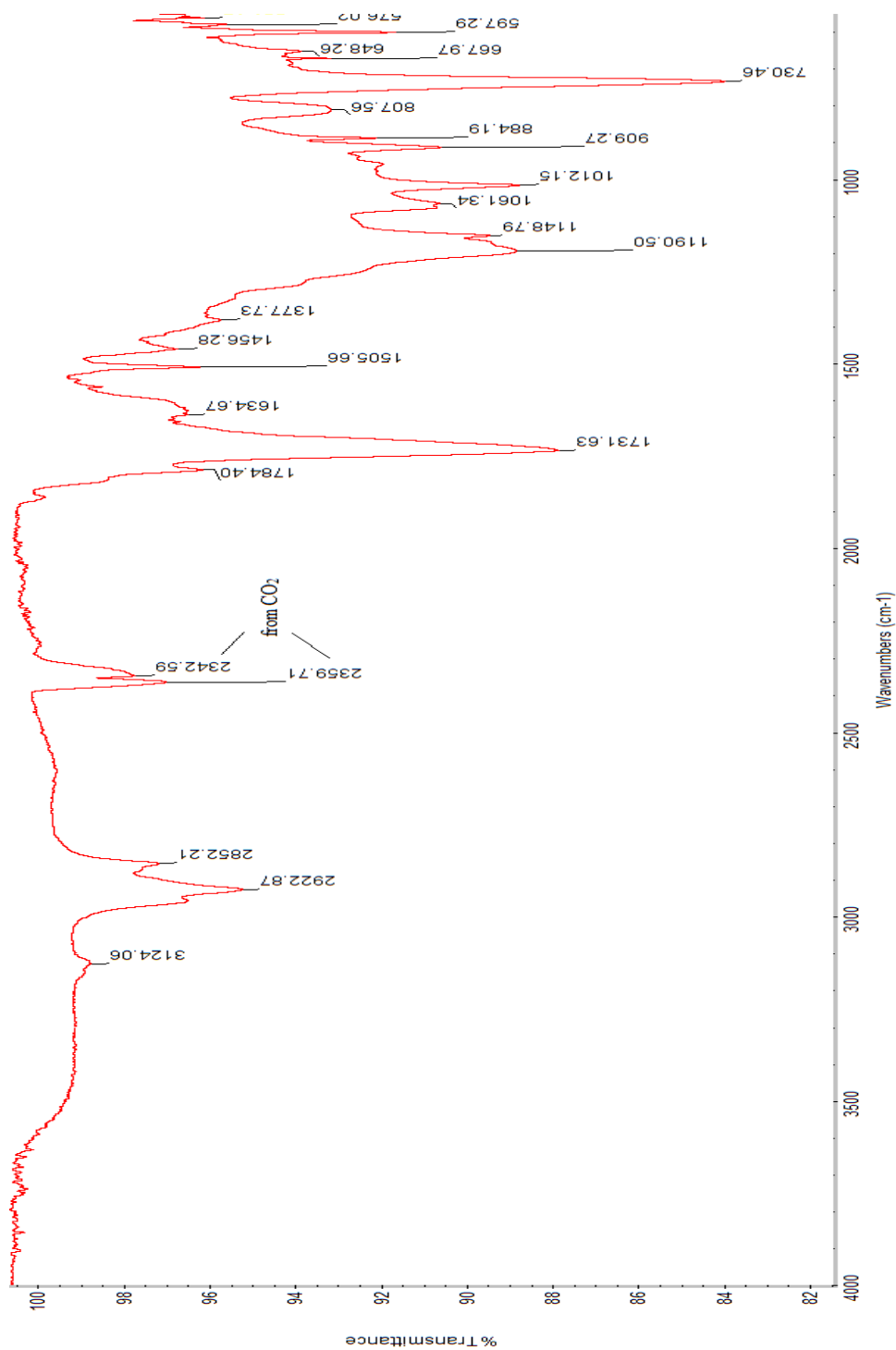


Figure 44. IR spectrum of the polymer product from 3,4-di(furan-2-yl)cyclobutane-1,2-dicarboxylic acid **12** and glycerol.

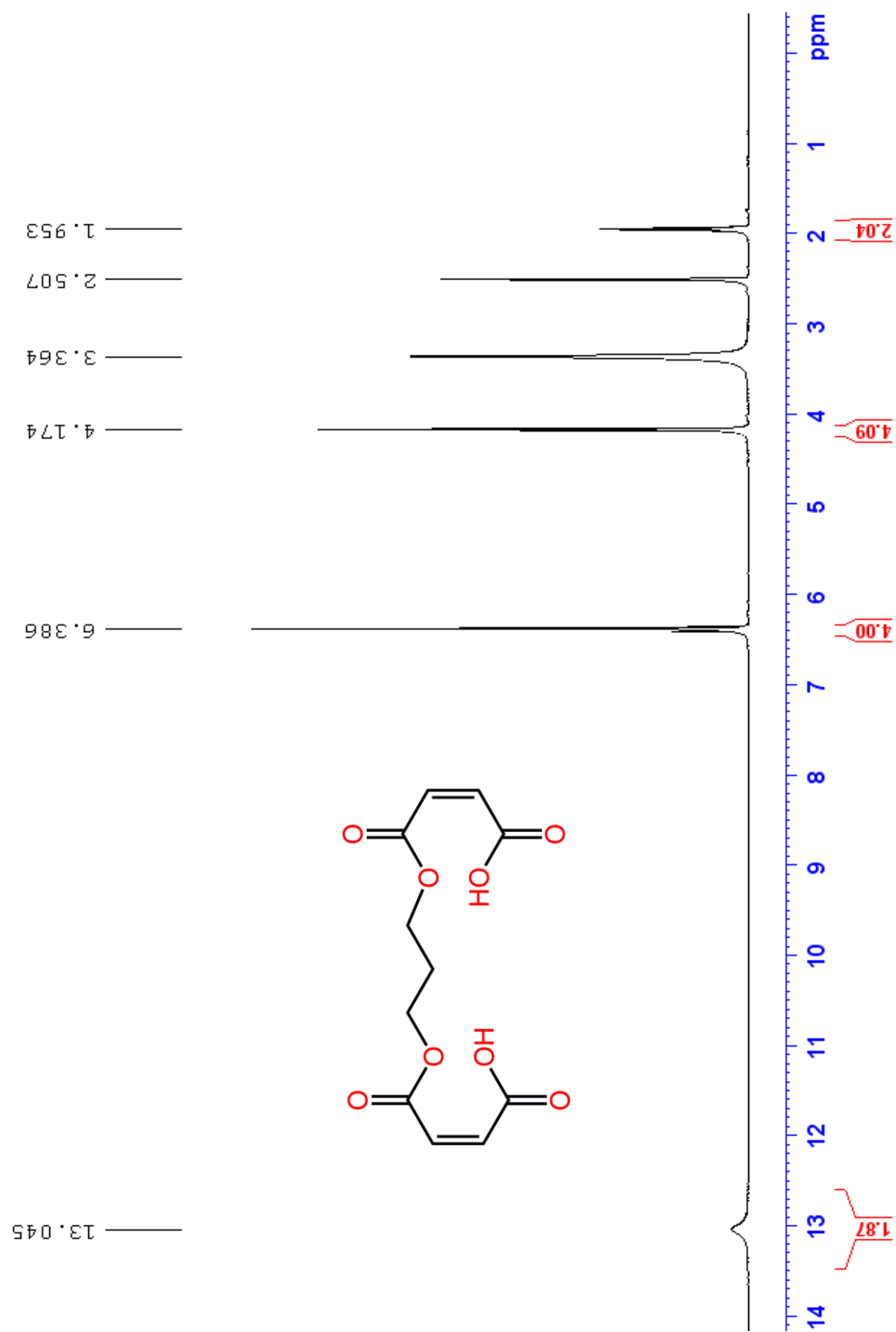


Figure 45. ^1H NMR spectrum of (2Z,2'Z)-4,4'-[propane-1,3-diylbis(oxy)]bis(4-oxobut-2-enoic acid) **13** in $\text{DMSO-}d_6$.

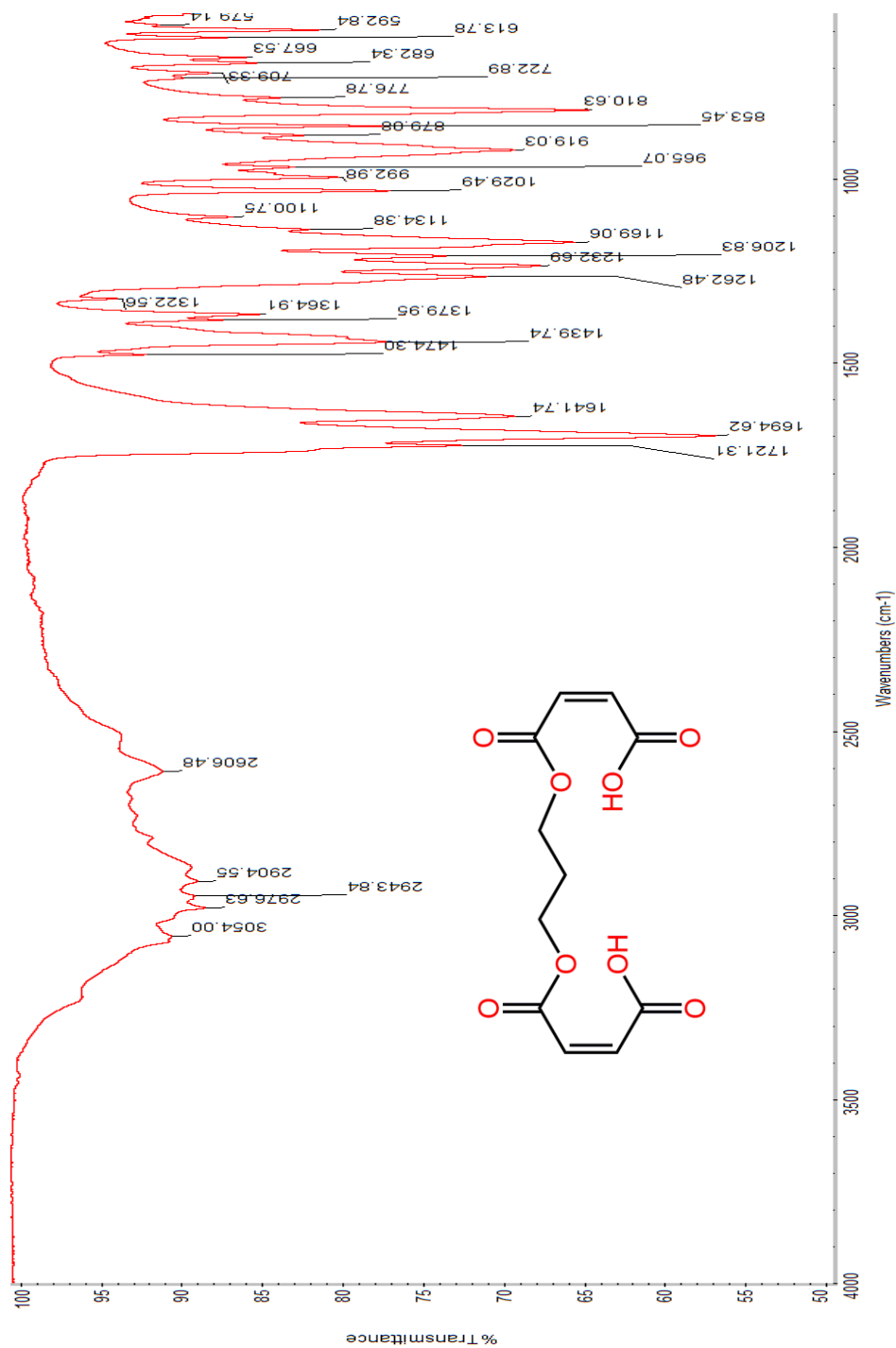


Figure 46. IR spectrum of (2Z,2'Z)-4,4'-[propane-1,3-diylbis(oxy)]bis(4-oxobut-2-enoic acid) **13**.

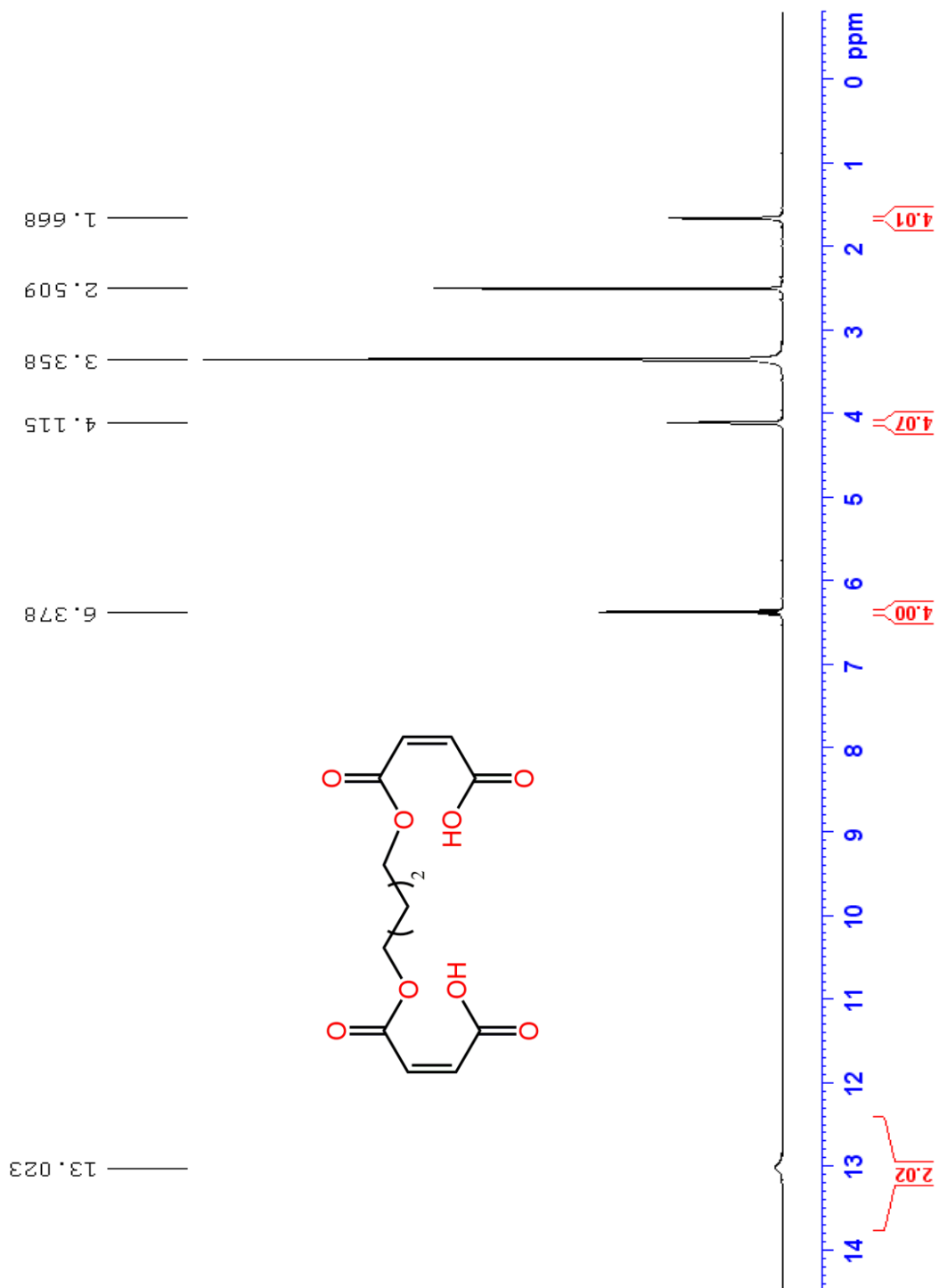


Figure 47. ¹H NMR spectrum of (2Z,2'Z)-4,4'-[butane-1,4-diylbis(oxy)]bis(4-oxobut-2-enoic acid) **14** in DMSO-*d*₆.

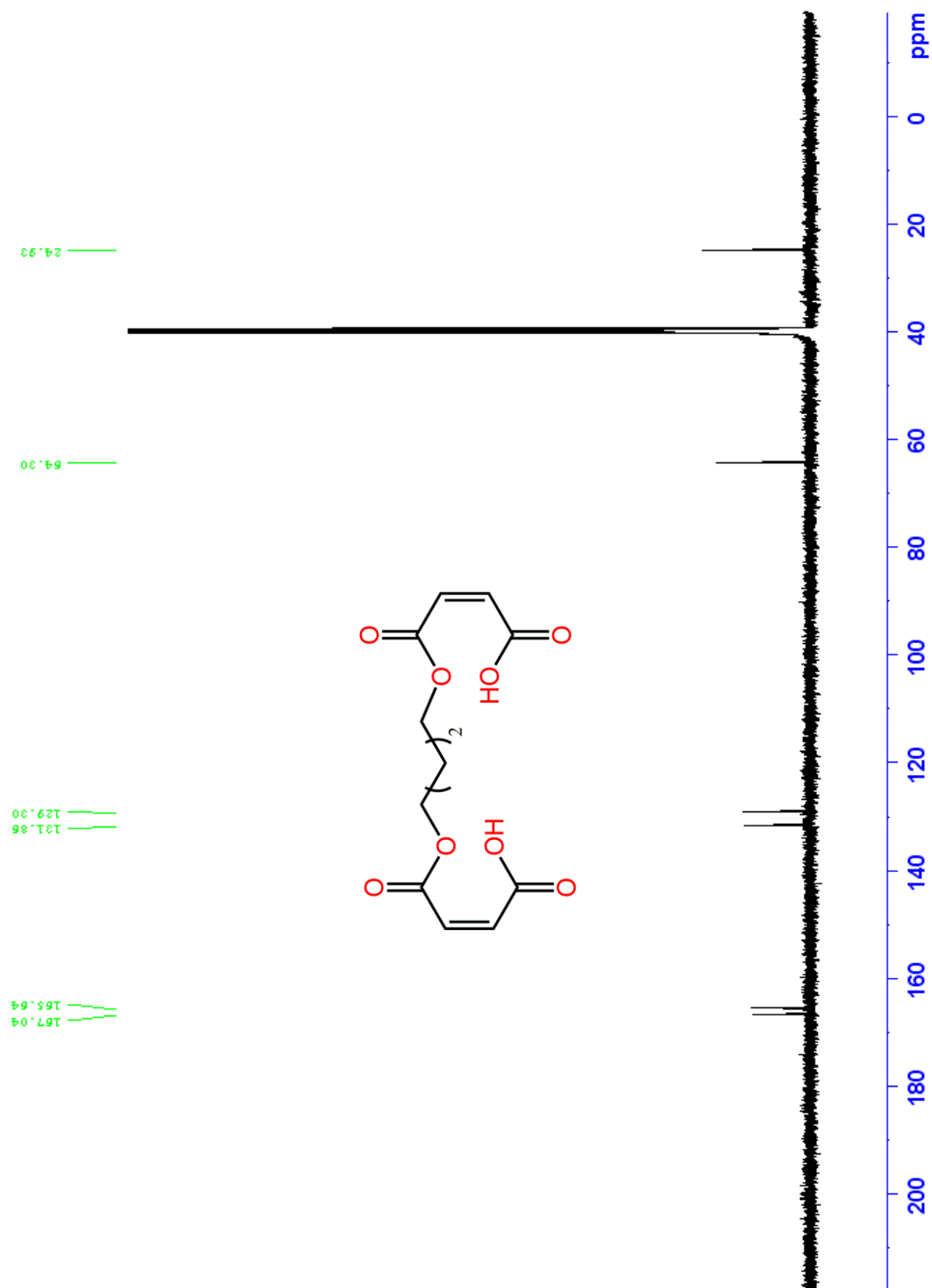


Figure 48. $^{13}\text{C}\{^1\text{H}\}$ NMR spectrum of $(Z,Z,2'Z)$ -4,4'-[butane-1,4-diylbis(oxy)]bis(4-oxobut-2-enoic acid) **14** in $\text{DMSO-}d_6$.

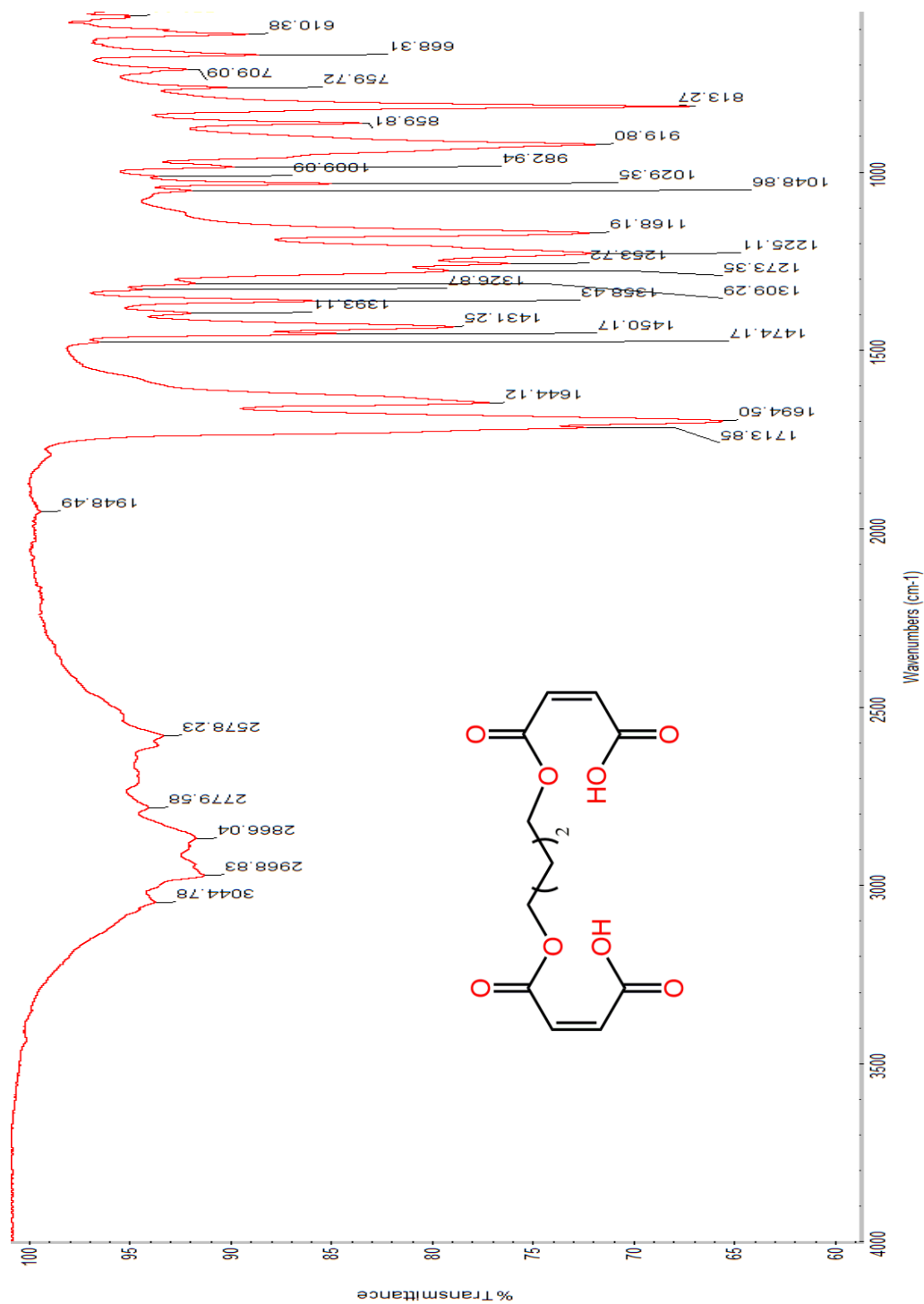


Figure 49. IR spectrum of (2Z,2'Z)-4,4'-[butane-1,4-diylbis(oxy)]bis(4-oxobut-2-enoic acid) **14**.

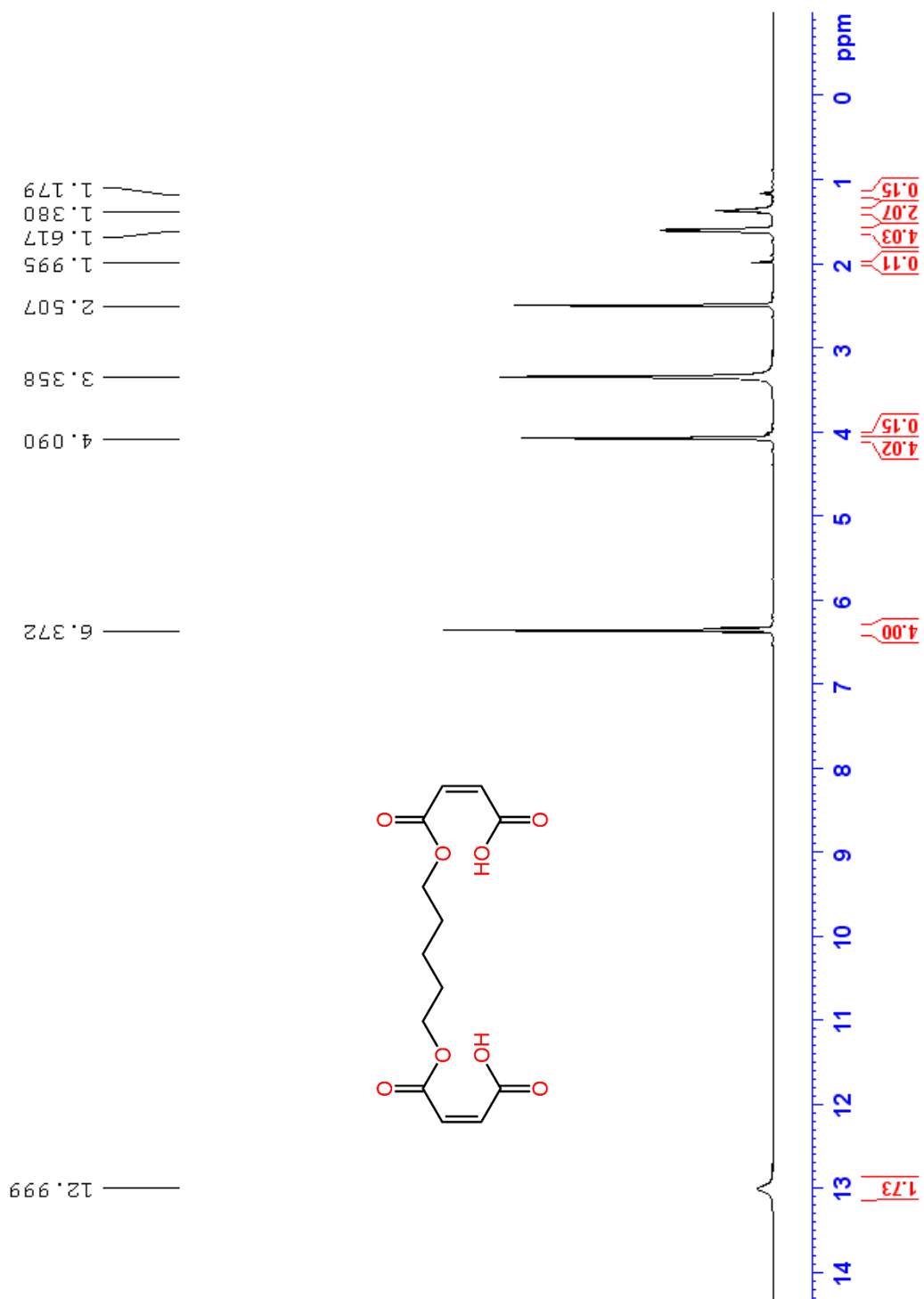


Figure 50. ¹H NMR spectrum of (2Z,2'Z)-4,4'-[pentane-1,5-diylbis(oxy)]bis(4-oxobut-2-enoic acid) **15** in DMSO-*d*₆.

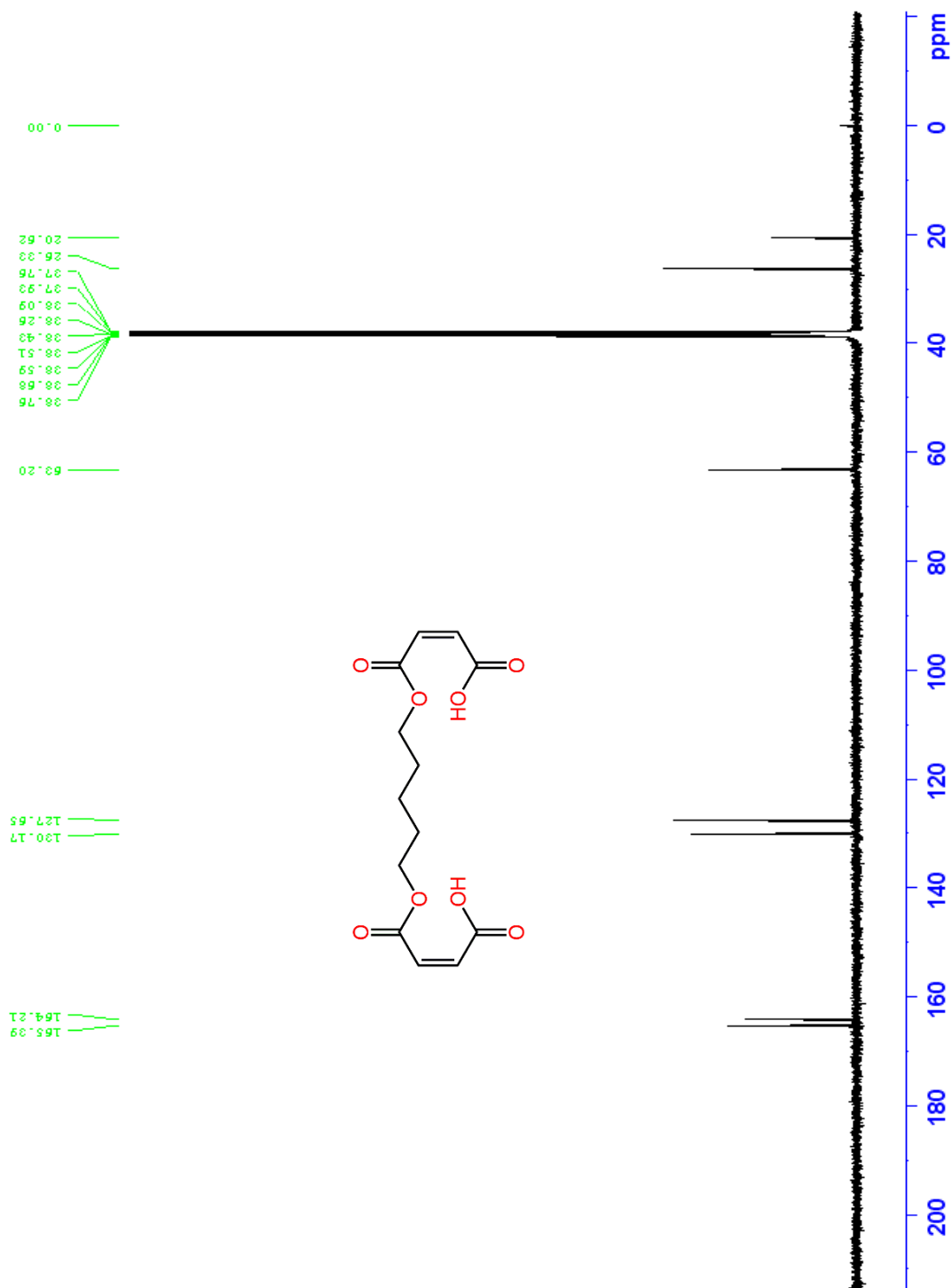


Figure 51. $^{13}\text{C}\{^1\text{H}\}$ NMR spectrum of (2Z,2'Z)-4,4'-[pentane-1,5-diylbis(oxy)]bis(4-oxobut-2-enoic acid) **15** in $\text{DMSO-}d_6$.

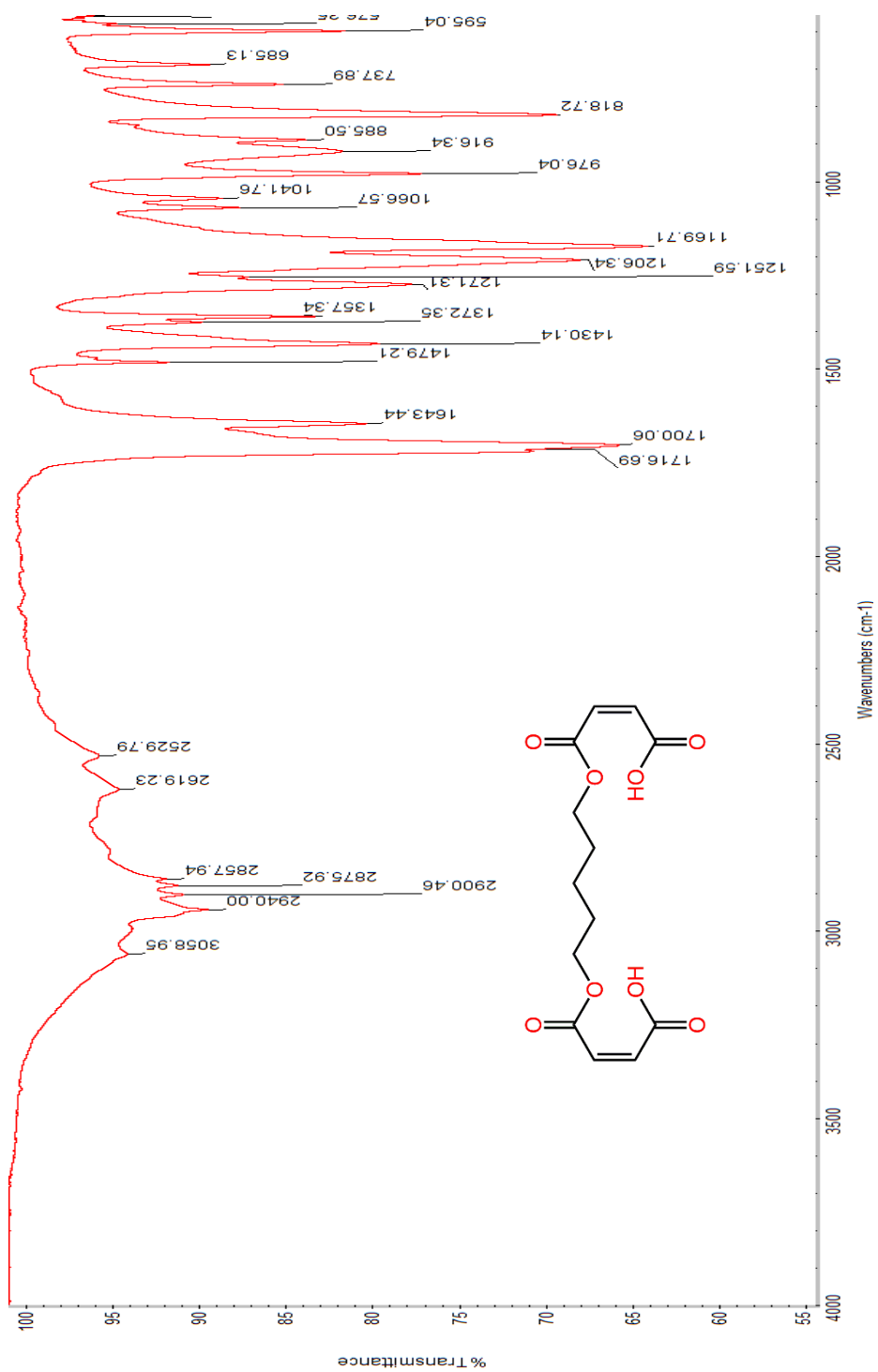


Figure 52. IR spectrum of (2Z,2'Z)-4,4'-[pentane-1,5-diylbis(oxy)]bis(4-oxobut-2-enoic acid) **15**.

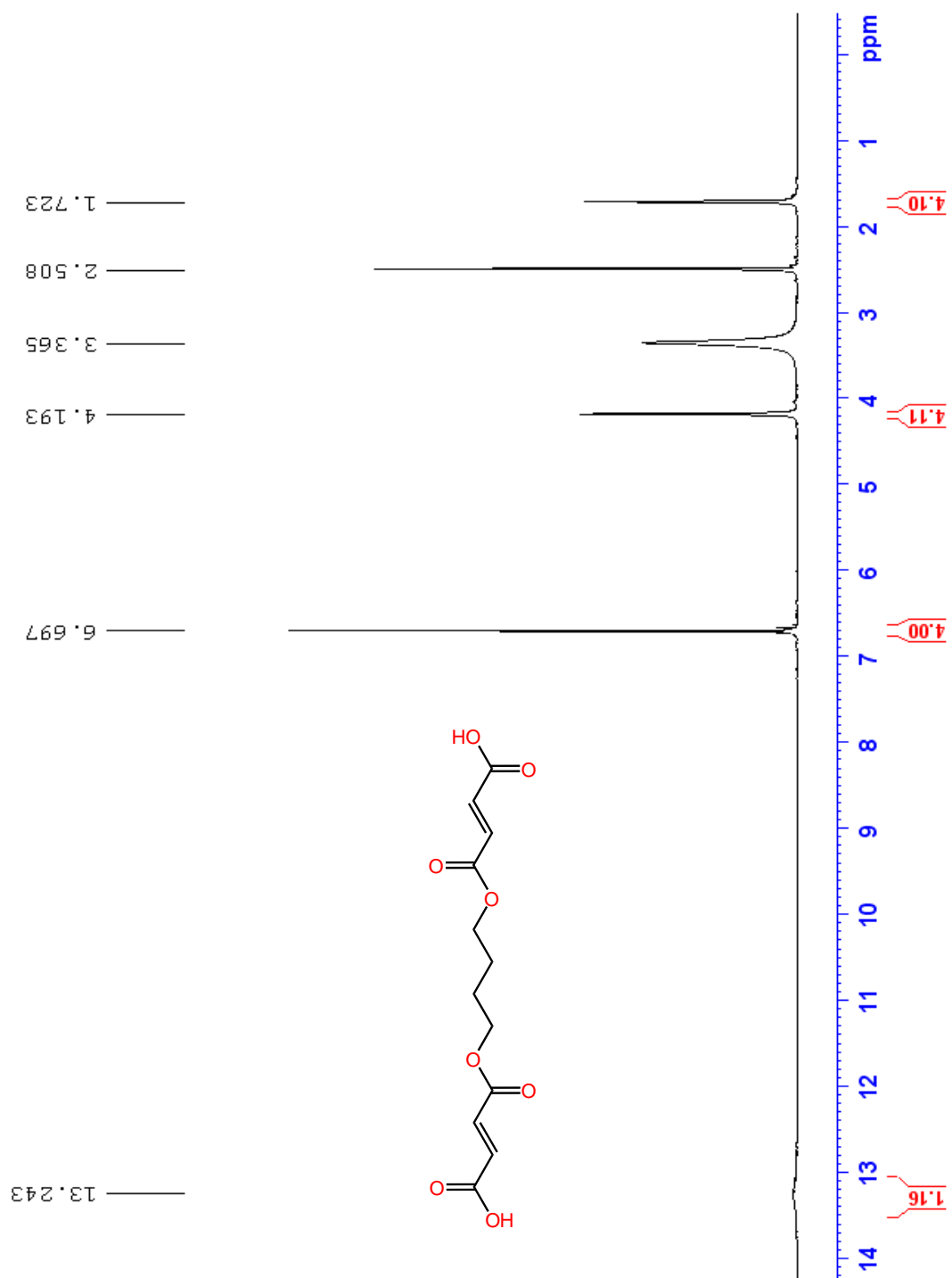


Figure 53. ^1H NMR spectrum of $(2E,2'E)$ -4,4'-[butane-1,4-diylbis(oxy)]bis(4-oxobut-2-enoic acid) **16** in $\text{DMSO-}d_6$.

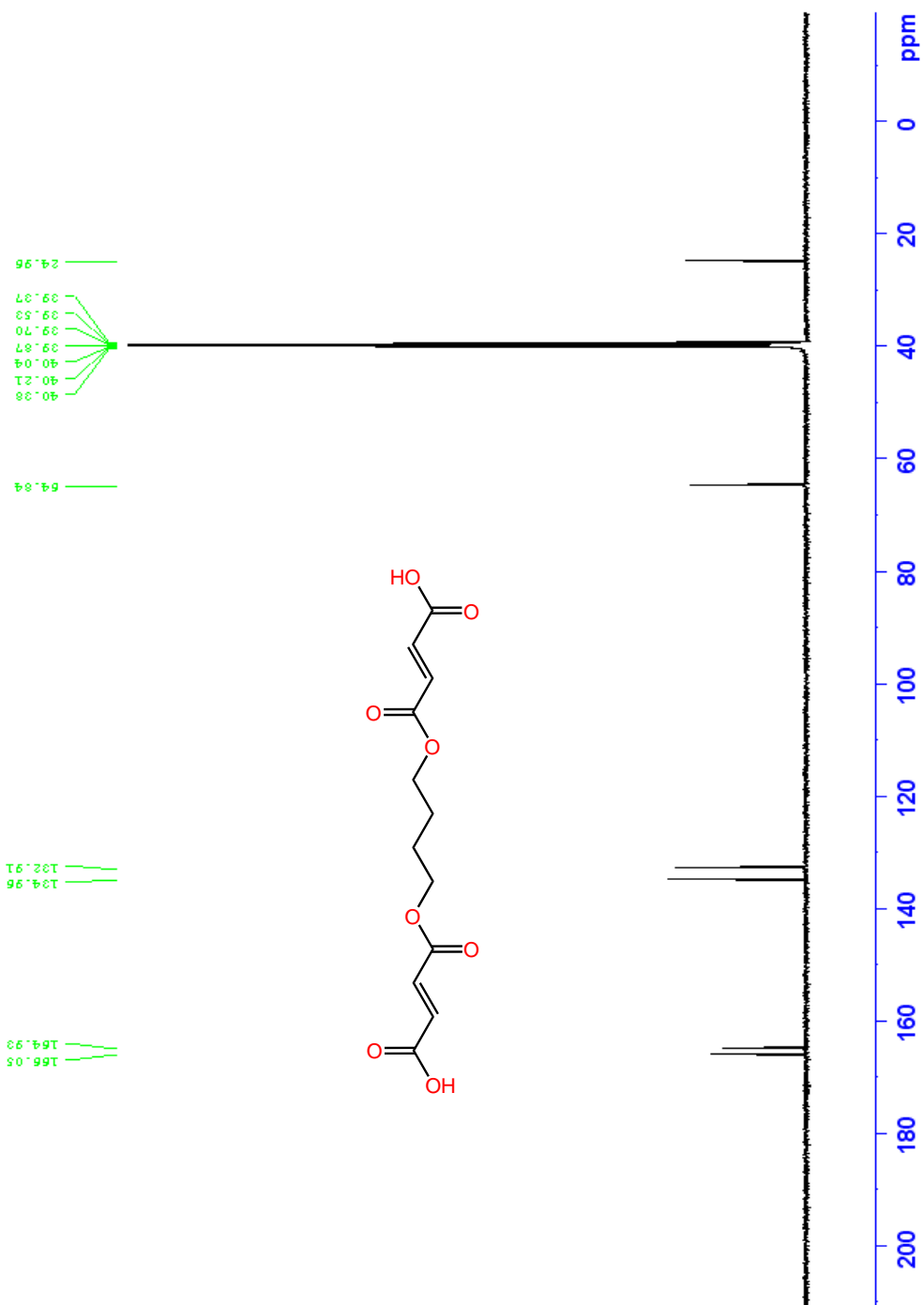


Figure 54. $^{13}\text{C}\{^1\text{H}\}$ NMR spectrum of $(2E,2'E)$ -4,4'-[butane-1,4-diylbis(oxy)]bis(4-oxobut-2-enoic acid) **16** in $\text{DMSO-}d_6$.

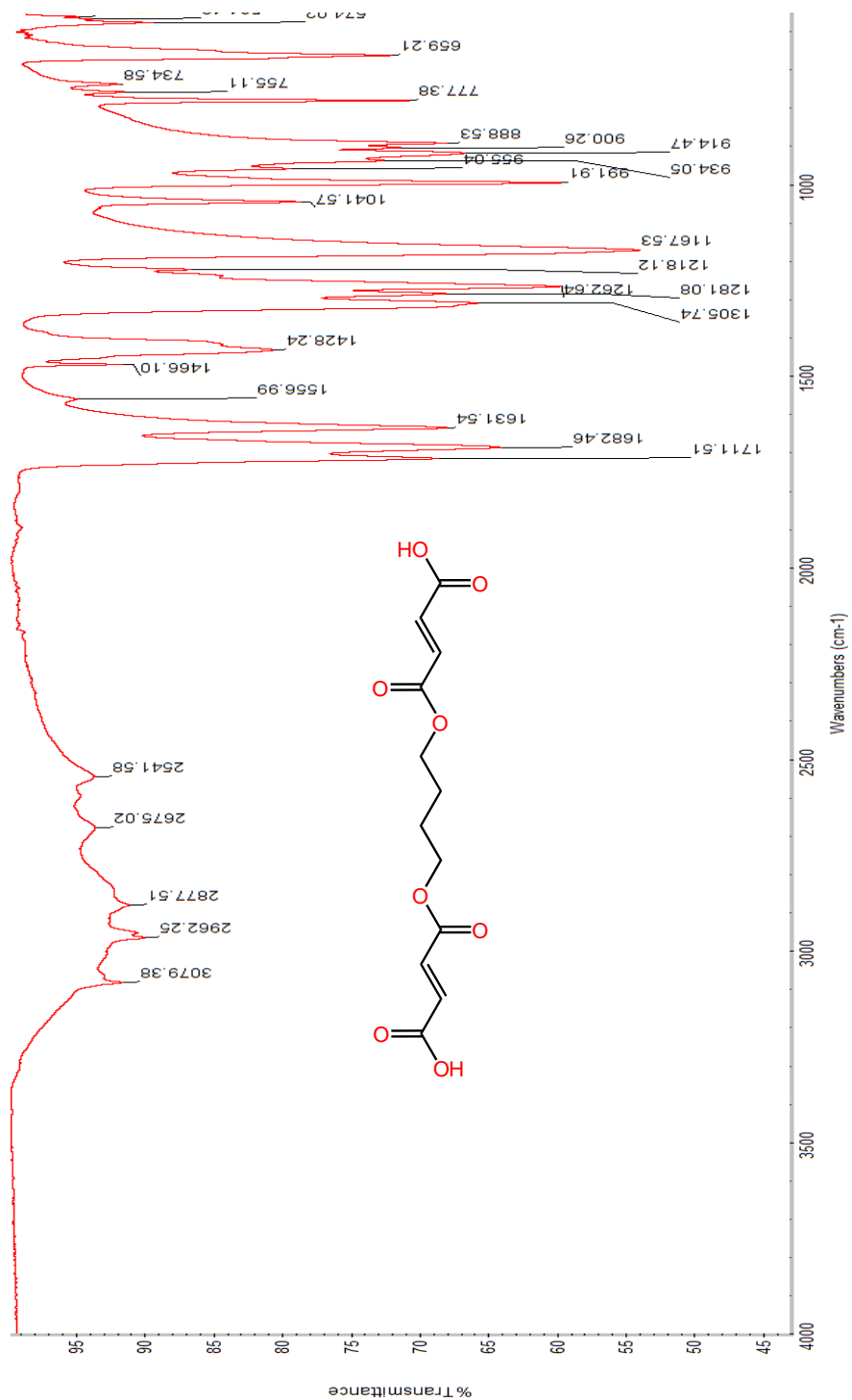


Figure 55. IR spectrum of (2E,2'E)-4,4'-[butane-1,4-diylbis(oxy)]bis(4-oxobut-2-enoic acid) **16**.

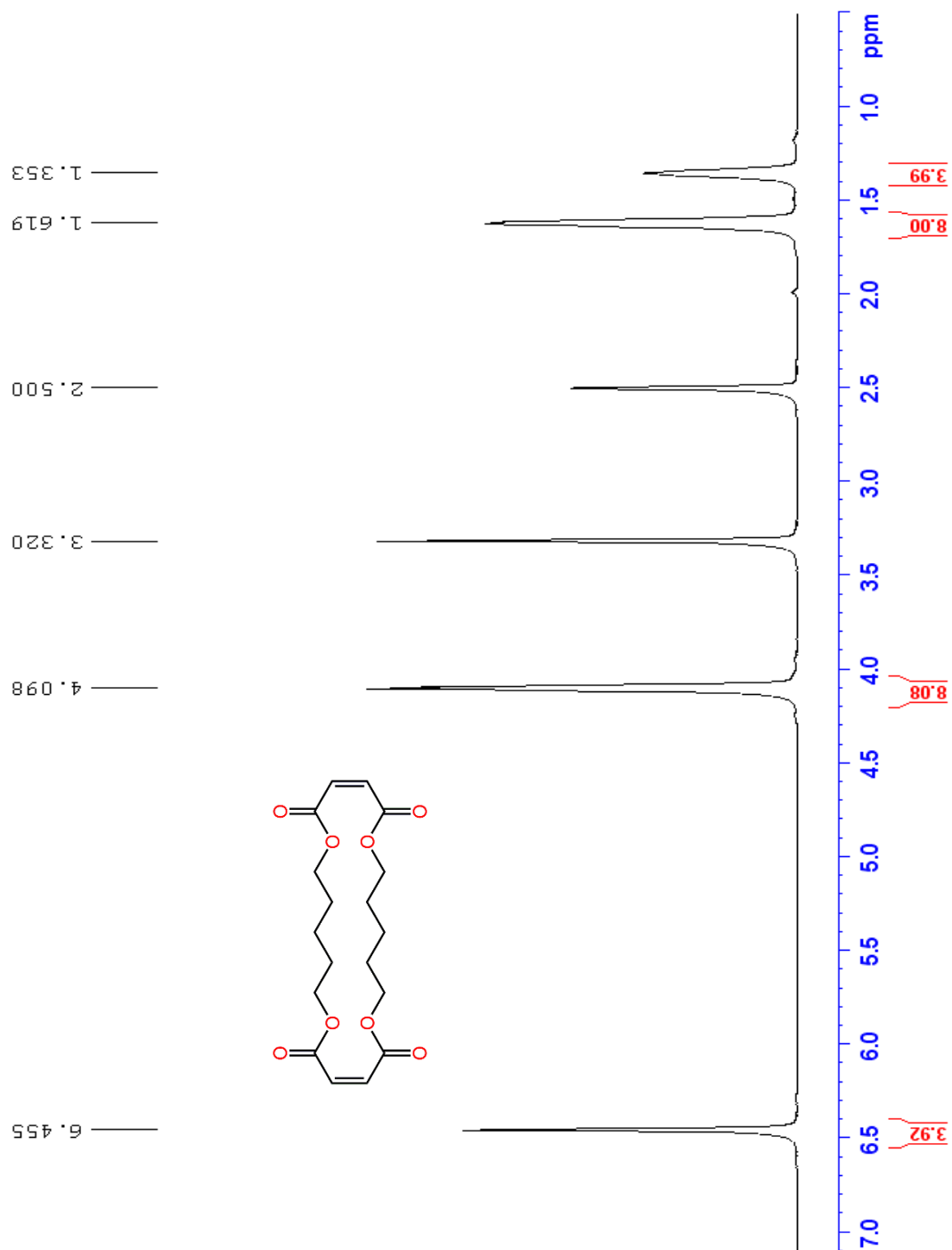


Figure 56. ^1H NMR spectrum of (3Z,14Z)-1,6,12,17-tetraoxacyclodocosa-3,14-diene-2,5,13,16-tetraone **17** in $\text{DMSO-}d_6$.

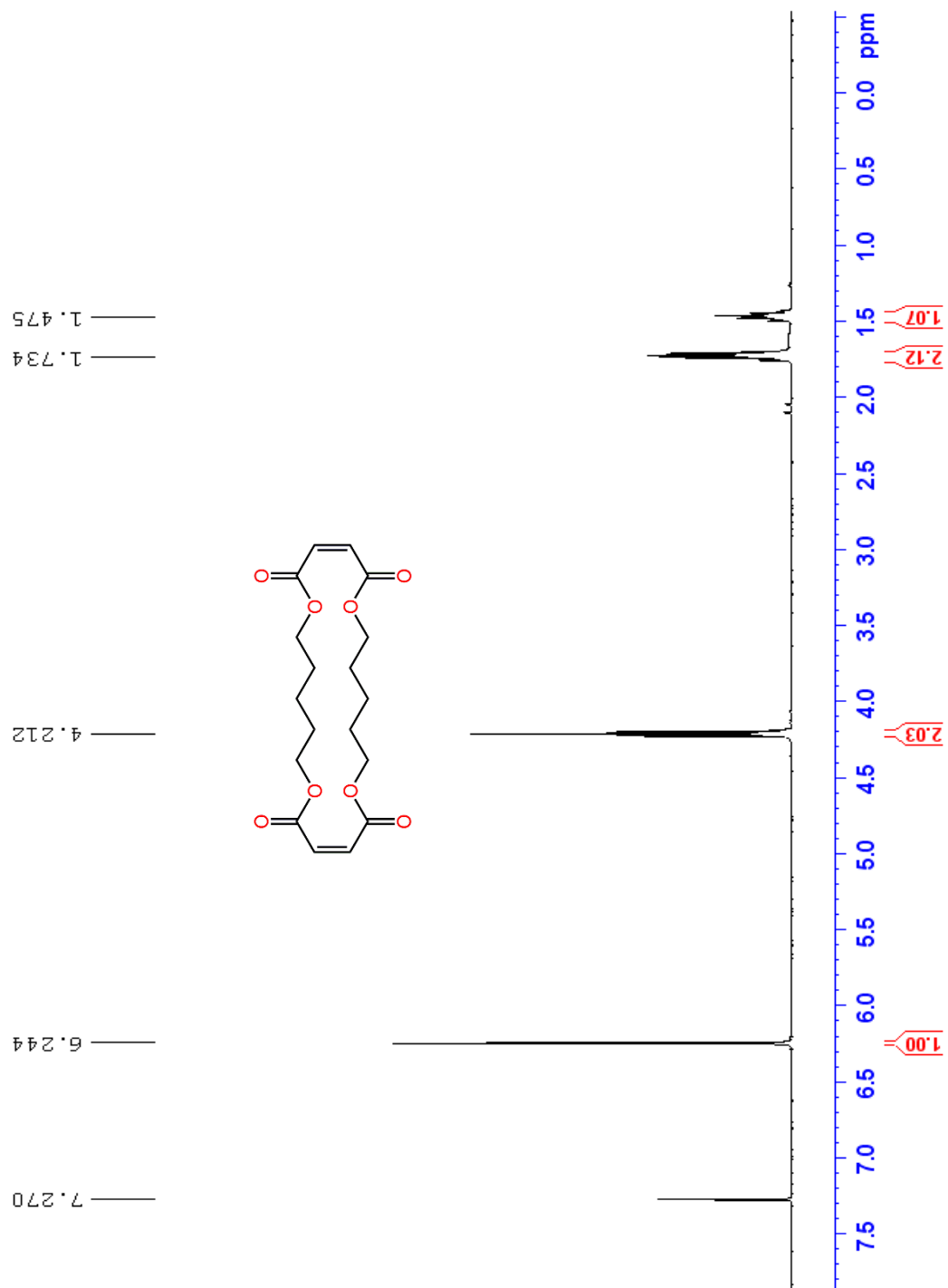


Figure 57. ^1H NMR spectrum of (3Z,14Z)-1,6,12,17-tetraoxacyclodocosa-3,14-diene-2,5,13,16-tetraone **17** in CDCl_3 .

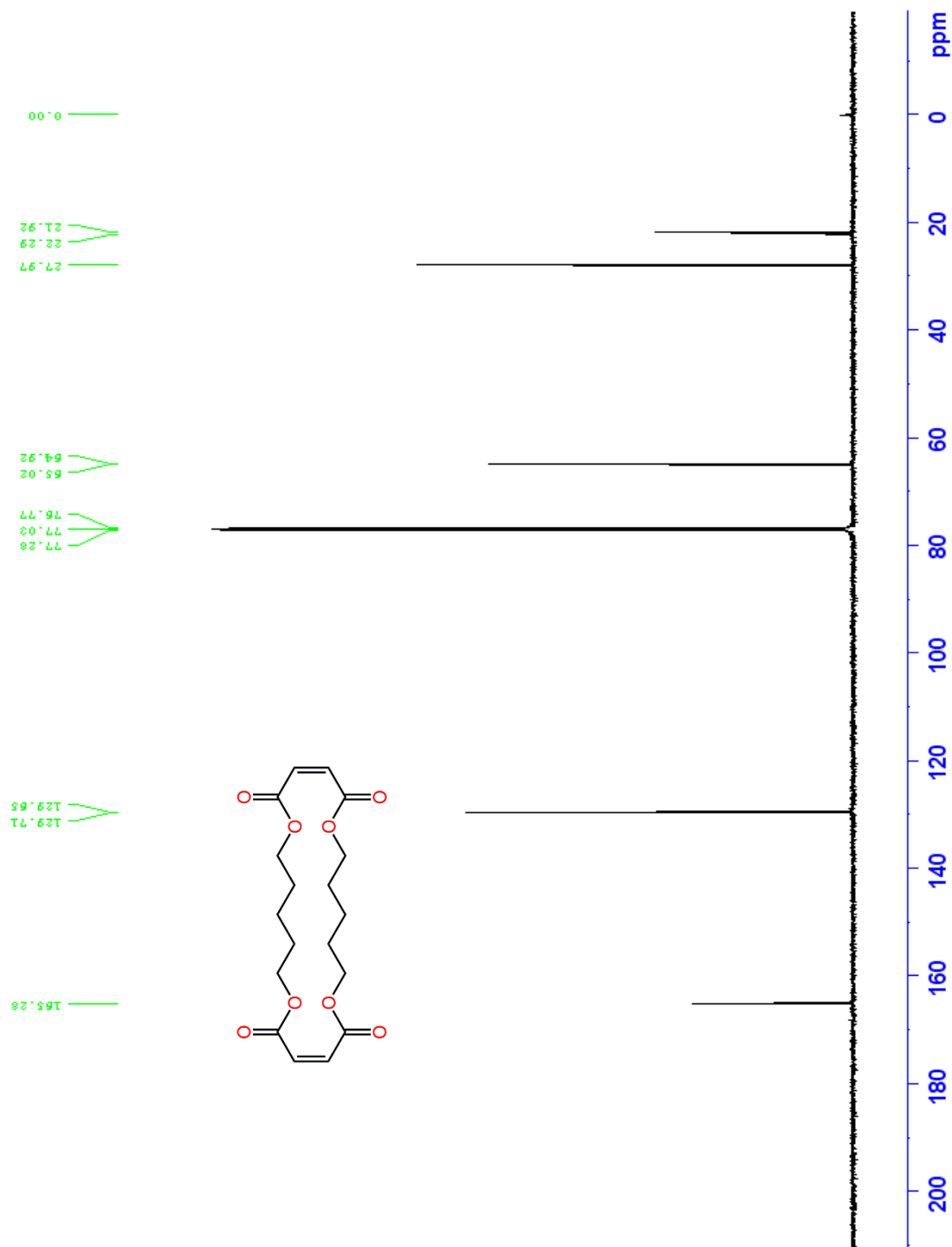


Figure 58. $^{13}\text{C}\{^1\text{H}\}$ NMR spectrum of (3Z,14Z)-1,6,12,17-tetraoxacyclodocosa-3,14-diene-2,5,13,16-tetraone **17** in CDCl_3 .

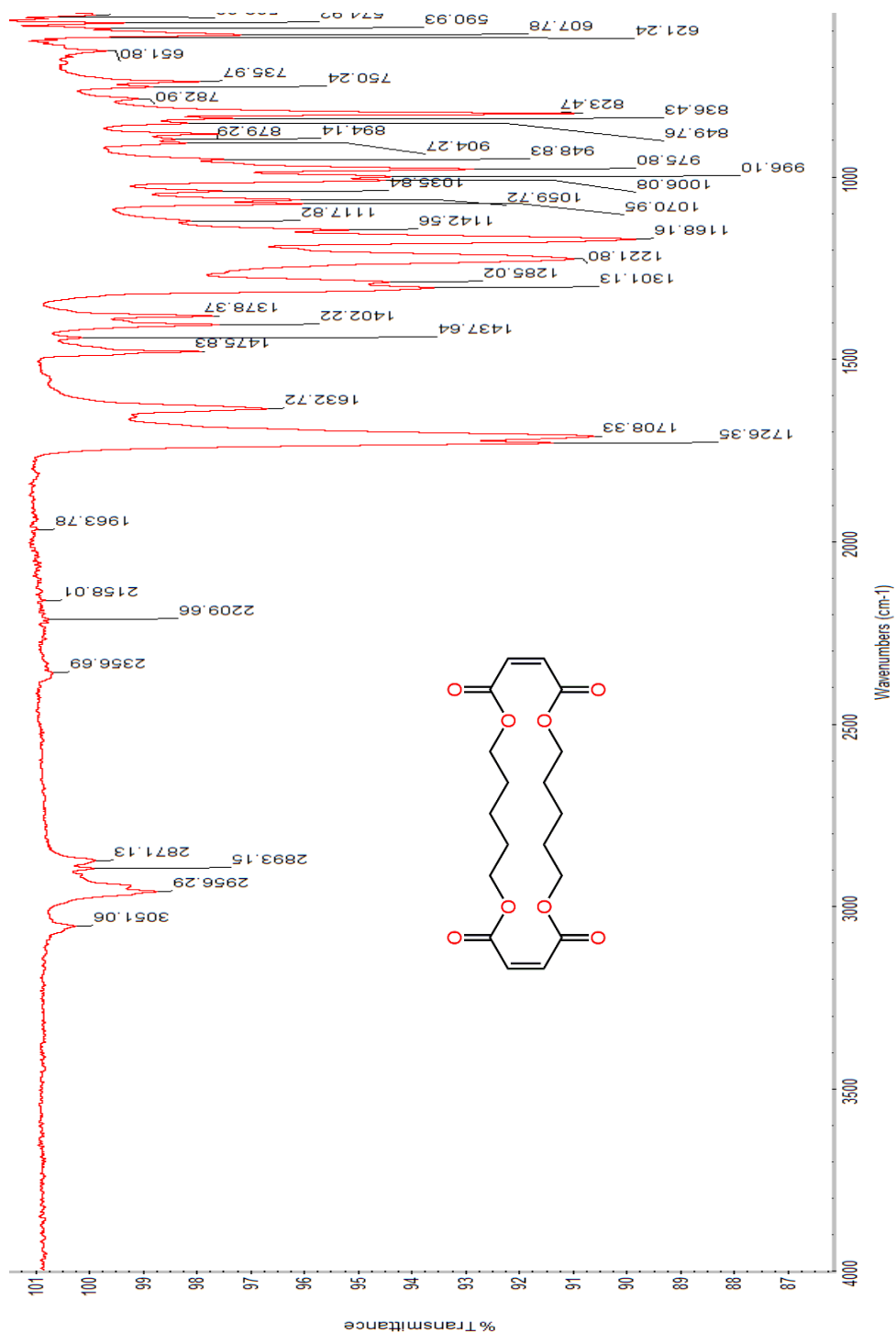


Figure 59. IR spectrum of (3Z,14Z)-1,6,12,17-tetraoxacyclodocosa-3,14-diene-2,5,13,16-tetraone **17**.

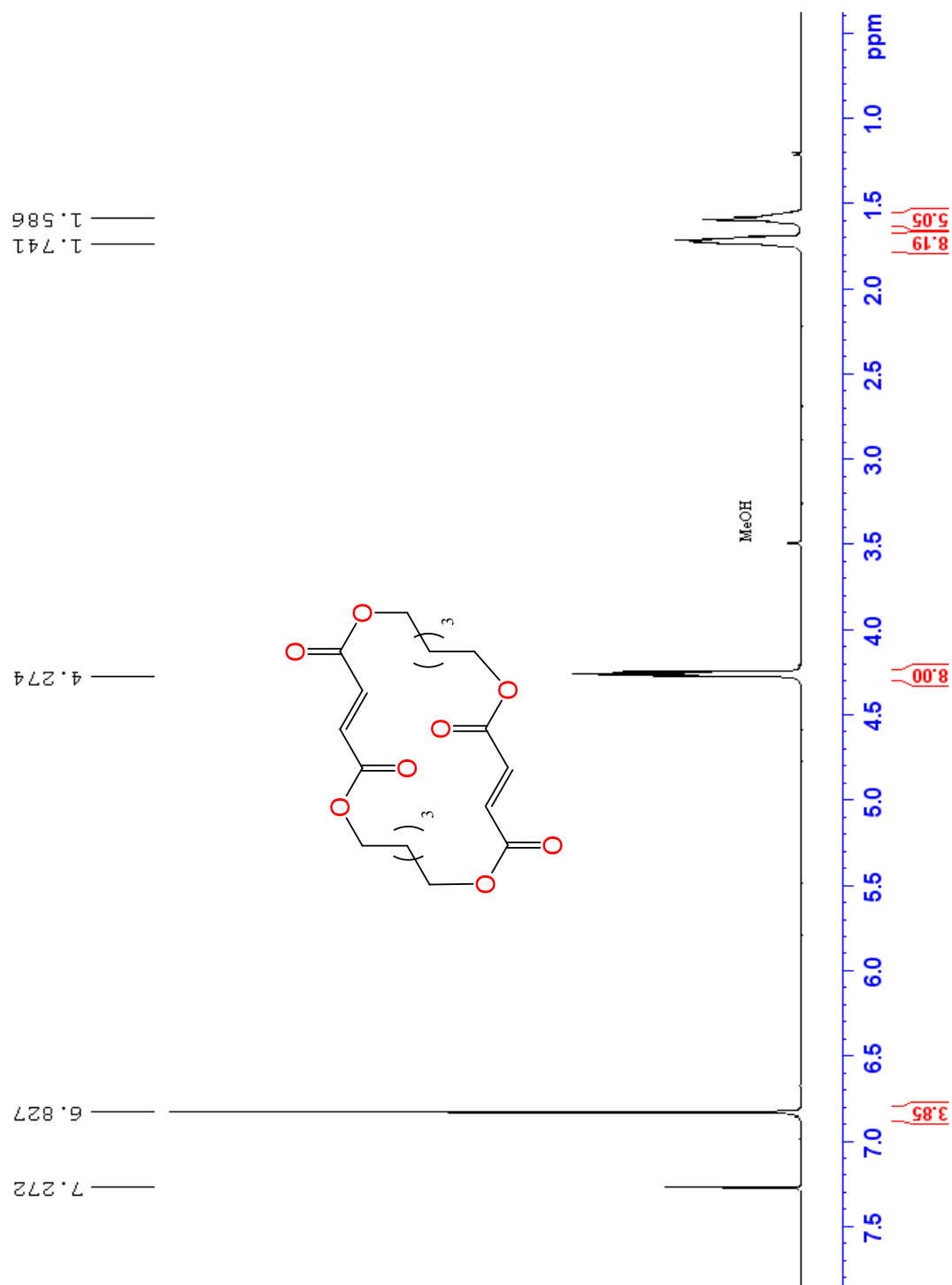


Figure 60. ¹H NMR spectrum of (3*E*,14*E*)-1,6,12,17-tetraoxacyclodocosa-3,14-diene-2,5,13,16-tetraone **18** in CDCl₃.

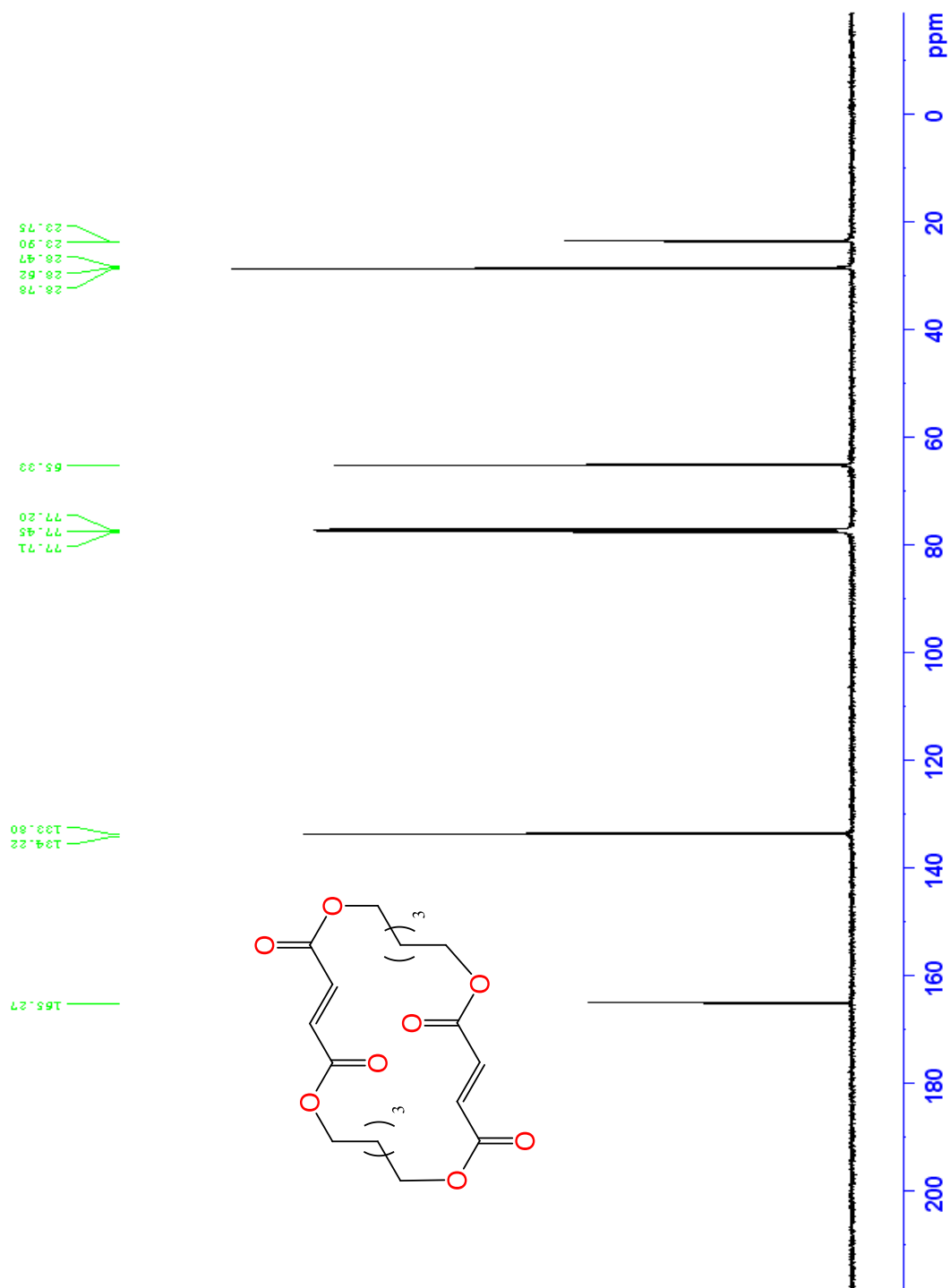


Figure 61. $^{13}\text{C}\{^1\text{H}\}$ NMR spectrum of (3*E*,14*E*)-1,6,12,17-tetraoxacyclodocosa-3,14-diene-2,5,13,16-tetraone **18** in CDCl_3 .

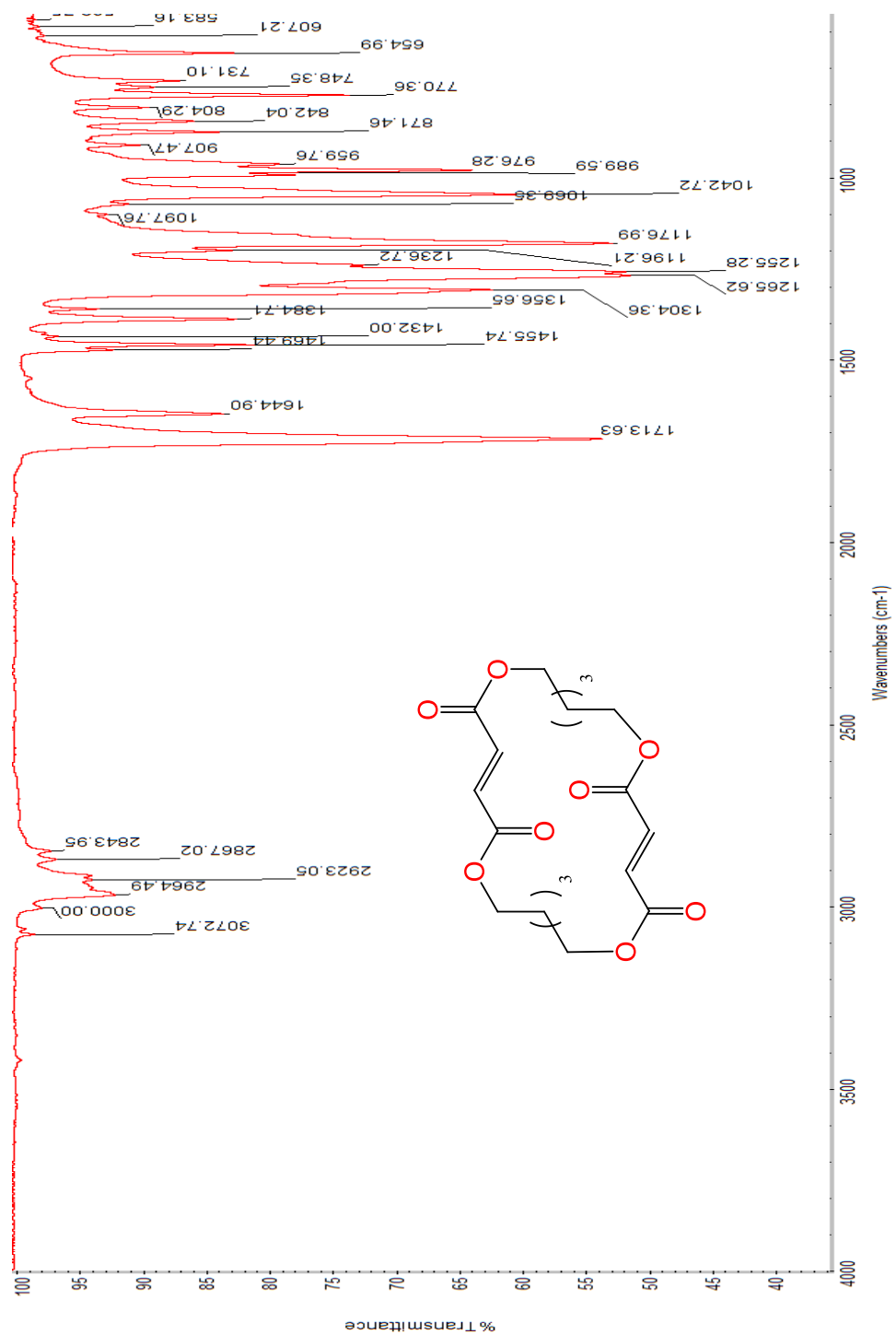


Figure 62. IR spectrum of (3E,14E)-1,6,12,17-tetraoxacyclodocosa-3,14-diene-2,5,13,16-tetraone **18**.

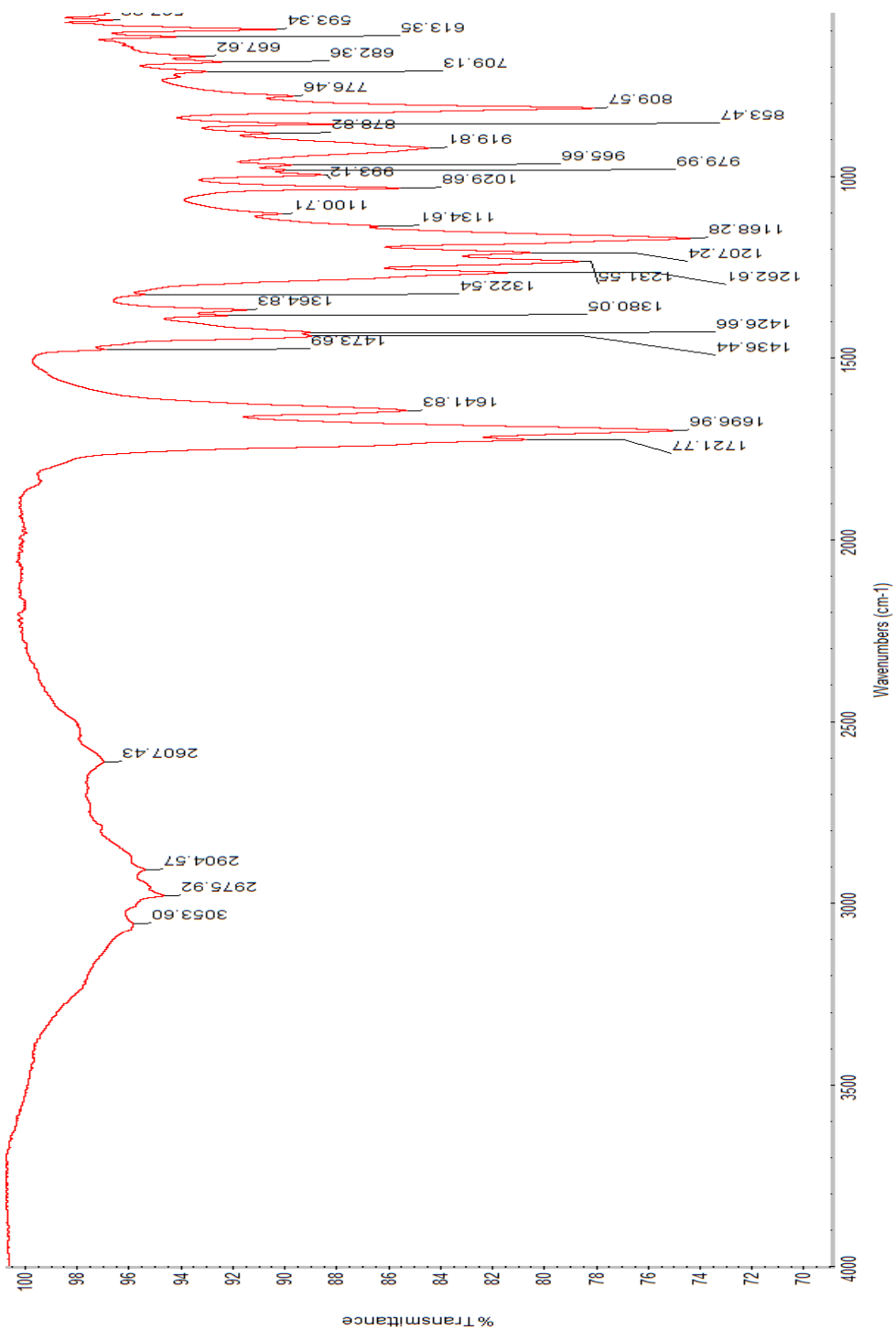


Figure 63. IR spectrum of (2Z,2'Z)-4,4'-[propane-1,3-diylbis(oxy)]bis(4-oxobut-2-enoic acid) **14** after 27 h mercury lamp UV irradiation.

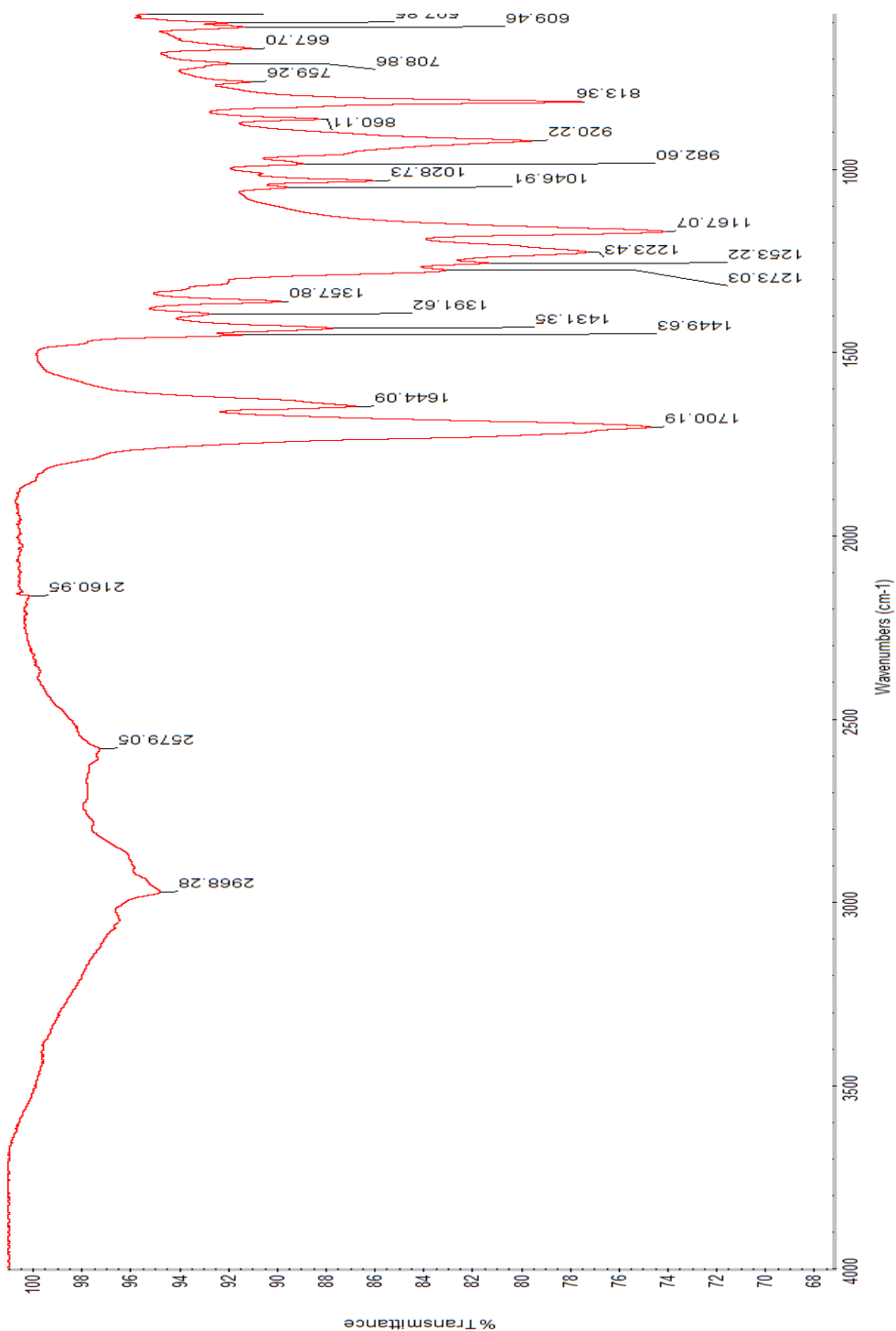


Figure 64. IR spectrum of (2Z,2'Z)-4,4'-[butane-1,3-diylbis(oxy)]bis(4-oxobut-2-enoic acid) **14** after 27 h mercury lamp UV irradiation.

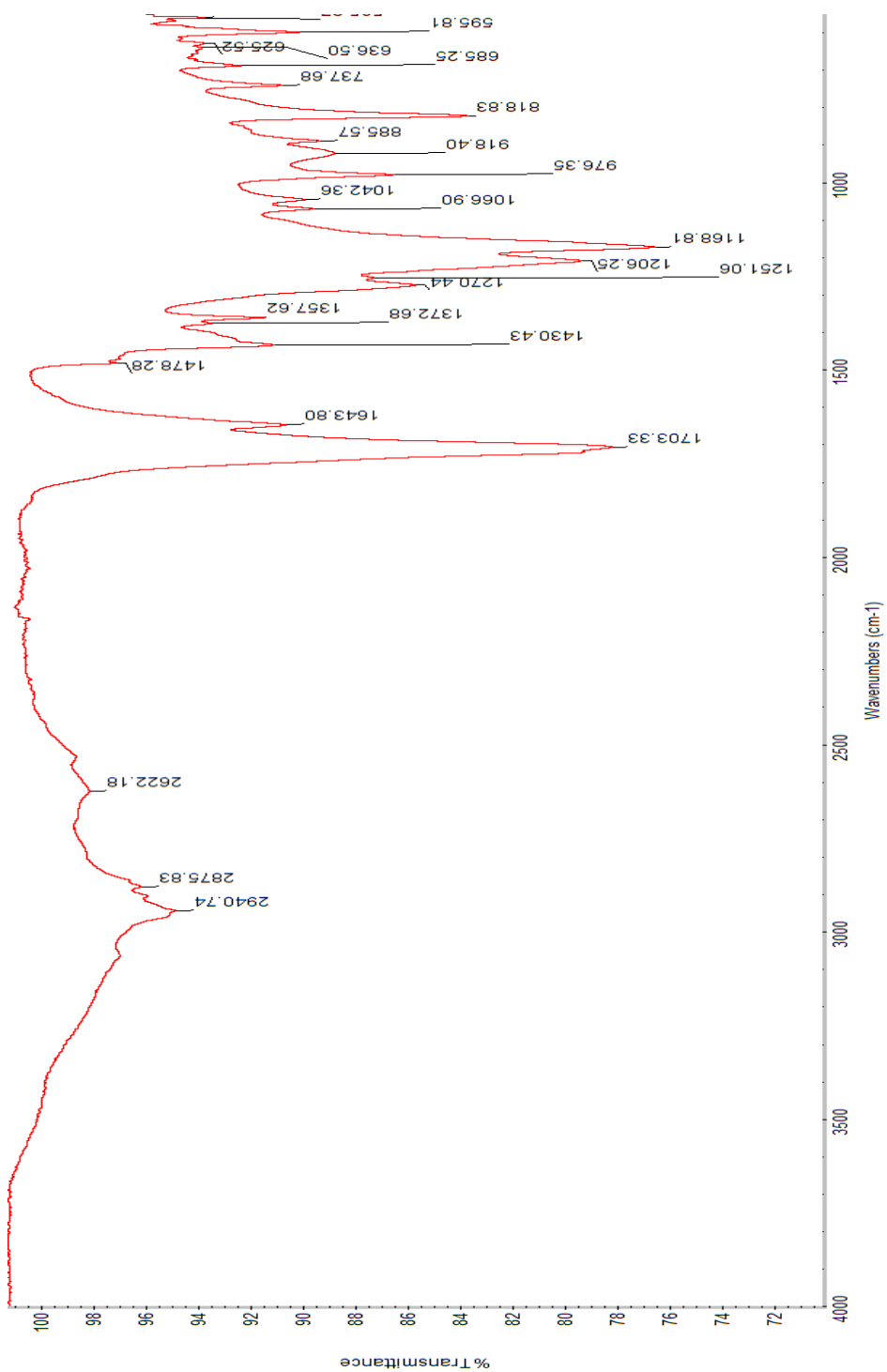


Figure 65. IR spectrum of (2Z,2'Z)-4,4'-[pentane-1,3-diylbis(oxy)]bis(4-oxobut-2-enoic acid) **15** after 27 h mercury lamp UV irradiation.

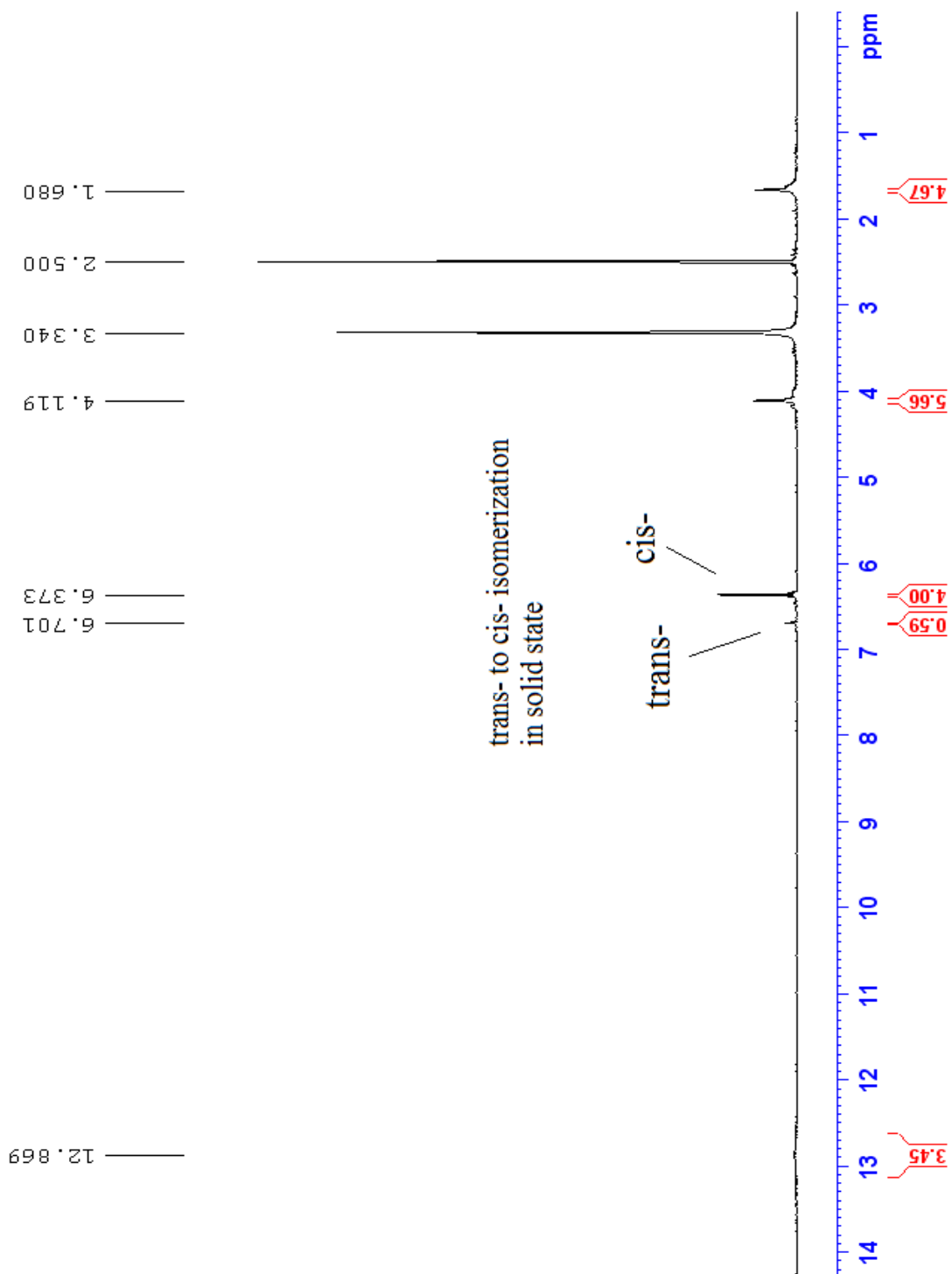


Figure 66. ¹H NMR (DMSO-*d*₆) spectrum of (2*E*,2'*E*)-4,4'-[butane-1,3-diylbis(oxy)]bis(4-oxobut-2-enoic acid) **16** after 72 h mercury lamp UV irradiation.

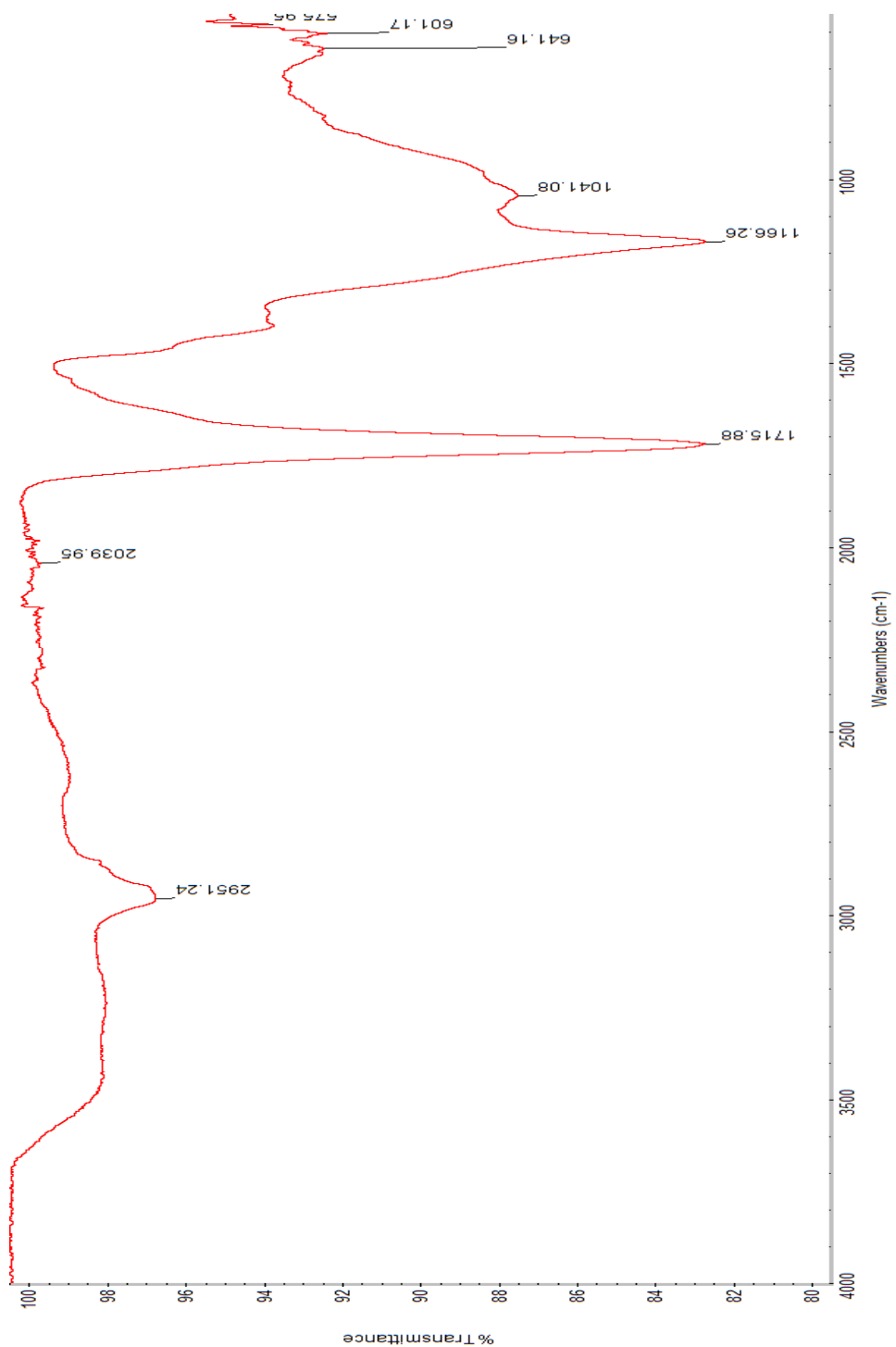


Figure 67. IR spectrum of (3Z,14Z)-1,6,12,17-tetraoxacyclodocosa-3,14-diene-2,5,13,16-tetraone **17** after 2-day mercury lamp UV irradiation.

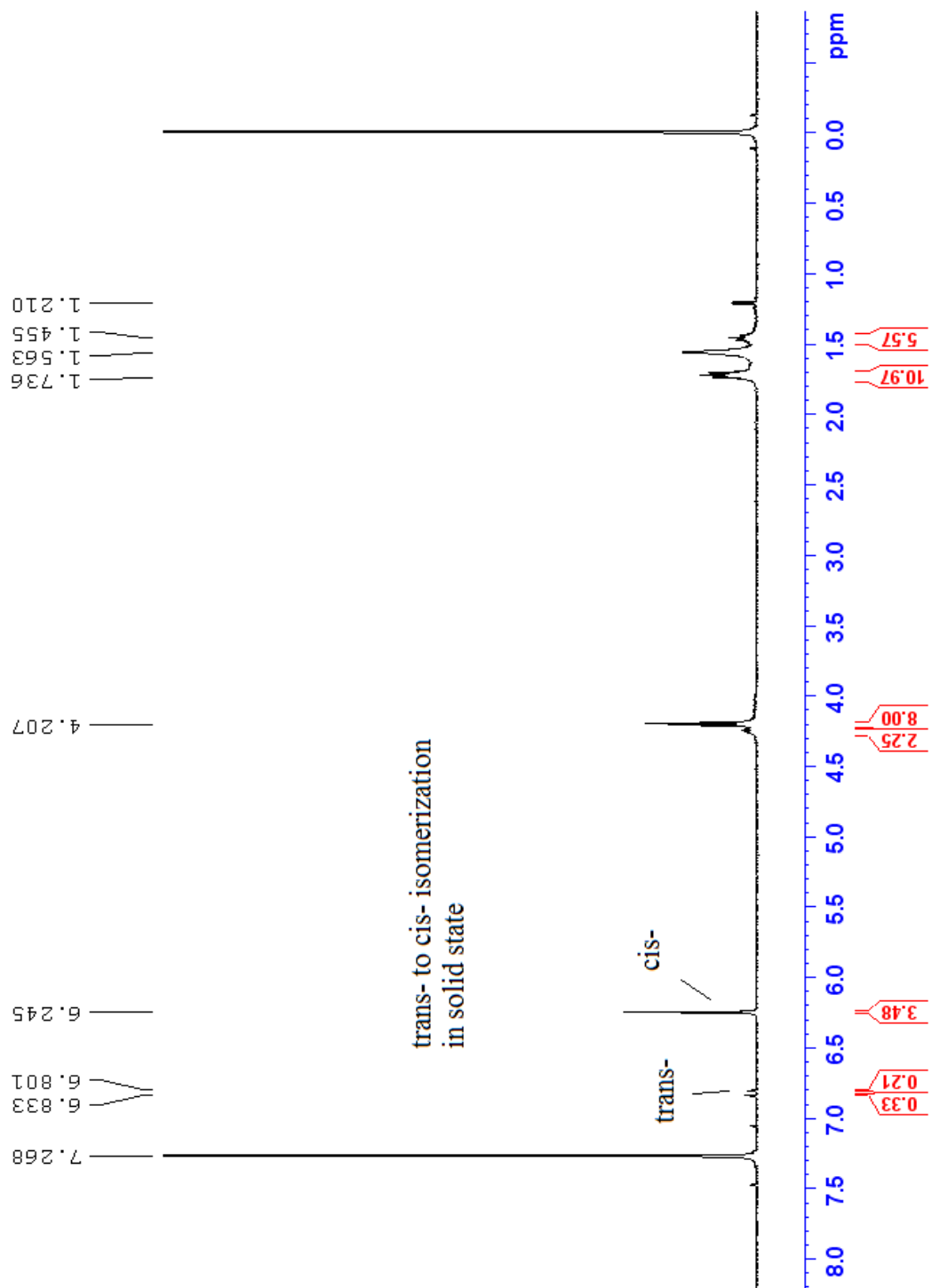


Figure 68. ^1H NMR (CDCl_3) spectrum of (3*E*,14*E*)-1,6,12,17-tetraoxacyclodocosa-3,14-diene-2,5,13,16-tetraone **18** after 12 h mercury lamp UV irradiation.

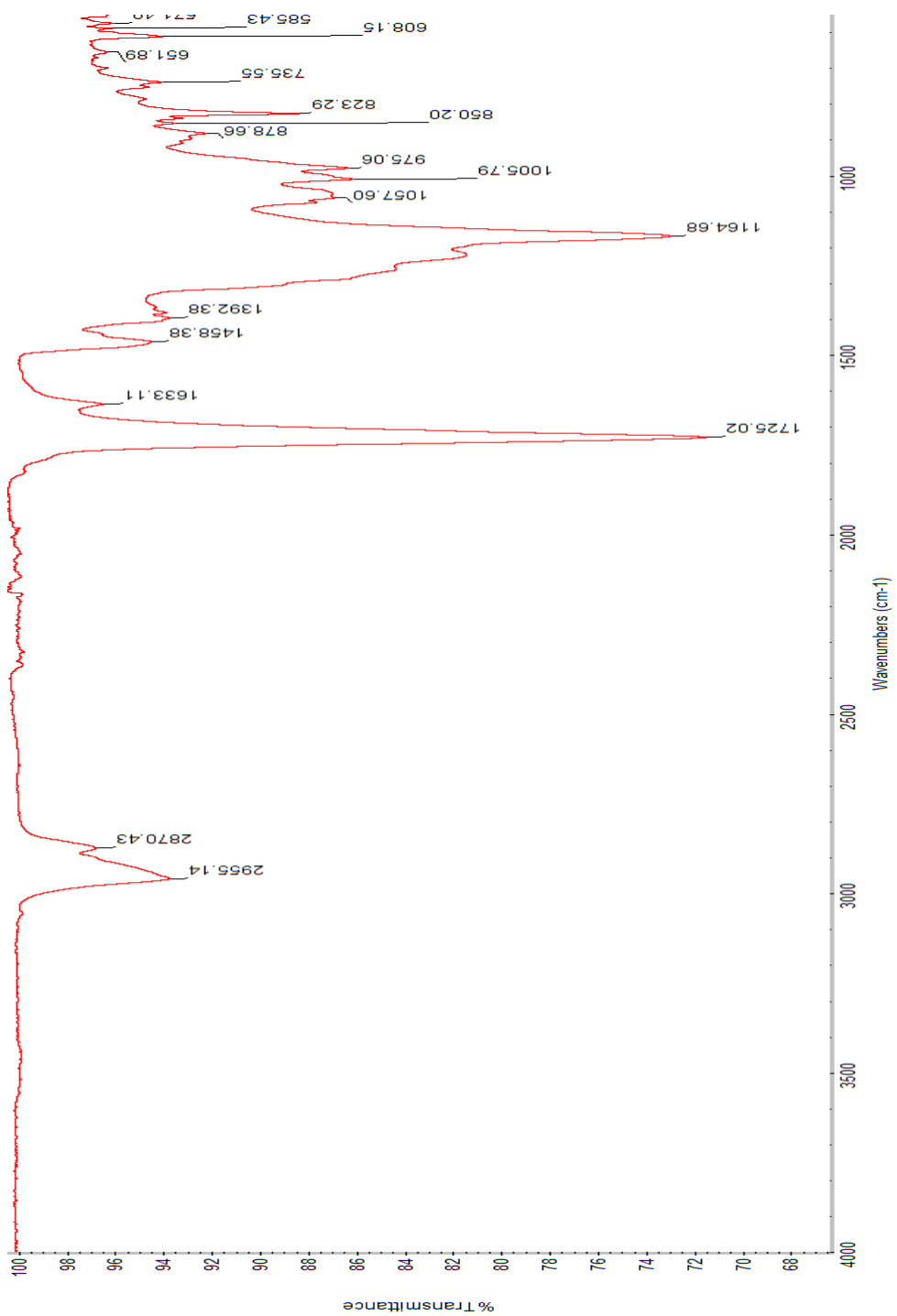


Figure 69. IR spectrum of the product obtained from the solution of (3Z,14Z)-1,6,12,17-tetraoxacyclodocosa-3,14-diene-2,5,13,16-tetraone **17** in hexane after 12 h mercury lamp UV irradiation.

REFERENCES

- (1) Saunders, K.J. Basic Concepts. *Organic polymer chemistry: an introduction to the organic chemistry of adhesives, fibres, paints, plastics, and rubbers*. 1st ed.; Springer Science & Business Media: New York, 2013; pp 1.
- (2) Harris, J.M. In *Poly (ethylene glycol) chemistry: biotechnical and biomedical applications*, 1st ed.; Harris, J.M., Eds.; Springer Science & Business Media: Berlin, New York, 2013; Chapter 1.
- (3) Percec, V. Introduction: frontiers in polymer chemistry. *Chem. Res.* **2001**, *101*, 3579-3580.
- (4) Carraher, C.E., Jr. *Carraher's polymer chemistry*, 9th ed.; CRC Press: Boca Raton, 2010; pp 571.
- (5) Ertl, P.; Schuffenhauer, A. Estimation of synthetic accessibility score of drug-like molecules based on molecular complexity and fragment contributions. *J. Cheminf.* **2009**, *1*, 1.
- (6) de Greef, T. F. A.; Meijer, E. W. Materials science: Supramolecular polymers. *Nature* **2008**, *453*, 171–173.
- (7) Aida, T.; Meijer, E. W.; Stupp, S. I. Functional Supramolecular Polymers. *Science* **2012**, *335*, 813–817.
- (8) Berg, J. M.; Tymoczko, J. L.; Stryer, L. *Biochemistry*, 6th ed., W. H. Freeman: New York, 2006; Chapter 1.
- (9) Nam, K. T.; Shelby, S. A.; Choi, P. H.; Marciel, A. B.; Chen, R.; Tan, L.; Chu, T. K.; Mesch, R. A.; Lee, B. C.; Connolly, M. D.; Kisielowski, C.; Zuckermann, R. N. Free-floating ultrathin two-dimensional crystals from sequence-specific peptoid polymers. *Nat. Mater.* **2010**, *9*, 454–460.
- (10) Davis, R.; Berger, R.; Zentel, R. Two-Dimensional Aggregation of Organogelators Induced by Biaxial Hydrogen-Bonding Gives Supramolecular Nanosheets. *Adv. Mater.* **2007**, *19*, 3878–3881.
- (11) Hou, X.; Schober, M.; Chu, Q. A Chiral Nanosheet Connected by Amide Hydrogen Bonds. *Cryst. Growth Des.* **2012**, *12*, 5159–5163.
- (12) Singh, R. K.; Hou, X.; Overby, M.; Schober, M.; Chu, Q. Hydrogen bonded chiral sheet self-assembled from a C₃-symmetric tricarbamate. *CrystEngComm.* **2012**, *14*, 6132–6135.

- (13) Hou, X.; Wang, Z.; Overby, M.; Ugrinov, A.; Oian, C.; Singh, R.; Chu, Q. R. A two-dimensional hydrogen bonded organic framework self-assembled from a three-fold symmetric carbamate. *Chem. Commun.* **2014**, *50*, 5209–5211.
- (14) Hansen, J.; Sato, M.; Ruedy, R. Perception of Climate Change. *Proc. Natl. Acad. Sci. U. S. A.* **2012**, *109*, E2415-E2423.
- (15) Keith, D. A.; Mahony, M.; Hines, H.; Elith, J.; Regan, T. J.; Baumgartner, J. B.; Hunter, D.; Heard, G. W.; Mitchell, N. J.; Parris, K. M.; Penman, T.; Scheele, B.; Simpson, C. C.; Tingley, R.; Tracy, C. R.; West, M.; Akçakaya, H. R. Detecting Extinction Risk from Climate Change by IUCN Red List Criteria. *Open Conserv. Biol. J.* **2014**, *28*, 810–819.
- (16) Shafiee, S.; Topal, E. When Will Fossil Fuel Reserves Be Diminished? *Energy Policy* **2009**, *37*, 181–189.
- (17) Hamilton, J. D. Historical oil shocks. In *Handbook of Major Events in Economic History*; Parker, R.E.; Whaples, R. Eds.; Routledge New York, 2011; Vol. 21; p 239.
- (18) Yang, S.; Madbouly, S. A.; Schrader, J. A.; Srinivasan, G.; Grewell, D.; McCabe, K. G.; Kessler, M. R.; Graves, W. R. Characterization and Biodegradation Behavior of Bio-Based Poly (Lactic Acid) and Soy Protein Blends for Sustainable Horticultural Applications. *Green Chem.* **2015**, *17*, 380–393.
- (19) Ma, Q.; Liu, X.; Zhang, R.; Zhu, J.; Jiang, Y. Synthesis and Properties of Full Bio-Based Thermosetting Resins from Rosin Acid and Soybean Oil: The Role of Rosin Acid Derivatives. *Green Chem.* **2013**, *15*, 1300–1310.
- (20) Fleischer, M.; Blattmann, H.; Mülhaupt, R. Glycerol-, Pentaerythritol- and Trimethylolpropane-Based Polyurethanes and Their Cellulose Carbonate Composites Prepared via the Non-Isocyanate Route with Catalytic Carbon Dioxide Fixation. *Green Chem.* **2013**, *15*, 934–942.
- (21) Ninomiya, W.; Sadakane, M.; Matsuoka, S.; Nakamura, H.; Naitou, H.; Ueda, W. An Efficient Synthesis of α -Acyloxyacrylate Esters as Candidate Monomers for Bio-Based Polymers by Heteropolyacid-Catalyzed Acylation of Pyruvate Esters. *Green Chem.* **2009**, *11*, 1666–1674.
- (22) Quirino, R. L.; Garrison, T. F.; Kessler, M. R. Matrices from Vegetable Oils, Cashew Nut Shell Liquid, and Other Relevant Systems for Biocomposite Applications. *Green Chem.* **2014**, *16*, 1700–1715.
- (23) Muñoz-Guerra, S.; Lavilla, C.; Japu, C.; de Ilarduya, A. M. Renewable Terephthalate Polyesters from Carbohydrate-Based Bicyclic Monomers. *Green Chem.* **2014**, *16*, 1716–1739.

- (24) Martin, R. T.; Camargo, L. P.; Miller, S. A. Marine-Degradable Polylactic Acid. *Green Chem.* **2014**, *16*, 1768–1773.
- (25) European Commission. Innovating for Sustainable Growth: A Bioeconomy for Europe. http://ec.europa.eu/research/bioeconomy/pdf/official-strategy_en.pdf (accessed September 24, 2016).
- (26) The Whitehouse. National Bioeconomy Blueprint Released. <http://www.whitehouse.gov/blog/2012/04/26/national-bioeconomy-blueprint-released> (accessed Sep 24, 2016).
- (27) Wiley Online Library. Furfural and Derivatives. http://onlinelibrary.wiley.com/doi/10.1002/14356007.a12_119.pub2/abstract?userIsAuthenticated=false&deniedAccessCustomisedMessage= (accessed September 24, 2016).
- (28) Binder, J. B.; Blank, J. J.; Cefali, A. V.; Raines, R. T. Synthesis of Furfural from Xylose and Xylan. *ChemSusChem.* **2010**, *3*, 1268–1272.
- (29) Gandini, A. The Irruption of Polymers from Renewable Resources on the Scene of Macromolecular Science and Technology. *Green Chem.* **2011**, *13*, 1061–1083.
- (30) Besson, M.; Gallezot, P.; Pinel, C. Conversion of biomass into chemicals over metal catalysts. *Chem. Res.* **2013**, *114*, 1827-1870.
- (31) Bozell, J. J.; Petersen, G. R. Technology Development for The Production of Biobased Products from Biorefinery Carbohydrates—the US Department of Energy’s “Top 10” Revisited. *Green Chem.* **2010**, *12*, 539–554.
- (32) Cai, C. M.; Zhang, T.; Kumar, R.; Wyman, C.E. Integrated furfural production as a renewable fuel and chemical platform from lignocellulosic biomass. *J. Chem. Technol. Biotechnol.* **2014**, *89*, 2-10.
- (33) Malinowski, A.; Wardzińska, D. Catalytic conversion of furfural towards fuel biocomponents. *CHEMIK* **2012**, *1*, 982–990.
- (34) Rackemann, D. W.; Bartley, J. P.; Harrison, M. D.; Doherty, W. O. S. The effect of pretreatment on methanesulfonic acid-catalyzed hydrolysis of bagasse to levulinic acid, formic acid, and furfural. *RSC Adv.* **2016**, *6*, 74525–74535.
- (35) Delidovich, I.; Hausoul, P.J.; Deng, L.; Pfützenreuter, R.; Rose, M.; Palkovits, R. Alternative Monomers Based on Lignocellulose and Their Use for Polymer Production. *Chem. Res.* **2015**, *116*, 1540-1599.

- (36) Knoevenagel, E. Condensation von Malonsäure mit aromatischen Aldehyden durch Ammoniak und Amine. *Ber. Dtsch. Chem. Ges.* **1898**, *31*, 2596-2619.
- (37) Zou, X.; Zhou, Y.; Yang, S. T. Production of Polymalic Acid and Malic Acid by *Aureobasidium Pullulans* Fermentation and Acid Hydrolysis. *Biotechnol. Bioeng.* **2013**, *110*, 2105–2113.
- (38) Li, Y.; Wang, X.; Ge, X.; Tian, P. High Production of 3-Hydroxypropionic Acid in *Klebsiella Pneumoniae* by Systematic Optimization of Glycerol Metabolism. *Sci. Rep. Scientific Reports* **2016**, *6*, 26932.
- (39) Lahav, M.; Schmidt, G. M. J. Topochemistry. Part XVIII. The solid-state photochemistry of some heterocyclic analogues of trans-cinnamic acid. *J. Chem. Soc. B* **1967**, 239–243.
- (40) Sonoda, Y. Solid-State [2+2] Photodimerization and Photopolymerization of α, ω -Diarylpolyene Monomers: Effective Utilization of Noncovalent Intermolecular Interactions in Crystals. *Molecules* **2010**, *16*, 119–148.
- (41) Guo, F.; Martí-Rujas, J.; Pan, Z.; Hughes, C. E.; Harris, K. D. M. Direct Structural Understanding of a Topochemical Solid State Photopolymerization Reaction. *J. Phys. Chem. C* **2008**, *112*, 19793–19796.
- (42) Mueller, J. O.; Guimard, N. K.; Oehlenschlaeger, K. K.; Schmidt, F. G.; Barner-Kowollik, C. Sunlight-Induced Crosslinking of 1,2-Polybutadienes: Access to Fluorescent Polymer Networks. *Polym. Chem.* **2014**, *5*, 1447–1456.
- (43) Schultz, D. M.; Yoon, T. P. Solar Synthesis: Prospects in Visible Light Photocatalysis. *Science* **2014**, *343*, 1239176.
- (44) Dewaele, A.; Meerten, L.; Verbelen, L.; Eyley, S.; Thielemans, W.; Van Puyvelde, P.; Dusselier, M.; Sels, B.F. Synthesis of Novel Renewable Polyesters and-Amides with Olefin Metathesis. *ACS Sustainable Chem. Eng.* **2016**, *4*, 5943-5952.
- (45) Faraji, F.; Bakker, F. A modified method for clearing, staining and mounting plant-inhabiting mites. *Eur. J. Entomol.* **2008**, *105*, 793.
- (46) Wang, Z.; Kastern, B.; Randazzo, K.; Ugrinov, A.; Butz, J.; Seals, D. W.; Sibi, M. P.; Chu, Q. R. Linear Polyester Synthesized from Furfural-Based Monomer by Photoreaction in Sunlight. *Green Chem.* **2015**, *17*, 4720–4724.
- (47) Wang, Z.; Randazzo, K.; Hou, X.; Simpson, J.; Struppe, J.; Ugrinov, A.; Kastern, B.; Wysocki, E.; Chu, Q. R. Stereoregular Two-Dimensional Polymers Constructed by Topochemical Polymerization. *Macromolecules* **2015**, *48*, 2894–2900.

- (48) Yashima, E.; Maeda, K.; Furusho, Y. Single- and double-stranded helical polymers: synthesis, structures, and functions. *Acc. Chem. Res.* **2008**, *41*, 1166-1180.
- (49) Nielsen, P. E. Peptide nucleic acid. A molecule with two identities. *Acc. Chem. Res.* **1999**, *32*, 624-630.
- (50) Lehn, J. M. Toward self-organization and complex matter. *Science* **2002**, *295*, 2400-2403.
- (51) Cantekin, S.; Balkenende, D. W.; Smulders, M. M.; Palmans, A. R.; Meijer, E. W. The effect of isotopic substitution on the chirality of a self-assembled helix. *Nat. Chem.* **2011**, *3*, 42-46.
- (52) Hou, X.; Schober, M.; Chu, Q. A Chiral Nanosheet Connected by Amide Hydrogen Bonds. *Cryst. Growth Des.* **2012**, *12*, 5159-5163.
- (53) Wang, Z.; Lee, J.; Oian, C.; Hou, X.; Wang, Z.; Ugrinov, A.; Singh, R.K.; Wysocki, E. Chu, Q.R. An unsaturated hydrogen bonded network generated from three-fold symmetric carbamates. *CrystEngComm.* **2014**, *16*, 7176-7179.
- (54) Davis, M.C. Safer Conditions for the Curtius Rearrangement of 1,3,5-Benzenetricarboxylic Acid. *Synth. Commun.* **2007**, *37*, 3519-3528.
- (55) de Loos, M.; Feringa, B.L.; van Esch, J.H. Design and application of self-assembled low molecular weight hydrogels. *Eur. J. Org. Chem.* **2005**, *2005*, 3615-3631.
- (56) Abdallah, D.J.; Weiss, R.G. Organogels and low molecular mass organic gelators. *Adv. Mater.* **2000**, *12*, 1237-1247.
- (57) Menger, F.M.; Caran, K.L. Anatomy of a gel. Amino acid derivatives that rigidify water at submillimolar concentrations. *J. Am. Chem. Soc.* **2000**, *122*, 11679-11691.
- (58) Suzuki, M.; Nakajima, Y.; Yumoto, M.; Kimura, M.; Shirai, H.; Hanabusa, K. Effects of hydrogen bonding and van der Waals interactions on organogelation using designed low-molecular-weight gelators and gel formation at room temperature. *Langmuir* **2003**, *19*, 8622-8624.
- (59) Hou, X.; Schober, M.; Chu, Q. A Chiral Nanosheet Connected by Amide Hydrogen Bonds. *Cryst. Growth Des.* **2012**, *12*, 5159-5163.
- (60) Zehe, C.; Schmidt, M.; Siegel, R.; Kreger, K.; Daebel, V.; Ganzleben, S.; Schmidt, H.W.; Senker, J. Influence of fluorine side-group substitution on the

- crystal structure formation of benzene-1,3,5-trisamides. *CrystEngComm*. **2014**, *16*, 9273-9283.
- (61) Markvoort, A.J.; Ten Eikelder, H.M.; Hilbers, P.A.; de Greef, T.F.; Meijer, E.W. Theoretical models of nonlinear effects in two-component cooperative supramolecular copolymerizations. *Nat. Commun.* **2011**, *2*, 509.
- (62) Bejagam, K.K.; Fiorin, G.; Klein, M.L.; Balasubramanian, S. Supramolecular polymerization of benzene-1,3,5-tricarboxamide: a molecular dynamics simulation study. *J. Phys. Chem. B* **2014**, *118*, 5218-5228.
- (63) Cantekin, S.; Balkenende, D.W.; Smulders, M.M.; Palmans, A.R.; Meijer, E.W. The effect of isotopic substitution on the chirality of a self-assembled helix. *Nat. Chem.* **2011**, *3*, 42-46.
- (64) Leenders, C.; Jansen, G.; Frissen, M.M.; Lafleur, R.P.; Voets, I.K.; Palmans, A.R.; Meijer, E.W. Monosaccharides as Versatile Units for Water-Soluble Supramolecular Polymers. *Chem. Eur. J.* **2016**, *22*, 4608-4615.
- (65) Chheda, J.N.; Román-Leshkov, Y.; Dumesic, J.A. Production of 5-hydroxymethylfurfural and furfural by dehydration of biomass-derived mono- and poly-saccharides. *Green Chem.* **2007**, *9*, 342-350.
- (66) Mascal, M.; Nikitin, E.B. High-yield conversion of plant biomass into the key value-added feedstocks 5-(hydroxymethyl) furfural, levulinic acid, and levulinic esters via 5-(chloromethyl) furfural. *Green Chem.* **2010**, *12*, 370-373.
- (67) Dutta, S.; De, S.; Saha, B.; Alam, M.I. Advances in conversion of hemicellulosic biomass to furfural and upgrading to biofuels. *Catal. Sci. Technol.* **2012**, *2*, 2025-2036.
- (68) D'Auria, M.; Piancatelli, G.; Vantaggi, A. Photochemical dimerization of methyl 2-furyl- and 2-thienylacrylate and related compounds in solution. *J. Chem. Soc., Perkin Trans.* **1990**, *1*, 2999-3002.
- (69) Baker, W.R. Cyclobutane derivatives as inhibitors of squalene synthase and protein farnesyltransferase. U.S. Patent 5,783,593, Jul 21, 1998.
- (70) Brink, A.S. On the uses of glyptal in palaeontology. *Palaeontographica Africana* **1956**, *6*, 124-130.

- (71) Jordao, R.C.C.; Da Silva, N.H.; Carvalho, L.B. Jr. Glyptal as a support for enzyme immobilisation. *Biotechnol. Tech.* **1996**, *10*, 59-62.
- (72) Xu, Z.; Zhang, Y.; Li, P.; Gao, C. Strong, conductive, lightweight, neat graphene aerogel fibers with aligned pores. *ACS Nano.* **2012**, *6*, 7103-7113.
- (73) Meza, L.R.; Das, S.; Greer, J.R. Strong, lightweight, and recoverable three-dimensional ceramic nanolattices. *Science* **2014**, *345*, 1322-1326.
- (74) Sharma, M.; Singh, M.P.; Srivastava, C.; Madras, G.; Bose, S. Poly (vinylidene fluoride)-based flexible and lightweight materials for attenuating microwave radiations. *ACS Appl. Mater. Interfaces* **2014**, *6*, 21151-21160.
- (75) Paul, D.R.; Robeson, L.M. Polymer nanotechnology: nanocomposites. *Polymer* **2008**, *49*, 3187-3204.
- (76) Thompson, E.; Narasimhan, D.; Moreland, J.C.; Ghazaly, H.M. Lightweight robust thin flexible polymer coated glove. U.S. Patent 8,640,504, Mar 20, **2014**.
- (77) Schmidt, G. Photodimerization in the solid state. *Pure Appl. Chem.* **1971**, *27*, 647-678.
- (78) Leong, S.W.; Faudzi, S.M.M.; Abas, F.; Aluwi, M.F.F.M.; Rullah, K.; Wai, L.K.; Bahari, M.N.A.; Ahmad, S.; Tham, C.L.; Shaari, K.; Lajis, N.H. Synthesis and sar study of diarylpentanoid analogues as new anti-inflammatory agents. *Molecules* **2014**, *19*, 16058-16081.